Imperial College London
Centre for Environmental Policy
Centre for Process Systems Engineering

Economic, process and reservoir modelling for evaluating large-scale deployment of carbon capture and storage

by Clea Kolster

London, May 2018

Submitted in part fulfillment of the requirements for the degree of
Doctor of Philosophy from the Faculty of Natural Sciences of
Imperial College London

First supervisor: Niall Mac Dowell

Second supervisor: Samuel Krevor

Academic mentor: Nilay Shah

Funding body: Natural Environment Research Council Science and Solutions for a Changing Planet Doctoral Training Program

Declaration of originality

I certify, to the best of my knowledge, that the work presented in this thesis is primarily my own and that I am the primary person responsible for the preparation of this manuscript. Any work that was the result of a collaborative effort has been referenced and acknowledged in this thesis.

Clea Kolster, April 2018.

Copyright declaration

The copyright of this thesis rests with the author and is made available under a Creative Commons Attribution Non-Commercial No Derivatives licence. Researchers are free to copy, distribute or transmit the thesis on the condition that they attribute it, that they do not use it for commercial purposes and that they do not alter, transform or build upon it. For any reuse or redistribution, researchers must make clear to others the licence terms of this work.

Abstract

Carbon capture and storage (CCS) is a key technology for least-cost climate change mitigation, but its deployment rate is significantly slower than projected. This thesis provides novel, quantitative insight into the myriad of risks associated with CCS and provides pragmatic solutions to the development of large-scale CCS from multiple angles.

Using the financial metrics that inform private sector investments, this work shows that lack of investor confidence adds a large risk premium to the cost of CCS, contributing 40-70% of its cost. Lowering perceived risk is found to provide a more significant cost reduction than technological innovation would (*e.g.* with better solvents for capture). Reduced risk could result from governments acting as a 'loan guarantor' in the event of CO_2 transport and storage failing to meet demand.

The value of the oil market, CO_2 storage credits, and technological learning on the deployment rate of CCS are assessed through the development of MIICE, a model of iterative investment in CCS with CO_2 enhanced oil recovery (CO_2-EOR). With a highly detailed representation of cost metrics, financing, the CO_2-EOR process and characteristics for thousands of fields, MIICE demonstrates that even with an increasing storage credit (starting at 25\$/tCO_2), technological learning available and oil prices below 85\$/bbl, CCS deployment with CO_2-EOR revenue is not lucrative enough to trigger gigatonnes worth of investment by mid-century.

With a UK example, the impact of CCS deployment and operation scenarios on reservoir behavior is assessed by simulating varying CO_2 injection rates, in their frequency and amplitude, into a geological reservoir model of the UK's main storage sink: the Bunter Sandstone saline aquifer. This work demonstrates the resilience of the storage sink to such variations and provides evidence for accurately representing CO_2 storage in energy systems models.

By developing detailed process models of four variations of CO_2 compression and purification units (CPUs), the potential for an accommodating capture process, in its cost and product purity, is exhibited. Considering a multi-source to sink approach, this result is used to demonstrate the value of a transport network in reducing total system cost *i.e.*, of a group of capture plants. The value of shared capture infrastructure in reducing total capture cost for multiple point sources is also demonstrated.

This body of work demonstrates the importance of commercial innovation and a holistic view of CCS in order to achieve its large-scale deployment. The public-sector can play a key role in enabling this with: greater focus on policies eliminating the cross-chain risk of CCS, stronger incentives for CO_2 market development, measures to improve public perception and representation of CO_2 storage, and schemes attributing greater value to multi-project CCS development rather than individual, isolated projects.

Acknowledgements

I would like to thank my supervisors Niall Mac Dowell and Samuel Krevor for the opportunity to pursue this thesis as a PhD candidate. Thank you both for your time, years of insight and expertise in the wide variety of fields in and around CCS. Thank you Sam for your support and for having provided me with the tools to gain expertise in a whole new discipline and for my initial bridge to Stanford and then California. I also had the opportunity to work with Adam R. Brandt in Energy Resources Engineering at Stanford, whom I would also like to thank for taking me into his research group with open arms, for a great collaboration, sharing a breadth of knowledge, and for having opened me up to more opportunities in the Bay Area. I would also like to thank the many more I have had the chance to collaborate with and who have provided great contributions to the work in this thesis including Mohammad S. Masnadi, Simeon Agada, Evgenia Mechleri and Sam Jackson, and the researchers who have inspired me in the CleanFab group, the Krevor Lab group and the Brandt EAO group. I would also like to thank those who have taken the time to meet with me, providing insight, guidance and collaboration as well as funding opportunities for the work that is presented here; including Hayley Vosper and Gareth Williams from the British Geological Survey, the scholars of the UK Carbon Capture and Storage Research Center, Paul Fennel from Imperial College, Kurt House from Stanford University and Lynn Orr. I would also like to thank Nilay Shah for the many wise words shared and invaluable mentoring provided over the years.

I would like to thank and recognize my funding body, the SSCP NERC DTP, provided through the Grantham Institute for Climate Change and the Environment at Imperial. I would like to thank all those at the Grantham Institute and their directors, for always being a great inspiration, source of support - both financially and mentally - and for always allowing me to pursue new ideas and opportunities. I also want to note how much I have appreciated the cohort that came as part of the DTP and the great friends I have gained through the program; I could not have gotten through this without you.

I would like to thank the friends that have always been there for me, to care for me, listen to me and guide me; I am very lucky to have always had you by my side whether in London, Paris, Milan, Amsterdam, New York or San Francisco. Throughout the course of the PhD, I have also been lucky to have made great new friends, who have challenged me and stood by me in these years through the good times and hard times and with whom I will always share a special bond. Most importantly, I would like to thank my family for always believing in me, always standing by me, supporting me in my decisions and advising me on the most important questions in life. To you Azita, Jacob and Alexander I am forever grateful and to Maman Victoria for your unconditional love.

Contents

List of Tables

List of Figures

Chapter 1

Introduction

This introductory chapter presents the motivation and background of the work for this thesis, first in sections 1.1 and 1.2, followed by the justification and structure of the rest of this thesis in section 1.3, and a list of publications resulting from this work.

1.1 Motivation

Carbon capture and storage (CCS) is recognized as an essential technology to limit greenhouse gas emissions (GHG) in order to avoid dangerous climate change[1]. The Intergovernmental Panel on Climate Change (IPCC), a United Nations (UN) scientific, inter-governmental body, reviews integrated assessment models (IAMs) from literature that propose portfolios of solutions to limit global warming to well below 2°C, which in 2015 has been set as the goal of the UNFCCC's COP21 Paris Agreement[2]. The scenarios evaluated by these IAMs have demonstrated with "high confidence" that CCS is needed in order to have a "likely" chance of limiting warming to below 2°C. This means greater than 66% probability of stabilizing atmospheric CO_2 concentrations to 450 ppm by the end of the century. Only 4 of the 12 models analyzed by the IPCC were able to solve without CCS in the their portfolio of technologies. The long term mitigation costs resulting from the 4 models without CCS were found to be, on average, 138% more expensive than with CCS between 2015 and 2100[1]. One of the key reasons for this is that the models rely on negative emissions technology (NET), bioenergy with CCS (BECCS), being available to make up for predicted overshoots of atmospheric CO_2 concentrations[1]. BECCS is the most technologically advanced and well understood of NETs[1,3].

While the development of CCS has been in progress since the 1970s, proven

since on an industrial scale, and recognized as a least-cost climate change mitigation technology, its deployment has been significantly slower than what was expected and said to be needed in future[1,4–7]. By the end of 2017, according to the Global CCS Institute Database, there were 21 large-scale CCS facilities in operation or in execution totaling 37 $MtCO_2$/year capture capacity[4], but over 40 CCS projects canceled or on hold[8]. The emissions reduction potential from CCS, both in the energy and industrial sectors, is estimated to amount to 2 $GtCO_2$/year by 2030[9], or 54 times the current capacity.

The IPCC's 2005 Special Report on Carbon Capture and Storage highlighted the importance that CCS was to play in mitigating climate change by reducing emissions from fossil fuel driven industries, including primary energy generation and heavy industry sectors[5]. However, since then, all around the world, focus and subsidies have been directed towards other key, cost-effective energy generating technologies, such as wind turbines, solar photovoltaics and concentrated solar power. As a result their costs have been driven down and their deployment accelerated[10,11]. CCS, meanwhile, is complimentary to renewable energy generation as it can make up for these sources' intermittent nature by providing dispatchable power with a low CO_2 emissions intensity. CCS also remains the only means to decarbonize industrial sources, such as steel, iron, cement and fertilizer production. Dependency on fossil fuels for energy security, particularly in developing countries such as India and coal-rich nations such as Australia and Canada, reluctant to strand their assets, will also continue to set a place for CCS in the power sector[12]. China, the largest consumer of coal globally, contributed 50% of global demand in 2016 and while its consumption is predicted to peak within the next two decades, it continues to build and consume more unabated coal capacity[9,13,14]. If China, and the rest of the world, plan to continue to use their existing, under construction and planned coal power plant capacities, then retrofitting these plants with CCS is currently the only solution to reduce these emissions[9].

Nevertheless, there are a number of reasons why CCS has yet to be deployed at the scale that is expected. Some of what needs to be done to trigger economically sound deployment of CCS on a large scale, and globally, is addressed here in this thesis. None of these reasons, however, stem from a lack of technical feasibility of CCS[3,4].

Several reviews have been published describing the technical status, costs and challenges of CCS[5,15–17], the political upheavals around CCS and financial challenges[18,19] and most recently the review by Bui et al. 2018[3]. There is a lot of perceived uncertainty and risk around CCS and this typically has translated into a high cost of capital[4,20,21] and there is a common notion that reducing this

perceived uncertainty and risk to CCS will reduce its cost of capital and thereby allow for the large-scale deployment needed[20–22]. Establishing a value to this reduction of risk, however, is not straightforward.

A key element of risk is the multi-component nature of the full CCS chain and the reliance on external factors to the CCS process. These have created steep barriers to its large-scale deployment. Few studies have attempted to address CCS deployment issues by focusing on multiple components of the process at once. Here, techno-economics and feasibility of CCS deployment are assessed from the perspective of an individual or group of investors and from the perspective of the CO_2 off-taker. This is done by looking at multiple components of the process at once, from the energy system's CO_2 supply and capture system, transport, CO_2 storage and usage. Thus, this work seeks to identify and address key issues hindering the large-scale deployment of CCS. These include:

1. The proportion of CCS cost that is paid for in financial risk and thus establishing key focus points for reducing overall system cost.

2. The policy and economic risk of CCS that stems from the lack of a long-term and reliable market incentive for CCS. This is considered through either a value of CO_2 as a raw material and/or a universal incentive to reduce CO_2 emissions from fossil fuel based industries.

3. The representation of CO_2 storage in energy systems models considering CCS deployment that will inform the public perception of long-term CO_2 storage. This is done by assessing CO_2 storage reservoir response to fluctuations in CO_2 injection as a result of varying CO_2 capture deployment and demand.

4. The limiting cost and purity requirements associated with CCS when adopting a myopic, single-facility viewpoint. By considering a large-scale plan for CCS deployment with multiple facilities, cost reduction benefits are drawn from the transport network infrastructure that links streams at varying levels of purity and more or less expensive CO_2 capture facilities.

1.2 Background to carbon dioxide capture, transport and storage

Multiple pathways of carbon dioxide capture, transport and storage exist. With regards to CO_2 capture, three main variations are considered to have

reached a high level of technological readiness[3](above 6 on a scale of 1 to 10) [1]: post-combustion, oxy-combustion and pre-combustion[17,24]. In this thesis, some elements of post-combustion and oxy-combustion capture are discussed, and recommendations on measures for their deployment are provided. Part of the capture process has been modeled in detail in this work (Chapter 5), but the selection process for each of these is not discussed here. Currently all industrial CCS projects in operation or under construction have amine-based post-combustion technology capturing carbon dioxide[4]. In October 2014, oxy-combustion capture was the method of choice for one of two large-scale CCS demonstration projects in the United Kingdom, the White Rose CCS project, and therefore was considered a viable CO_2 capture method. Today, with the White Rose CCS project canceled[8], one CCS project planned with oxy-combustion capture remains and is in early stages of development: the Shanxi International Energy Group CCUS based in China[4]. Oxy-combustion capture is also worth considering as the means to capture CO_2 from cement production and in iron and steel production where an air separation unit is already present.

Transporting CO_2 is considered to be most efficient via pipeline for distances of up to 1,000 km and as a supercritical fluid at conditions above the critical point of 31.1°C and 74 bar, and typically held at a pressure of 100 - 120 bar[17]. The oil and gas industry has decades of experience transporting CO_2 via pipelines, e.g. in getting CO_2 from its point source to an oil field for enhanced oil recovery (EOR) or from a natural gas processing site to a designated storage site[25,26]. Carbon dioxide is transported safely through over 6,000 km of pipelines in the United States since the 1970s and more recently in Norway, the North Sea, North Africa and the Middle East, provided pressure and single phase conditions are maintained[26,27]. The costs associated with building pipeline transport for CO_2 are comprised mostly of upfront costs for licensing, network design, materials and labour. Operating costs for transport are minor in comparison and will include operating and maintenance of the pipeline and booster stations typically needed for transport over 100 km[15,16,28,29]. Transportation of CO_2 as a cryogenic liquid via ship is also considered to be a viable option particularly for distances over 1,000 km or for small quantities of gas, but is substantially more energy intensive than pipeline transport[3,17].

Carbon dioxide injection and storage, similarly to transport, has also been taking place for decades in certain parts of the world, both onshore *e.g.*, in the Permian Basin in Texas for EOR, and offshore *e.g.*, at Sleipner in the Norwegian part of the North Sea for storage[3,17,26]. The availability of the largest CO_2 storage sinks are proven to be in deep geological reservoirs that may have previ-

[1] Technological readiness levels are defined and described for CCS in the Global CCS Institute Status Report: 2011[23] and Bui et al. EES 2018[3]

ously or still contain oil and gas or are filled with brine *i.e.*, high salinity water. Various estimates are provided for global CO_2 storage capacity. Depleted oil and gas fields are estimated to be able to provide up to 920 $GtCO_2$[30] and deep saline aquifer storage is estimated as sufficient to store a century of CO_2 emissions from large point sources worldwide[31] with early estimates of 10,000 $GtCO_2$[30,31]. These estimates are based on a volumetric approach to calculating CO_2 storage capacity. Meanwhile, estimations of storage capacity based on a dynamic injection approach that incorporates reservoir pressure limitations have been conducted for certain regions, such as North America and Europe, and demonstrate more limited storage capacities[26,30–33]. The deep geological reservoirs considered for CO_2 storage are sealed with impermeable or very low permeability rock and are therefore expected to be able to store CO_2 safely for thousands of years via the same mechanisms with which these reservoirs have stored other hydrocarbons (oil & gas) for centuries.

Of the 21 large-scale CCS facilities operating or under construction, 16 of these are to use CO_2 for EOR (CO_2-EOR), gaining revenue from crude oil production, and then using the depleted hydrocarbon reservoir as a storage sink[4]. Capturing CO_2 to be able to use it for CO_2-EOR is particularly appealing in oil-rich regions where infrastructure for CO_2 transport and storage already exist from EOR activities or can easily be converted from existing oil production operations. These 16 facilities are located in the US and then in Canada, Saudi Arabia, UAE and Brazil[4]. In China, two CCS projects are under construction with enhanced oil recovery as the main sink for CO_2 although the Asia-Pacific region is scarce with EOR capacity: about a tenth of its CCS target[3]. Globally, it has been estimated that, in the 54 largest oil basins, there is the capacity to store 140 $GtCO_2$ for 470 billion barrels of oil produced from proven reserves and up to 320 $GtCO_2$ stored for 1,070 billion barrels of oil recovered when considering 'undiscovered' resources from known large hydrocarbon reservoirs[34].

Detailed descriptions of the variation of pathways for CCS can be found in the breadth of CCS review literature, including, most recently, Bui et al. 2018[3], and previously Gale et al. 2015[35], De Connick et al. 2014[36], Boot-Handford et al. 2014[17] and earlier, the IPCC special report on CCS[5].

1.3 Objectives and structure

The work presented in this thesis assesses dynamics and links between the energy system, CO_2 capture, transport and storage, and a market presence for CO_2 (sequestration or use). This work moves away from a 'myopic view' of CCS where analyses are conducted on a project by project basis. Instead, outcomes

of large-scale CCS deployment (*i.e.*, multiple projects and facilities) are modeled and analysed, focusing on the effects this can have on multiple moving parts of the process: from emissions point sources to the CO_2 grave.

The rest of this thesis is structured as follows. Chapter 2 defines the financial metrics used to calculate the levelized cost of CCS and the value of perceived risk, in order to better target cost reduction opportunities for CCS. Chapter 3 presents the development and results of MIICE (model of iterative investment in CCS with CO_2-EOR) that demonstrates the breadth of conditions under which the revenue from CO_2-EOR will not prove to be sufficient to catalyze gigatonnes worth of CCS investment, even when considering a US-type transport and storage infrastructure set-up. MIICE provides insight to policy makers on the value of factors like oil price, CO_2 tax, capital cost and technological learning. Chapter 4 demonstrates, through reservoir simulation, that a CO_2 storage reservoir can be robust and resilient to varying CO_2 injection rates, in frequency and amplitude. Such variations may come as a result of a changing energy system and gradual CCS deployment needs. Chapter 5 models the value transport and storage infrastructure can provide for CO_2 capture cost reduction and the financial benefit that can be drawn from planning CCS deployment for multiple future point sources at once. Finally, Chapter 6 summarizes the conclusions of this thesis and scope for further research.

This thesis builds heavily on the following open access and peer-reviewed journal papers, as a first author and co-author, and listed in reverse chronological order. The work contributing to each publication is presented and discussed in the respective chapters indicated here and restated at the beginning of each relevant chapter.

- *The impact of time-varying CO_2 injection rate on large scale storage in the UK Bunter Sandstone*, C. Kolster, S. Agada, N. Mac Dowell, S. Krevor. **International Journal of Greenhouse Gas Control**, 68, 77-85, January 2018[37]. `https://doi.org/10.1016/j.ijggc.2017.10.011`. Chapter 4.

- *CO_2 enhanced oil recovery: a catalyst for gigatonne-scale carbon capture and storage deployment?*, C. Kolster, M. S. Masnadi, S. Krevor, N. Mac Dowell, A. R. Brandt. **Energy & Environmental Science**, 2594-2608, November 2017[38]. `pubs.rsc.org/en/content/articlelanding/2017/ee/c7ee02102j`. Chapter 3.

- *The impact of energy systems demands on pressure limited CO_2 storage in the Bunter Sandstone of the UK Southern North Sea.* S. Agada, S.

Jackson, C. Kolster, N. Mac Dowell, G. Williams, H. Vosper, J. Williams, S. Krevor. **International Journal of Greenhouse Gas Control**, 65, 128-136, October 2017[39]. `https://doi.org/10.1016/j.ijggc.2017.08.014`. Chapter 4.

- *The role of CO_2 purification and transport networks in carbon capture and storage cost reduction*, C. Kolster, E. Mechleri, S. Krevor, N. Mac Dowell. **International Journal of Greenhouse Gas Control**, 58, 127-141, March 2017[40]. `https://doi.org/10.1016/j.ijggc.2017.01.014`. Chapter 5.

- *Cost and performance of some carbon capture technology options for producing different quality CO_2 product streams*, R. T. J. Porter, M. Fairweather, C. Kolster, N. Mac Dowell, N. Shah, R. M. Woolley, **International Journal of Greenhouse Gas Control**, 57, 185-195, February 2017[41]. `https://doi.org/10.1016/j.ijggc.2016.11.020`.Chapter 5.

Chapter 2

Financial risk and the cost of CCS

The work presented here was conducted following that described in chapters 3, 4 and 5 with the aim of providing a clear methodology for calculating the levelized cost of CCS and demonstrating in a quantitative manner, why it is vital to focus on commercial incentives for CCS rather than isolated single technological improvements. This work responds to a perceived gap in the literature around the nature of CCS cost calculations, that have failed to clearly outline financial assumptions used to obtain a levelized cost of CCS and the link between cost and financial risk. The initial hypothesis is that the cost of CCS is likely driven by the financial and material risks associated with the technology as seen by potential investors. In order to validate this hypothesis, this work draws on the capital asset pricing model (CAPM), an economic model widely used in the energy sector and with solid theoretical foundation. The CAPM demonstrates the relationship between an asset's risk and an investor's expected return. The values of expected return obtained from the CAPM are then used to calculate the cost of CCS and the proportion of its cost that is paid in risk aversion. The full methodology is outlined in the next sections of this chapter.

2.1 Introduction

The elevated cost of carbon capture and storage (CCS) has very often been the focal point in discussions on the deployment need for CCS as a global emissions reduction solution. However, no single method or definition of CCS cost has been universally established and a wide range of costs are still quoted in literature[15,16,21,22,28]. The upfront capital cost of CCS is high. However, it is

the cost of capital *i.e.*, the rate of return on the investment, that will determine whether or not that investment is worthwhile. The cost of capital is calculated by following a financing method of choice for CCS and determining the perceived investment risk. To date, most projects that had a large reliance on government backing for CCS have failed, whether regional (*e.g.* EU NER300) or national (*e.g.* Mongstad in Norway, the UK CCS competition or US FuturGen)[8,19]. Attracting private sector investment is seen as vital to establish a 'best value for money' perception of CCS and is key to the roll out of any large-scale technology (similarly to nuclear power plants)[18,42]. This work argues that, with private sector involvement, taxpayers' willingness to bear the burden of CCS cost is likely to improve, which in turn enables easier government budget allocation to support CCS (*e.g.* through insurance on capital or CO_2 liability allocation) and thereby reducing an investor's perception of CCS risk. This chapter clearly defines the key financial metrics used to determine CCS cost and assesses the proportion and the allocation of risk included in the cost of CCS in order to better orientate the focus of researchers and policy makers for improved monetization of the CCS process.

2.2 Financing metrics and the capital asset pricing model (CAPM) for energy sector investments

When deliberating over a potential investment, an investor will establish their expected rate of return as a function of the amount of risk to be taken on. The Capital Asset Pricing Model (CAPM) of Sharpe[43] and Lintner[44], has historically been used in the energy sector to calculate this investment risk and hence define an investor's expected asset return or equity return (R_E). It assumes a value of systematic risk β for the security (typically between 0 and 2), the market return R_M of the security's sector [1] and scales it against the risk free rate of return R_F (typically taken as the percentage yield on a long term government bond *e.g.* 3% for a US 10 year Treasury Bill and 1.55% for a UK 10 year government bond[47])[48]. The CAPM defines the equity return with:

$$R_E = R_F + \beta \times (R_M - R_F) \tag{2.1}$$

[1] R_M is typically taken as the return/performance of a portfolio of companies *e.g.* the S&P 500 with a 2016 annual return 2016 11.59%[45] or the FTSE 100 with a 2016 annual return of 11.4%[46]

CCS is not an energy generating technology, but it is likely to be deployed initially for the energy sector, either as part of a new power plant or retrofitted onto a refurbished plant build. Hence, it is reasonable to define its equity return similarly to that of an asset in the energy and power generation sector. The CAPM equity return R_E is then used to define the weighted average cost of capital (WACC) or is assumed as the internal rate of return (IRR) on investment for a 100% equity financed investment. In literature, the IRR value assumed/desired by investors is typically used as the nominal discount rate (NR) in a discounted cash flow analysis to define the net present value (NPV) of an investment. WACC is defined as:

$$WACC = R_D \times D/E + R_E \times (1 - D/E) \tag{2.2}$$

where R_D is the cost of debt, R_E the cost of equity , D/E is the fraction of capital financed by debt and (1- D/E) the fraction financed by equity.
The real discount rate, DR, is the nominal discount rate adjusted for inflation. DR is taken as the interest rate to calculate the capital recovery factor (CRF) on an investment (see Equation 2.3), which is used to obtain a levelized or annualized cost on the investment. The capital recovery factor (CRF) is defined as:

$$CRF = \frac{DR \times (1 + DR)^n}{[(1 + DR)^n] - 1} \tag{2.3}$$

where n is the number of years over which the investment is to be recovered and DR is the real discount rate assumed. CRF decreases with higher investment period n and increases with DR. In order to get from a nominal rate such as IRR to a real rate such as DR, adjusted for inflation i the following equation is applied:

$$DR = \frac{1 + IRR}{1 + i} - 1 \tag{2.4}$$

As defined by the WACC equation, DR will be closest to the cost of debt (R_D) or the cost of equity (R_E) as defined by the CAPM, depending on whether the ratio of debt to equity is greater or lower than 50:50, respectively.

Here, it is assumed that the equity return R_E, adjusted for inflation, serves as the upper bound for the assumed DR and therefore the minimum required rate of return or IRR on investment (*N.B.* R_E is used as the nominal discount rate). This is because, for countries in Europe and North America or China, where debt can be financed at relatively low interest rates (2% - 8%)[49], factoring in the cost of debt to calculate WACC will typically bring it below the equity return R_E.

In literature, different assumptions are made on discount rates and financing

methods, whether assumed to be equity financed or split between equity and debt, and most often CCS costs are given in relation to a power plant with and without CCS[15,50,51]. Rubin et al. 2015 reports capital recovery factors of 9% - 12 % for investment in a supercritical coal-fired power plant with CCS[15]. A case study example of an investment in a coal-fired power plant with CCS presented in NETL report "Cost and Performance Baseline for Fossil Energy: Volume 1" assumes a debt to equity ratio (D:E) of 45:55, an R_E of 12% and R_D of 5.5% and a 30 year project lifetime[51]. Other reports on fossil-based energy projects suggest a D:E of 60:40, an R_E of 20% and R_D of 8.5%, a D:E of 50:50 with 20% R_E and 10% R_D, or 100% equity financed for example[50]. While these assumptions will vary from project to project, it is critical that assumptions made are clearly outlined.

The CAPM provides a means to define quantitatively the value of risk on CCS and therefore the discount rate that should be used. The CAPM security line is plotted to define the appropriate R_E based on the market risk premium assumed (*i.e.* [R_M - R_F]) and as a function of the systematic risk β associated with the asset to receive investment. The value of systematic risk β is a measure of the deemed volatility of the security when compared to the security's market sector. If β is equal to 1, the asset or security's value moves with that of the market. If β is less than 1, the security is less volatile than the market and would appeal to risk averse type investors, and if greater than 1, the security is deemed more volatile than the market, appealing to more risk loving investors. The risk free rate R_F taken here is the yield on a US 10YR T-Bill (10 year treasury bill) or 2.4% in December 2017[52]. A 3% inflation rate is assumed, leading to negative real interest rates on government bonds[16].

Based on a selection of energy sector published equity return values[47], the security lines for high, medium and low market risk premium values are plotted in Figure 2.1. equivalent to 13%, 10% and 8%. Highlighted in the CAPM formula (see equation 2.1), the market risk premium is the slope of the CAPM security line (Figure 2.1). Because there are no publicly listed companies that are solely invested in CCS, the best proxy for β values are those of publicly listed companies that have CCS investments in their portfolio or energy companies that could be investing in CCS in the future. These are most likely to be oil & gas companies as precedent has shown. These are summarized in Table 2.1. Petra Nova CCS, the second large-scale deployment of CCS in the power sector, operational in early 2017, located in Houston, Texas, was a 50/50 joint venture by NRG Energy and JX Nippon Oil & Gas Exploration. The parent company of the latter is JXTG Holdings Inc. The CO_2 capture technology used at Petra Nova was developed jointly by Mitsubishi Heavy Industries Ltd and Kansai

Electric Power Co[53]. The first power sector deployment of CCS, Boundary Dam, took place in October 2015 by SaskPower, which is owned by the government of Saskatchewan[54] and therefore does not have a known measure of systematic risk β. Other energy companies, such as EDF, Total, BP and Shell have at some point shown interest in investing in CCS and may be amongst the first to do so in the future and therefore are good benchmarks for financial metrics for CCS investing entities.

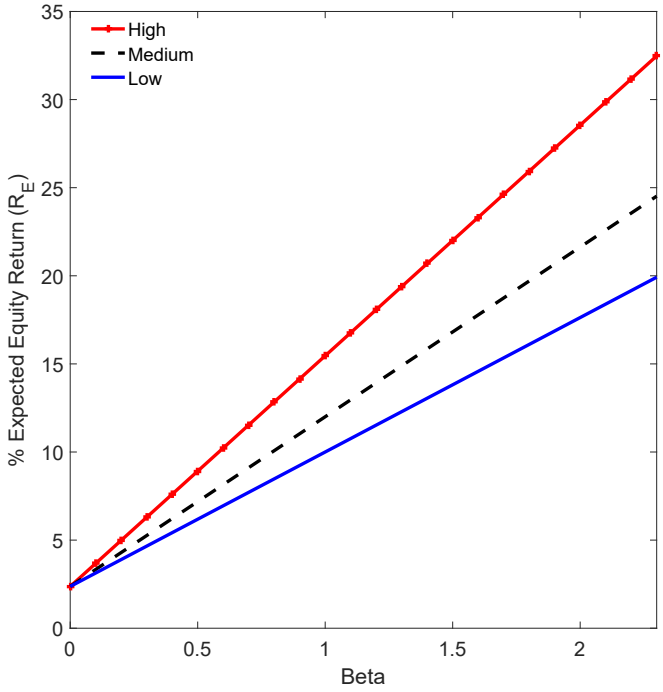

Figure 2.1: CAPM security line for high, medium and low energy sector market risk premium values ([R_M - R_F]).

Table 2.1: Systematic risk β of a sample of energy sector listed companies, February 6, 2018[47]

Listed Company	Listing	β
NRG Energy Inc.	NRG.N	1.09
JXTG Holdings Inc	5020.T	0.58
Mitsubishi Heavy Industries Ltd	7011.T	1.37
Kansai Electric Power Co. Inc	9503.T	1.25
Electricite de France SA	EDF.PA	1.28
Total SA	TOTF.PA	0.94
BP PLC	BP.L	0.93
Royal Dutch Shell PLC	RDSa.L	0.80

The CAPM security lines (see Figure 2.1) show that for CCS interested companies with β values below or equal to 1, expected asset return R_E will always

be smaller or equal to the market risk premium (*i.e.* below a high 13%, medium 10% or low 8%), while those valuing CCS risk with β above 1 will face higher systematic risk but expect to get a return higher than the market risk premium (*i.e.* greater than a high 13%, medium 10% or low 8%). Hence, for the range of β values given in Table 2.1 (0.58 - 1.37), if a low market risk premium value is assumed (*i.e.* 8% blue line), a CCS investment estimated to have low systematic risk, the expected rate or return or IRR would be between 7% and 10%, while high systematic risk assumptions are expected to be matched with an IRR between 11% and 13%. At medium market risk premium (*i.e.* 10% black dotted line), low systematic risk investments would have an expected return of 8% to 12%, and high risk investments a return of 13% to 16%. Finally, at high market risk premium (*i.e.* 13% red line), low systematic risk investments would have an expected return of 10% to 15% and high systematic risk investments, 16% to 21%. Here, we assume a 10% IRR for deemed low risk CCS investment and 20% IRR for high risk CCS investment.

2.3 Evaluating the cost of CCS

The cost of CCS is typically given as a cost per unit of CO_2 emissions avoided (*e.g.* \$/tCO_2) or, when referring specifically to CCS with power, as a cost per unit of energy (*e.g.* \$/MWh). In this work, cost per unit of CO_2 emissions avoided is used since this metric allows for leveled comparison of CCS across sectors and across different power generating sources [2]. These costs are given on an annualized (*i.e.* levelized) basis by grouping capital and operating costs and normalized to a metric tonne of CO_2 basis. Most often, the cost metric chosen is then split into cost allocated to capture, transport and storage of CO_2.

Here, two perceptions of CCS investment risk are translated into annualized CCS cost and distinguished as 'High Risk' and 'Low Risk'. At 'High Risk', a 20% IRR is assumed, equivalent to the CAPM equity return R_E for systematic risk values β of 1.3, 1.8 or 2.3 based on security lines of decreasing slopes, *i.e.* the security's value is more volatile than the sector's market (see Figure 2.1). At 'Low Risk', a 10% IRR is assumed, which, following the CAPM security lines, is equivalent to the CAPM R_E for β of 0.6, 0.8 and 1, *i.e.* the security's value is less volatile or equivalent to its sector's market.

In order to distinguish the proportion of CCS cost that is attributed to the

[2]The amount of CO_2 avoided per MWh of energy production varies substantially depending on the efficiency and type of system and fossil fuel e.g. assuming these are combined with an amine-based post combustion capture plant natural gas combined cycled would output about 2.65 MWh/tCO_2 captured whereas a supercritical pulverized coal fired power plant would output 0.96 MWh/tCO_2 captured[16]

relevant level of perceived risk on capital in juxtaposition to the actual or risk free based cost of capture, transport and storage, the following steps are taken. The upfront capital cost of CO_2 capture, transport and storage (CAPEX) is first levelized based on the CRF of the risk free rate R_F over a 30 year investment span of 2.4%, which is equivalent to an inflation-adjusted CRF of 2.9% (see equation 2.3) [3]. The same levelization is done based on the IRR assumed for the 'High Risk' and 'Low Risk' investments (*i.e.* 20% and 10%), equivalent to an inflation-adjusted CRF of 16.3% and 7.6%. To the cost of capital (given on an annualized $/t$CO_2$ basis), the equivalent operating cost for capture, transport and storage (OPEX) are added, resulting in a total levelized cost for CCS in $/t$CO_2$ (LCOCCS) and illustrated with equation 2.5.

$$LCOCCS = CAPEX \times CRF + OPEX \tag{2.5}$$

The difference between the 'High Risk' or 'Low Risk' LCOCCS and the LCOCCS based on a risk free rate of CRF is the risk premium paid for CCS[4]. The capital and operating cost of CO_2 capture, transport and storage costs are given in Table 2.2. These values were obtained and approximated based on the MIICE model developed as part of this work and published in Kolster et al. 2017[38]. The levelized cost of CCS will differ based on whether the project is assumed to be at first of a kind (FOAK) or Nth of a kind (NOAK) cost levels. This results in a risk free LCOCCS (*i.e.* annualized based on a CRF of 2.9%) of 25$/t$CO_2$ at FOAK conditions and 18$/t$CO_2$ at NOAK conditions.

Figure 2.2 shows this split in allocated cost and the cost reduction that results from technological learning (from FOAK to NOAK), but also separates out the part of cost that is attributed to perceived risk of capital. Here, technological learning is assumed only for CO_2 capture. This brings the upfront capital cost of CO_2 capture from an assumed $500 Million for an FOAK 1 Mtpa CO_2 capture facility down to $250 Million for an NOAK facility based on an assumed 10% learning rate. Assuming 0.11 kW/tCO_2 captured (post combustion capture on SCPC), the upfront capital cost of CO_2 capture is equivalent to 4,500 $/kW at FOAK conditions and 2,250 $/kW at NOAK conditions.

However, based on the breadth of CCS cost literature, it is clear that CCS cost analyses and values most often differ because of dissimilar assumptions, *e.g.* geography/topography, cost of materials, licensing, years of defined investment.

[3] All cost values are in 2016 USD

[4] NB: The market risk premium is [R_M - R_F], different from the risk premium paid on CCS and attributed to the cost of CCS

Table 2.2: Overnight capital cost and operating cost and assumptions for CO_2 capture, transport and storage based on simplified MIICE[55] data in 2016 USD, published in Kolster et al. 2017[38] and Rubin et al. 2015 storage costs[15].

Cost type	Value per $MtCO_2$ captured per year	Assumption
Upfront Capital Cost		
Capture FOAK	\$500 Million	Amine-based post combustion capture on supercritical pulverized coal firing power plant (SCPC)
Capture NOAK	\$250 Million	Same as above
Transport	\$10 Million	100km pipeline transport onshore
Storage	\$20 Million	Average for geological reservoir storage offshore or onshore[15]
Operating cost		
Capture	\$9 Million	Fixed and variable O&M and fuel cost
Transport	\$0.5 Million	O&M cost only
Storage	\$1 Million	O&M, fluid pumping and injecting

Therefore, the specifics of cost figures is best understood as an approximate range rather than a fixed value. The work of Rubin et al., 2015, quotes capital cost values between \$300 Million and \$400 Million per $MtCO_2$ captured using post combustion technology on a supercritical pulverized coal flue gas stream[15], but is not clear on whether this refers to FOAK or NOAK costs. Meanwhile, for the same type of process, the Petra Nova CCS project was delivered at a cost of \$714 Million per $MtCO_2$ captured (it cost \$ 1 Billion and captures 1.4 $MtCO_2$ per year[53]). Also quoted in the Rubin et al. CCS cost review: \$ 1 Million to \$ 10 Million per $MtCO_2$ transported over 250 kilometers of pipeline onshore or offshore and \$ 5 Million to \$ 25 Million per $MtCO_2$ stored, whether in a saline aquifer or a depleted oil and gas reservoir onshore or offshore[5]. The cost for capture here is based on the assumption that the CO_2 capture process is amine-based post combustion applied to a supercritical pulverized coal firing power plant as these are widely cited in literature, and this is the first type of CO_2 capture plant associated with a primary energy producing facility[4,15,16,28,53,54]. Estimates of cost of CO_2 capture for natural gas combined cycle (NGCC) power plants and for industrial plants are estimated to be less costly, but may be less

[5]All values have been converted from the original quoted currency to 2016 USD based on CPI inflation factors and exchange rate average on January 31st of the given year.

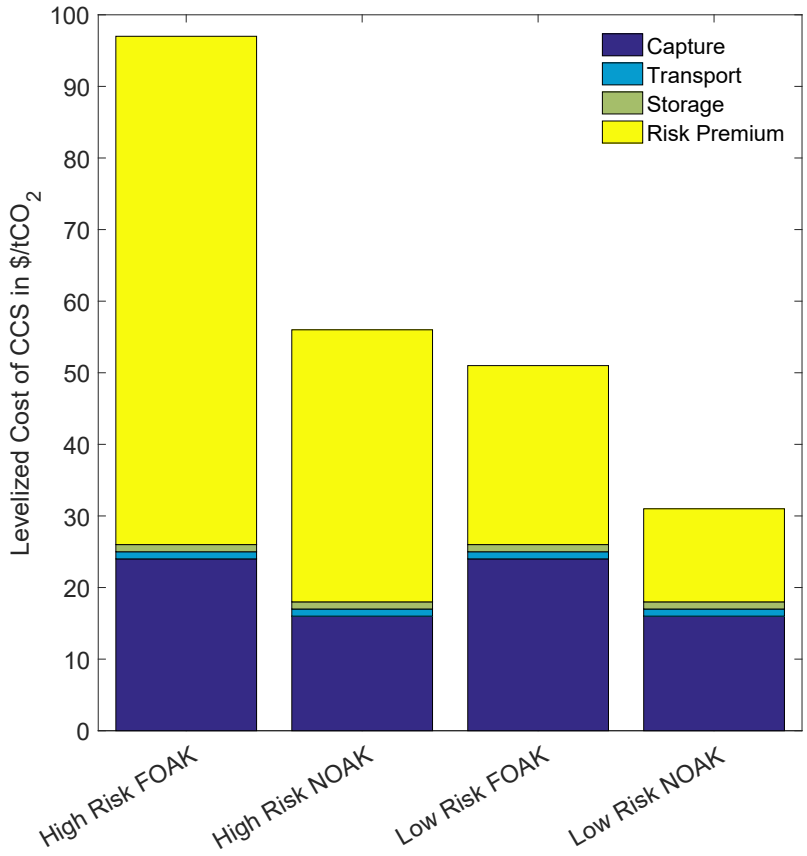

Figure 2.2: Estimated CCS levelized cost breakdown into risk premium, capture, transport and storage costs when CCS is considered either a high risk investment (at 20% IRR to investors) or a lower risk investment (at 10% IRR to investors) at FOAK cost level or NOAK cost level assuming 10% learning rate to reach gigatonne-scale CCS deployment.

willing to bear the cost of CO_2 capture as they are less likely to be first to be phased out with regulations on emissions[15].

Figure 2.2 shows that, most importantly, the proportion of cost attributed to the risk premium is lowest at 42% for Low Risk NOAK CCS and highest at 74% with High Risk FOAK CCS. Hence, the cost reduction attributed to reducing perceived risk is more significant than the value attributed to technological learning. At FOAK conditions going from high to low risk perception reduces the overall levelized CCS cost by 48% and at NOAK conditions by 44%, reducing the value of risk premium by as much as 65%. In contrast, when the investment is considered 'High Risk' the levelized cost reduction achieved through technological learning (FOAK to NOAK) is of 42% and when deemed 'Low Risk' is 38%, which is an effective reduction in the cost of CO_2 capture, transport and storage (i.e. only blue and green bars) of 28%. We may also consider that while CCS goes from FOAK to NOAK conditions the investment risk is associated with it transitions from 'High Risk' to 'Low Risk'. Hence, the combination of techno-

logical improvement and reducing perceived investment risk takes the LCOCCS from 97 \$/tCO_2 to 31 \$/tCO_2 or a 68% total annualized cost reduction.

From a UK perspective, 2016 IChemE report, "The Commercialisation of CCS: What needs to happen next?", stresses the importance of improving investor confidence and reducing perceived risk in order to reduce CCS cost[21]. The report describes several factors attributed to the perceived 'High Risk' of CCS to investors, which is then reflected in its cost[21]. A cross-chain risk for CCS arises from the need for reliable transport and storage infrastructure to meet the supply of CO_2 captured. This is because, while the contracts and equipment for CO_2 capture at a power plant are well understood and widely available, the large infrastructure requirements for pipelines suitable for CO_2 transport, equipment for CO_2 injection and monitoring are novel for the UK. Indeed, perceived investor risk may also vary by location and precedent. In North America, for example, CO_2 transport infrastructure and underground injection are well understood and developed as a result of decades of experience of using CO_2 for enhanced oil recovery. Hence, that cross-chain risk associated with large infrastructure costs required to develop CO_2 pipelines and ensure the availability of appropriate storage sink development, will not exist. Meanwhile, in areas of the US where CO_2-EOR has been deployed for decades, the investment risk will initially be associated with the ability to capture CO_2 at low cost[19,56].

Liability over the CO_2 as it moves from the capture plant to transport network and storage reservoir also poses a cross-chain risk to CCS in managing the risk of leakage[20,21,57]. The cost and risk of a first mover project will also be higher than the next because of the oversized infrastructure developed to meet additional demand from the next project, which contributed to the cancellation of the UK CCS competition projects in 2015, White Rose and Peterhead[19,21,57]. Other attributable risks to CCS include the lack of clear and long-term policy and market for CCS and a tainted public perception as a result of costly projects [6] or canceled projects [7][3,8,58,59]. In the IChemE report, Hackett argues that putting in place policy mechanisms and government support to reduce these risks and improve investor confidence will significantly reduce CCS cost and improve deployment with private sector actors.

Hence, it is critical to recognize that focusing solely on technological innovation (*e.g.* through improved solvents for absorption of CO_2) for CCS cost reduction may not be as fruitful as commercial innovation.

[6] Kemper County CCS project is billions of dollars over-budget[58]

[7] Over 40 canceled CCS projects globally today[8], including the cancellation of EU-led initiatives to promote CCS through the NER300 and the cancellation of the UK CCS competition in 2015[3,59]

2.4 Public sector role in CCS risk reduction

This work has shown that reducing perceived investor risk may be most significant in reducing the cost of CCS and boosting its deployment. The government and public sector have a key role to play in driving this risk reduction. The Oxborough report suggests having government owned transport and storage (T&S), which would help reduce some or all of the cross-chain risk of CCS by assuring the availability of adequate T&S infrastructure to meet CO_2 capture demand and eliminating the issue of long-term CO_2 liability since this would be taken on by government[57]. Fully government owned CCS followed by its subsequent privatization, as suggested in the Oxborough report[57], could completely eliminate the initial cross-chain risk that comes with first mover projects and the burden of oversized T&S infrastructure by the private sector. In contrast, Hackett suggests that the government can reduce this risk by acting as a 'loan guarantor' or 'insurer of last resort', *i.e.* guaranteeing liability over the CO_2 in case of lack of CO_2 transport and storage availability[21].

Having government secure a predictable revenue stream for CCS, to ensure a positive return, could also help to reduce perceived investment risk. This could be through a CO_2 tax credit for example, similarly to the US 45Q bill that rewards CO_2 storage and usage[60–62], through a contract for difference (CfD) that rewards CCS deployment as a low carbon technology in the UK[3,20,21]. Furthermore, similarly to the implementation of landfill regulations on waste in the UK or flue gas desulphurisation on power plants in the US, regulation that imposes a limit on a power plant's CO_2 emissions will reduce an investor's decision to either investing in CCS or stranding the asset[20]. Drawing from the way the storage of radioactive waste in the nuclear power sector was handled in the UK, the transparency of site selection and improved understanding of CO_2 storage reliability and location through public engagement and outreach are also key to reducing perceived CCS risk[19,20]. Finally, governments can also provide schemes to benefit over-sized projects and boost economies of scale for larger shared infrastructures, paving the way for future deployment, in order to reduce the capital cost burden of capture and T&S infrastructure fueling investor's risk perception of CCS[20,21]. Efforts to quantify the value of such solutions, better understand and reduce this perceived risk, are explored in the following chapters of this thesis.

2.5 Contributions made

In this work, a fully transparent methodology for assessing the levelized cost of CCS was developed using a well-understood economic model, the CAPM. The

CAPM is used to establish a clear relationship between the assumed systematic risk (β) of an investment in CCS and the required return for an investor. The value of required rate of return then translates into a capital recovery factor (CRF), the metric used to levelize (or annualize) the cost of a technology and obtain a cost per metric tonne of CO_2 avoided. The aim of this was then to quantify the risk proportion of the CCS cost by measuring it against the cost obtained as a result of a 'risk free' return on investment and CRF. Through this analysis, it was demonstrated that, depending on the level of technological learning achieved, the proportion of the levelized cost of CCS associated to financial risk can range from 40% to 75% of the total cost of CCS on a $\$/tCO_2$ basis. In fact, reducing the required rate of return by 50% (from 20% IRR to 10% IRR) can reduce the levelized cost of CCS by as much as 47%. Meanwhile, reducing the capital cost of CO_2 capture by 50% as a result of technological learning, can reduce the levelized cost of CCS by 38% to 42% depending on the assumption on risk. Combining both effects - risk reduction and technological learning - this analysis shows that the cost of CCS, on the two extremes, can start at $97\$/tCO_2$ and be driven down to $32\$/tCO_2$.

This work is the first to provide such a clear and simple quantification of the value of risk on the cost of CCS, proving that financial risk is a key driver of high CCS cost. Hence, measures to reduce this financial risk are very important in order to render CCS investment more appealing and path the way for its large-scale deployment. The methodology established here is easily replicable and can be followed to establish the relationship between any assumption on systematic risk of CCS and the levelized cost of CCS.

Chapter 3

Can CO_2 enhanced oil recovery act as a catalyst for gigatonne-scale CCS deployment?

The work presented in this chapter aimed to quantify the impact of coupling CCS with CO_2-EOR on the actual deployment level of CCS on a large scale. Also, to what extent and by how much, external economic factors (*e.g.* oil price, CO_2 tax, R&D, subsidies or grants) could influence the level of CCS deployment. This chapter describes the methodology and characterization of the iterative investment model (MIICE) developed to answer these questions while maintaining a high level of detail into the CCS and CO_2-EOR process.

The majority of the work presented in this chapter was conducted during an 8-month research visit at Stanford University in the Energy Resources Engineering Department with Assistant Professor Adam R. Brandt and in collaboration with Dr. Mohammad Masnadi. Key contributions were provided by Kurt House, Visiting Professor at Stanford University, as well as supervisors Niall Mac Dowell and Samuel Krevor at Imperial College. This work is also presented in Kolster et al. 2017 published in Energy & Environmental Science (`http://pubs.rsc.org/en/content/articlehtml/2017/ee/c7ee02102j`) and the open-source model of iterative investment in CCS with CO_2-EOR (MIICE) developed can be downloaded here (originally coded in MATLAB and transcribed into GNU Octave, a free software equivalent to MATLAB): `http://doi.org/10.1039/C7EE02102J`[55].

Given the availability and expertise at hand while conducting this work at Stanford, a majority of the assumptions made are based on North American data

and cater mostly to the region's experience.

3.1 CCS and CO_2 enhanced oil recovery

Countries and regions that have been most pro-active about the deployment of CCS, including the USA, Canada, UK, Norway, China and Australia for example, often quote the reliance of CCS on using CO_2 for enhanced oil recovery (CO_2-EOR) as being a key trigger for improving the economics of CCS[4,18,63]. In countries like the USA, where infrastructure for CO_2 transport and underground injection is already in place, this reliance is of particular relevance and has been vocalized by policy makers with the 45Q bill providing tax credits of 50\$/tCO_2 and 35\$/tCO_2 for CO_2 sequestration and use respectively[60,61]. In the power sector, the two CCS plants that are operational today, capturing a total of 2.4 MtCO_2/year (Saskpower Boundary Dam in Saskatchewan, Canada and Parish Petra Nova CCS in Texas, U.S.A.)[53,54,64–68], both sell their CO_2 for use in EOR. In this chapter, an open-source technology investment model is built to examine whether CO_2-EOR might actually serve as a "catalyst" to reduce long-run costs of CCS and induce gigatonne-scale deployments.

During CO_2 enhanced oil recovery (CO_2-EOR) supercritical CO_2 is injected into the pay zone [1] of an oil reservoir to increase oil production. In the most typical approach, the injection occurs after more conventional production techniques have been applied, having recovered 30% - 45% of the original oil in place (OOIP)[69]. The CO_2 acts as a solvent, mobilizing previously trapped isolated pockets of immobile oil, while also swelling and reducing the viscosity of the fluid[70,71]. Combined, these effects can boost oil recovery by several percentage points over what is possible with conventional production, typically adding another 5% - 20% recovery from the OOIP. Carbon dioxide EOR has been conducted primarily in North America since the 1970s due to abundant sources of natural CO_2. In recent years, a lack of cheap CO_2 supply, 'low' oil prices (with WTI[2] crude prices averaging at 43 - 50 \$/bbl from 2015 to 2017 included[72]), and a lack of strong universal incentives for CO_2 usage (e.g., a widespread CO_2 usage credit) has stymied new projects. From 2012 - 2014, 11 new miscible CO_2-EOR projects were reported in the US, while 2014 - 2016 only saw 3 new projects. Approximately 80% of current CO_2 used for EOR comes from natural sources of CO_2 instead of abundant anthropogenic sources[73].

[1] Pay zone refers to the part of the reservoir that contains extractable hydrocarbons

[2] WTI (or West Texas Intermediate) is the price of crude sourced from mostly U.S. fields while Brent crude is that of crude produced from fields in the North Sea. The two prices are usually very similar with Brent crude typically priced slightly higher due to crude density and transportation costs involved.

In 2010, Herzog[74] challenged how to get CCS deployment from the megatonne-scale to the gigatonne-scale. The study highlighted the need for a clear business model for large scale investment and the uncertainty around sufficient storage capacity for gigatonne-scale CCS deployment. However, with the increasing interest and literature around CCS alone, CCS with bioenergy (BECCS) and CCS with CO_2-EOR across the globe, it is clear that there is scope for upscaling CCS[3,9,75–80]. Storage capacity and availability for CO_2, in depleted oil reservoirs with EOR or in saline aquifers, has also since been clarified and studied extensively[25,31,39,81,82].

The utilization rate of CO_2 for EOR affects net emissions abatement. Life cycle assessments (LCAs) have been conducted on CO_2-EOR, with a wide range of results[25,83–87]. For CO_2-EOR, the LCAs differ most significantly on the accounting treatment of produced oil. An assumption of *additionality* assumes that producing oil via CO_2-EOR will add to the global supply of oil and therefore LCAs should include emissions from the combustion of the resulting petroleum products (*i.e.* diesel fuel). Additionality results in CO_2-EOR with net positive emissions[25,84]. The alternative assumption of *displacement* assumes that EOR-derived oil displaces oil that would have come from another source. Displacement results in a net reduction in emissions from CO_2-EOR[85,86]. ARI and Melzer Consulting Group found total CO_2 emissions from CO_2-EOR operations are of 470 $kgCO_2$/bbl of oil produced and 40 $kgCO_2$/bbl of oil produced when excluding refining and end-use of crude oil recovered[25]. Cooney et al. studied the gate-to-gate GHG emissions from CO_2-EOR, drawing the boundary around the EOR facility, which excludes emissions associated with the source of CO_2 and end-use of crude oil. They found that for advanced EOR operations, the GHG emissions are between 59.2 and 99.5 $kgCO_2e$/bbl of crude[88]. Such ranges in emissions to be considered for the life cycle analysis of CO_2-EOR activities demonstrate the complexity of accurately assessing environmental impacts.

Commercial CO_2-EOR practice does not emphasize long-term storage; at end of pattern life CO_2 is often produced from the well to induce last oil production, then CO_2 is recycled for other oil fields, resold, or vented. This does not reflect the ability to store CO_2 in depleted oil fields[56]. Scott et al. 2015[89] categorize storage with CO_2 EOR as "easy to manage and inherently safe" due to the volume (and pressure) replaced in the process (i.e. volume of produced oil replaced by equivalent volume of dense phase CO_2 injected), comparing it to saline aquifer storage which is "complex to manage although expected to be secure" [89].

This work presents efforts to simulate CCS deployment to determine the conditions that would result in gigatonne-scale CCS deployment. This work presents one of the first detailed studies to assess the commercial value of CCS

with CO_2-EOR in this new and unfavorable economic environment. It does so by developing a novel and open-source model of iterative investment in CCS with CO_2-EOR (MIICE) that takes into account the techno-economic dynamics of CCS and CO_2-EOR and assumes a large variety of well characterized oilfields in order to discuss what technological, economic, and regulatory advances are needed for CO_2-EOR to accelerate gigatonne-scale CCS deployment. One of the major novelties of this work is the dynamic approach to assessing CCS coupled with CO_2-EOR whereby costs and revenue streams change over time as a result of changing prices and accumulated experience, modelled as technological learning or learning-by-doing. Another novel aspect of this work relies on the fact that here a dynamic production of oil and CO_2 is considered rather than using a constant ratio of CO_2 injected to oil produced. Another novelty lies in the way CO_2-EOR operations are modelled. While the model does not include a reservoir simulation study for each oil field considered, the model does includes extensive detail on thousands of potential fields, *i.e.* characteristics such as permeability, porosity, depth, initial water saturation and area, which determine a unique production schedule for each project, and field development parameters. Altogether, and with the randomized nature of field parameter selection incorporated in the model, this strives to replicate an uncertainty in real-world CO_2-EOR dynamics.

In the rest of this chapter, first, the methodology is outlined, including the development of the techno-economic CCS model and the modelling of EOR projects. Next, five indicative scenarios are described and explored in detail, and sensitivity cases that explore key drivers of model outcomes are outlined. Results for the five indicative scenarios are then presented, as well as sensitivity plots illustrating single-variable and multi-variable explorations of outcome. The chapter is concluded with qualitative lessons learned and points for further work.

3.2 Model of iterative investment in CCS with CO_2-EOR (MIICE)

3.2.1 Methodology overview

First, an overview of the basic MIICE (model of iterative investment in CCS with CO_2-EOR) work-flow is provided (Figure 3.1). MIICE begins by generating a candidate world containing illustrative oil fields. In the initial model year, potential EOR projects in these oil fields are evaluated given the oil price, CO_2 tax, and cost of CO_2 capture in that time period. Projects with positive net present value (NPV) are developed in accordance with standing limits on

investment rate. A positive NPV is also defined by an investment's internal rate of return (IRR) being greater than the discount rate assumed. The simulation then steps forward, updating the list of potential EOR fields, removing those with developed projects, simulating technological learning, and tracking CO_2 stored and oil produced from operating projects. The remaining potential projects are re-evaluated given updated conditions (e.g., updated CO_2 tax and oil price, learning-adjusted cost of CO_2 capture). The model continues year-by-year until the simulation period is complete.

The baseline assumptions made for key model parameters are listed below in Table 3.1. The study boundary includes capturing, transporting and injecting CO_2 and producing oil via EOR. Our boundary excludes power plant investment (i.e., assumes a separate stakeholder investment in a new power plant or continuation of an existing power plant). NPV is calculated by performing a discounted cash flow analysis of revenues from oil production and CO_2 storage. Negative cash flows include CO_2 tax for CO_2 that is not captured, leaked in EOR, or not stored in field operations, as well as variable and operating and maintenance (O&M) costs for CO_2 capture, transport, storage and EOR management. All cash flows are adjusted for inflation. Initial upfront capital investment includes all project inputs, amortized over project lifetime/investment horizon of 30 years with a fixed charge factor (also referred to as capital recovery factor)[15], of 0.118 [1/y]. MIICE is initiated in year 2016 and runs to year 2050. Though based largely on North American data, particularly in considering CO_2-EOR field data and operation, the model is assumed to be geographically neutral.

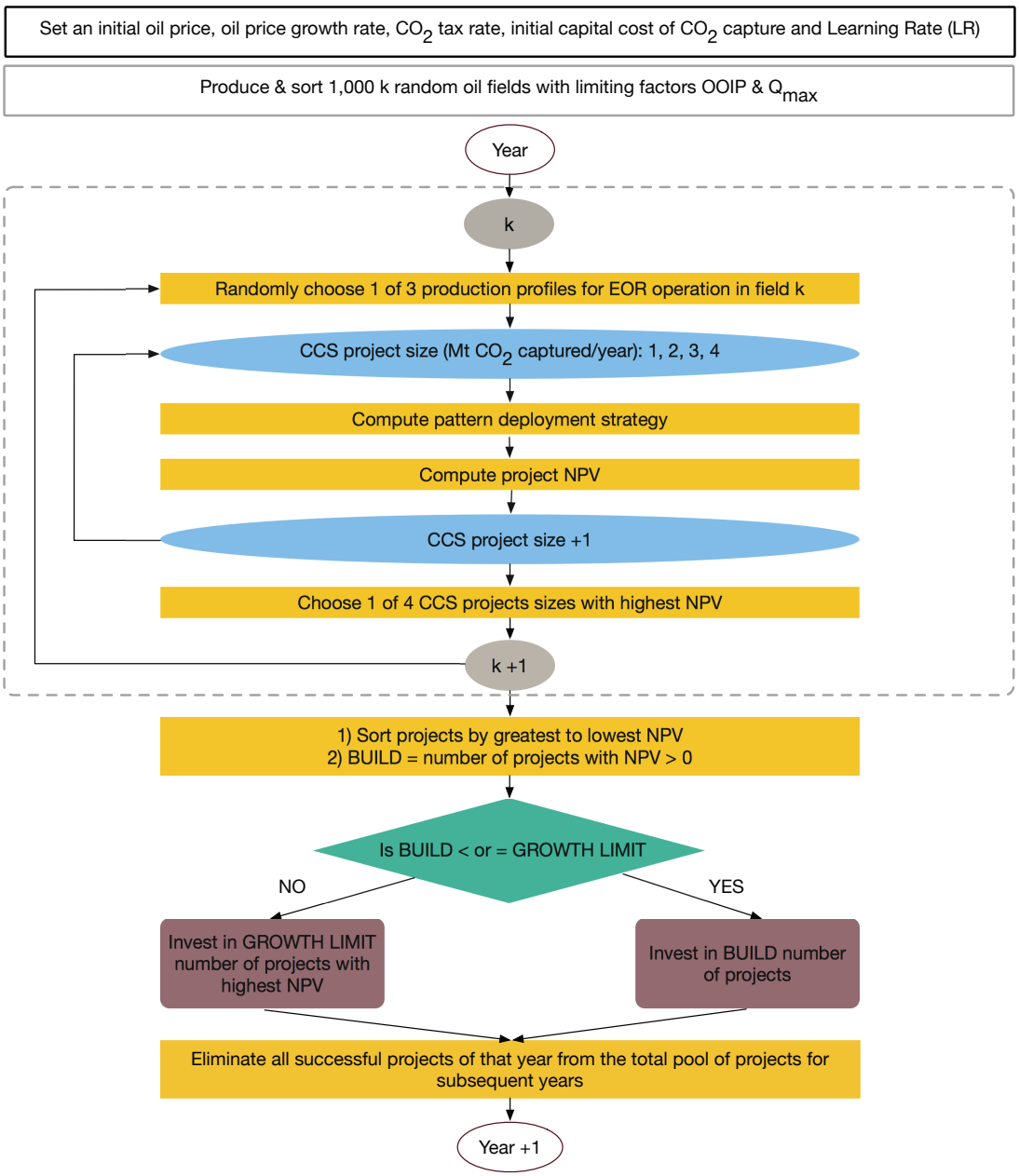

Figure 3.1: Flow diagram representing the process and economic evaluation mechanism adopted in MIICE. GROWTH LIMIT refers to the industry growth rate ceiling. The dotted line focuses on pattern deployment strategy and illustrated in more detail in Figure A3.

Table 3.1: Parameters used to compute net present value (NPV) of a CCS with CO_2-EOR project

Parameter	Value	Assumption/Reference
Project lifetime	30 years	Model based assumption[16]
Nominal discount rate (NDR)	15 %	High risk fossil fuel projects[50]
Currency value	2016 US$	All costs are adjusted for constant $
Equity	100%	High risk fossil fuel projects[50]
Yearly inflation rate	3.3%	Model based assumption[16]
Fixed charge factor	0.1185	Calculated based on NDR and inflation rate
Tax rate on oil revenue		North America based oil production practice[29,90]
Royalties	15%	Will depend on state legislation (W. Texas based[90])
Severance tax	2%	Percentage of royalty tax (W. Texas based[90])
Ad valorem tax	1.5%	Percentage of royalty tax (W. Texas based[90])
Corporate tax on CO_2 storage revenue	0%	Unclear on the taxation scheme of a credit
Limit on technological learning	First 1000 projects	Study based assumption

3.2.2 CO_2 enhanced oil recovery

The model initially generates 10,000 possible oil fields based on randomized combinations of characteristics with ranges derived from a database of existing CO_2-EOR projects[91] (see Table 3.2). The model eliminates nonsensical combinations and keeps 1,000 fields randomly from the population of feasible fields. By using a database of existing CO_2-EOR projects, we assume that similar fields will be chosen going forward. The database provides characteristic values for reservoir permeability, porosity, depth, and field areal extent. Distributions are drawn to include 85% of database observations (see Appendix Figure A2). These are limited to fields in which miscible EOR is conducted as this is most widely applied and understood, achieving better recovery than immiscible EOR[69,92]. Initial water saturation and net pay thickness[3] are not tabulated in the database, so representative values are obtained from literature and personal communications[93–96].

Table 3.2: Characteristic values for potential CO_2-EOR fields based on existing data from the Oil & Gas Journal EOR Survey and field data of miscible EOR operations[91,97].

Characteristic	Lower Bound	Higher Bound	Unit
Permeability	1	110	milliDarcy
Porosity	5	30	fraction
Reservoir depth	914	3140	meters
Reservoir area	8,094,000	80,920,000	m^2
Initial water saturation	15	75	fraction
Net pay thickness	10	50	meters

The CO_2-EOR industry has historically been limited by a lack of low-cost CO_2[70]. Operations have therefore sought to minimize fresh CO_2 purchased. This

[3]Net pay thickness: the thickness (one dimensional) of the targeted hydrocarbon rich region of the oil field

is manifested by CO_2 recycling and alternating injection of CO_2 with water *i.e.* water-alternating-gas (WAG). WAG is common in the CO_2-EOR industry and is said in some instances to improve the contact between CO_2 and oil in the reservoir[25,70,98], while others find that WAG does not necessarily improve the recovery of oil compared to continuous CO_2 injection[99–102]. In a world of emissions limits, continuous CO_2 injection and limited CO_2 recycling could be incentivized[103]. MIICE assumes operations and costs for continuous CO_2 injection only. For a limited project and field lifetime of 30 years, as assumed here, including WAG would change project economics by reducing CO_2 storage. Hence, MIICE provides an upper bound of sequestration potential for CO_2-EOR.

Fluid properties for CO_2 and oil are functions of multiple quadratic equations that would significantly increase the computational intensity of the model. Hence, constant fluid properties are assumed for CO_2 and oil. The hydrostatic pressure gradient is equivalent to the US Gulf coast at 10.52 kPa/m (0.465 psi/-foot)[104], the temperature gradient assumed is 30°C/km and surface temperature is 15°C[105]. CO_2 density and viscosity are estimated at the median of the reservoir depth range of 2026 m as 614.08 kg/m^3 and 47.8 microPa.S. The minimum miscibility pressure (MMP) sets a minimum CO_2 injection pressure (key for miscible CO_2-EOR). Average MMP is calculated using the Cronquist correlation (see Equation 3.1)[34]. Tank oil gravity of 37 API and oil formation volume factor at initial reservoir conditions of 1.3 are assumed[103,106]. These parameters are summarized in Table 3.3.

$$MMP = 15.988 \times T(0.744206 + 0.0011038 \times MWC5) \tag{3.1}$$

with MMP: minimum miscibility pressure (psi), T: reservoir temperature (Farenheit) and $MWC5$: molecular weight of pentanes & heavier fractions of oil.

Oil production rates and CO_2 production rates are a function of cumulative CO_2 injected. Both are dimensionless variables normalized by hydrocarbon pore volume (HCPV). HCPV refers to the pore volume of the reservoir that is filled with hydrocarbons:

$$HCPV = Ah\phi(1 - S_{wi}) \tag{3.2}$$

where $HCPV$ is the hydrocarbon pore volume at surface conditions [m^3], A is Pattern area [m^2] h is net pay thickness [m], ϕ is Average field porosity [fraction] and S_{wi} is initial water saturation [fraction]. The original oil in place is defined as $OOIP = HCPV/\beta_{oi}$ where β_{oi} is the initial oil formation volume factor. Each

Table 3.3: Reservoir characteristics assumed and calculated in order to obtain fluid properties

Parameter	Value	Unit	Reference
Median reservoir depth	2026	m	[91]
Pressure gradient	10.52	kPa/m	[104]
Temperature gradient	30	°C/km	[105]
Surface temperature	15	°C	Assumption of study
Reservoir pressure (P)	21.3	MPa	Calculated
Reservoir temperature (T)	75.8	°C	Calculated
CO_2 density at reservoir P & T	614.08	kg/m^3	[107]
CO_2 viscosity at reservoir P& T	47.8	microPa.s	[107]
CO_2 fluid phase	Supercritical		[107]
Average reservoir oil gravity	37	API	[91]
MWC5	183.67	g/mol	[34]
Average MMP	17.6	MPa	Calculated
Formation volume factor	1.3	m^3/m^3	Assumption of study

field has a unique HCPV, which will determine its production rates of CO_2 and oil.

An injection pattern refers to the arrangement of production and injection wells for EOR. Multiple well arrangement injection patterns exist including two-spot, three-spot, five-spot, nine-spot and twelve-spot. These can either be centered around a producer (called normal) or an injector (called inverted). Here, MIICE assumes that all patterns are 5-spot inverted patterns with 1 injector and 4 producers as this is commonplace in CO_2-EOR practice[29,34,90,108]. As a rule of thumb each pattern has a surface area of 40-acres and on a field-scale it is assumed that the ratio of producers to injectors is 1.8:1, which corresponds to nine adjacent 5-spot patterns. This is assumed constant in current MIICE version. However, as more patterns are developed together, side by side, this ratio would decrease. This can be modified in MIICE (access here: `http://doi.org/10.1039/C7EE02102J`)[55].

Reservoir simulations are typically used to model the rate of oil production and CO_2 injection and production from a CO_2-EOR process in one given field using proprietary tools such as ECLIPSE and CMG. However, these require large and complex data inputs for model initialization, history matching and pressure dynamics[69]. Therefore, in order to allow for MIICE to be broadly applicable, the CO_2-EOR process is modeled with a set of normalized outputs from such simulations: relationships defining the cumulative production profiles of oil and CO_2 as a function of the cumulative CO_2 injected. Data profiles for cumulative production of oil and cumulative production of CO_2 as a function of cumulative CO_2 injected are obtained for 6 fields from literature[109]. Also, P10, P50 and P90 statistical results for a U.S.-based CO_2 EOR reservoir simulation were obtained[110]. Each of these profiles is fitted with eq. 3.3 for cumulative oil production and

eq. 3.4 for cumulative CO_2 production[69,111]. Cumulative production of oil as a function of CO_2 injection follows a logistic curve with fitting parameters a, b, c and d, while the cumulative production of CO_2 as a function of cumulative CO_2 injected follows an exponential curve with fitting parameters a^*, b^*, c^* and d^*. The corresponding profiles are presented in Figure 3.2. All production profiles quoted refer to CO_2-EOR operations after primary and secondary recovery including water flooding.

$$Q_{oil} = \frac{a}{1 + \exp(-b\,(Q_{CO_2in} - c))} - d \tag{3.3}$$

with Q_{oil} representing normalized cumulative oil production (1/OOIP) and Q_{CO_2in} representing cumulative CO_2 injection (1/HCPV). Also:

$$Q_{CO_2out} = a^* \exp(b^*(Q_{CO_2in} - c^*)) - d^* \tag{3.4}$$

with Q_{CO_2out} representing cumulative CO_2 production (1/HCPV) and Q_{CO_2in} representing cumulative CO_2 injection (1/HCPV).

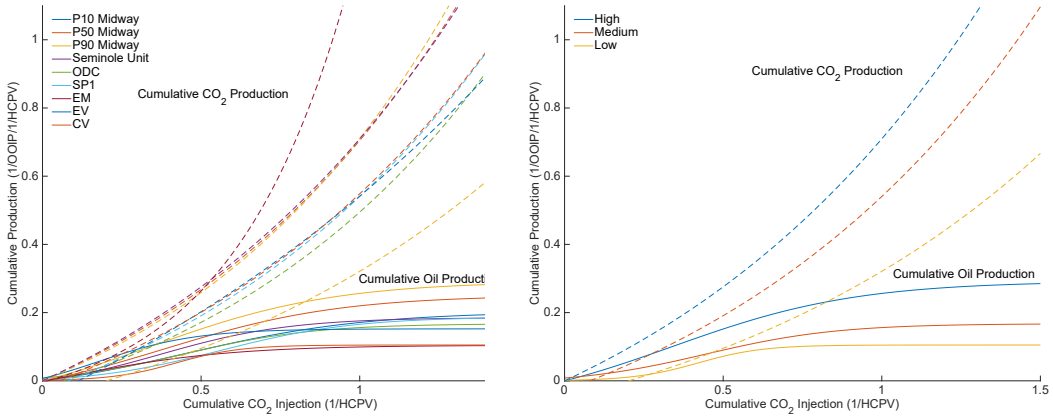

(a) (b)

Figure 3.2: Cumulative production of CO_2 (dash) and oil (solid) on a HCPV basis. (a) Reproduction of 9 empirical curves[109,110] (b) Low, medium, and high cases for simulation.

Three of the nine cumulative production profile pairs are used to represent low, medium and high oil recovery and CO_2 production cases (see Figure 3.2). The corresponding curve fitting parameters for low, medium and high oil recovery are given in Appendix Table A3. Each time the model assesses the economics of a CCS with CO_2-EOR project, a profile is chosen randomly. All patterns within one field follow the same profile and operations - CO_2 injection, production and storage rate, and oil productions rate - are modeled on a yearly basis. The model

assumes that during the lifetime of a field, CO_2 that is produced at one time step is recycled and re-injected into the field at the next time step. The recycled CO_2 is coupled with fresh CO_2 from the capture plant assumed to be distributed evenly into all open patterns. A total of 0.5 % of CO_2 produced is assumed to leak while the rest is recycled and re-injected. The rate of CO_2 storage is taken as the difference between the incremental CO_2 injected and the incremental CO_2 produced. The HCPV and OOIP, unique to each field, determine the total CO_2 stored and oil produced at each pattern.

Each field has an area A and a maximum number of patterns that can be deployed. At every field iteration, the model calculates the minimum amount of patterns p_{min} needed for injection of all the fresh CO_2 from the capture plant at a pressure differing by a safety factor f_{oil} of the maximum allowable injection rate, Q_{max}. Q_{max} for each well within a pattern is defined using Darcy's law for radial flow:

$$Q_{max} = \frac{2\pi kh(\Delta P)}{\mu \ln \frac{r_e}{r_w}} \tag{3.5}$$

with Q_{max} representing the maximum volumetric flow rate at the injection point [m^3/s], k, the average reservoir permeability [m^2], h, the field thickness (net pay thickness) [m]. ΔP, the pressure differential [Pa], μ the viscosity of CO_2 [Pa.s], $r_e$the drainage radius assumed to be 1000 feet (304.8 m), and $r_w$the wellbore radius assumed to be 6 inches (0.1524 m).

Production of oil progresses along the cumulative curve profiles, and injection ceases once the following condition is met: $Q_{oil}/Q_{CO_2in} \leq 0.1$. After a set of patterns p_{min} cease injection, a set of new patterns is opened, repeated until field area or the project duration limit is reached. f_{oil} is chosen so that the field size can process 30-years worth of CO_2 captured. This will vary with each project size and for each field coupling considered. The process is described in Appendix Figure A3. The fracture gradient assumed is 0.926 psi/ft and hydrostatic gradient is 0.465 psi/ft[112]. Also, the injection pressure is set never to exceed 80% of fracturing pressure.

The model computes well costs, CO_2 costs, and operating & maintenance (O&M) costs. Capital costs for CO_2-EOR include well design and installation of production and injection wells, drilling and completion (D&C), well conversion for CO_2-EOR operation, all of which are a function of the depth of the field. Capital costs also include CO_2 separation units, a function of the maximum recycling rate, and distribution infrastructure. Redevelopment of old fields is assumed, converting 3/4 of injection and production wells previously used for primary production and WAG, and only 1/4 of wells are assumed to be new[75,90]. Operating costs included are periodic O&M costs, which are a function of field depth, oil and water lifting costs, which are a function of oil price, and CO_2 recycling

O&M, a function of the initial oil price and CO_2 recycling volume. Monitoring cost is assumed at 2 M$/y per field[33]. These assumptions and values are clearly outlined in the MIICE script (`http://doi.org/10.1039/C7EE02102J`[55]). Qualitative details of the capital and operating cost parameters assumed for CO_2-EOR operations in MIICE are outlined in Tables 3.4 and 3.5. Detailed cost equations are provided and can be accessed in MIICE[55].

The model assesses four project sizes for each CO_2 capture plant: 1, 2, 3 and 4 $MtCO_2$/year. These sizes encompass current and planned CCS projects (current 1-2 $MtCO_2$/year from 100-300 MW coal plants, prospective 3-4 $MtCO_2$/year from coal plants of 450 - 600 MW[54]).

Table 3.4: Capital cost parameters and assumptions for CO_2-EOR with detailed equations presented in the MIICE script.

Cost Parameter	Function of	Assumption(s)	Reference
CO_2 processing & lease equipment			
Field Production equipment	Depth of site	L&A regression cost model, on a per pattern basis	[90,108] converted from 2004 US$
CO_2 Recycling plant	Maximum CO_2 injection rate	Capital cost of a recycling facility of sufficient size that can separate CO_2 from produced fluids at maximum production & injection rates	[29,93,113–115] converted from 2014 US$
CO_2 Trunkline cost	Fixed cost	Per pattern	[29]
CO_2 Transport & Distribution Cost	Trunkline distance, cost of trunkline	Per pattern basis, includes fixed and variable costs associated with transporting the volume of CO_2 from regional pipeline to EOR site as well as equipment required for on site distribution (from wells to recycling facility)	[29,93,113–115] converted from 2014 US$
Pattern equipment cost			
Production well equipment cost	Depth of site	New well cost, on a per pattern basis, based on L&A regression equation, includes tangible and tangible costs associated with production well equipment	[90,108] converted from 2004 US$
Injection well equipment cost	Depth of site	New well cost, on a per pattern basis, based on L&A regression equation,includes tangible and tangible costs associated with injection well equipment	[90,108] converted from 2004 US$
Drilling & Completion cost (D&C)	Depth of site	New well cost, on a per pattern basis, based on L&A regression equation, includes tangible and intangible costs associated with on-site drilling and completion phases for production & injection wells (e.g. casing, cementing, plugging)	[90,108] converted from 2004 US$
Production well work-over cost	Fraction of new well cost + D&C cost	3/4 of wells are worked over	[90,108] converted from 2004 US$
Injection well work-over cost	Fraction of new well cost + D&C cost	3/4 of wells are worked over	[90,108] converted from 2004 US$

Table 3.5: Operating cost parameters and assumptions for CO_2-EOR with detailed equations presented in the MIICE script.

Cost Parameter	Function of	Assumption(s)	Reference
Periodic O&M Costs	Depth of field, on a per pattern basis	Based on L&A regression model,includes periodic well work-overs and other surface/subsurface repairs	[90] converted from 2004 US$
Liquid Lifting Costs	Stock Tank Barrels of liquids processed (oil + water)	Typically provided by the user, on a per pattern basis, includes operating costs of pumping, managing and distributing liquids produced	[90,93] converted from 2004 US$
CO_2 Recycling O&M	Initial Oil Price & CO_2 volumetric flow rate	CO_2 density at STP 1.977 kg/m3 used to convert to surface conditions and cost given on a per pattern basis	[93] converted from 2004 US$
General& Administrative cost	Fraction of Periodic O&M Costs and Liquid Lifting Costs	Per pattern basis, includes staff salaries/wages, insurance, accounting, consulting, management and record keeping	[29,93] converted from 2014 US$
CO_2 Monitoring cost	Fixed cost assumed	Cost applied to a whole EOR site regardless of pattern number, 2010 USD 2 Million	[33] converted from 2010 US$

3.2.3 Cost of carbon capture and transport

CO_2 capture is the most cost intensive part of CCS and contributes 60% to 85% of total costs[15,17]. Actual costs of CCS plants have been higher than estimated first-of-a-kind (FOAK) costs[116]. Learning is initialized based on an existing CO_2 capture capacity on power plants of 2.4 $MtCO_2$/y.

In order to initialize the learning model, introduced in the next section, upfront capital cost as a function of capture capacity is needed and measured in M\$/$MtCO_2$/y.

In 2015, Rubin et al.[15] reviewed CCS costs and found current values for overnight capital cost of post-combustion capture of 242-453 M\$/$MtCO_2$/y. They find that older studies overestimate CCS costs because newer cost estimates use more-efficient proprietary amines. The study does not make a clear distinction whether FOAK or NOAK costs are estimated. The most recent real project of post-combustion capture on a coal-fired power plant had capital costs of 714 M\$/$MtCO_2$/y (Petra Nova project cost US\$ 1 billion to capture 1.4 $MtCO_2$/y)[64,65]. These are summarized in Table 3.6.

CCS prospects rely on its application to various types of thermal plants (e.g. coal-fired and gas-fired) as well as industrial plants (e.g. cement production, iron and steel production, hydrogen production) and costs will differ depending on plant application. CO_2 capture applications to industrial processes with high concentrations of CO_2 will have a substantially lower cost than when applied to power plants[117–119]. Therefore, a range of initial costs is explored, between 200

Table 3.6: Real-time and literature-based capital cost values of amine-based CO_2 post-combustion capture plants coupled with supercritical pulverized coal fired plants adjusted to 1 $MtCO_2$ captured per year

Reference Source	Capital Cost Value (2016 US$/$MtCO_2$ captured)	Information & Assumptions
Boundary Dam CCS[54]	$1.5 billion	Successfully deployed project, over-budget
Petra Nova Parish CCS[53,64–66]	$714 million	Successfully deployed project, on-budget
Rubin et al. Study[15]	$326 million	Literature based study for new build power plants with CCS
Adjusted SRCCS study[15]	$270 million	Literature based study conducted in 2005[5] for a new build power plant + CCS
Worley Parsons Report[16]	$209 million	Literature based study for a new build power plant + CCS

M$ and 714 M$/$MtCO_2$/y.

Power costs are wholesale electricity prices of US$ 39.67/MWh (Intercontinental Exchange (ICE) of the weighted average electricity cost for 2014-2016[120]). O&M costs include both variable and fixed O&M costs for labor, material and equipment[16,28].

For the range of capital costs considered, given a fixed charge factor of 0.1185, this is equivalent to an initial annualized cost of capture ranging from $100/t$CO_2$ to $39/t$CO_2$.

Capital and operating costs of transporting 1 - 4 $MtCO_2$/year are included[121]. Pipeline dimensions for transport are derived from NETL[122] and all pipelines are assumed 100km (62 miles) long. These are summarized in Appendix Table A2.

3.2.4 Technological learning and industry growth

The model assumes that technological learning reduces capital costs as cumulative CCS deployment increases. CO_2 capture infrastructure is assumed to decline in costs, while pipeline transport and EOR costs are assumed not to decline due to decades of experience with EOR. Learning is assumed to cross regional boundaries. The Wright progress curve, also defined as "learning-by-doing", has been established since the 1930s[123], and is used here as applied to CCS[124–127]:

$$C = C_i \left(\frac{Q}{Q_i} \right)^{-b} \tag{3.6}$$

with C, the updated capital cost, Q, the updated cumulative capacity installed, C_i, initial capital cost, and Q_i the initial capacity installed. The learning vari-

able b is defined as $b = -\log(1 - LR)/log(2)$ where LR is the cost reduction per doubling.

Learning rates are uncertain. Observed learning resulted in the second commercial CCS plant costing 50% less than the first[53,54]. Such learning is unlikely to continue: the high cost of capital of Boundary Dam have been explained with circumstantial, case-specific factors including high steel prices during the time of construction and dis-economies of scale due to the plant size being smaller than what it was designed for[116]. Circumstantial costs will include location of plant build, better company practices and market fluctuations affecting the price of materials. Literature on CCS learning rates have mostly assimilated it to large-scale chemical plants that take years to build, such as flue gas desulphurization and have assumed ranges of learning rates from 3% to 14%[125]. This differs from smaller scale products' technological learning that can be produced in larger quantities at a faster pace and have seen technological learning rates of over 20%, such as solar PV.

The model also includes a set of growth rate limitations. New energy technologies see rapid exponential growth until the technology reaches "materiality" (previously defined as a 1% market share)[128]. Here, materiality is defined as 100 $MtCO_2$/year installed capacity. Pre- and post-materiality growth rate limits are assumed to be 25% and 10%, respectively[129]. Furthermore, it is assumed that only one project can be commissioned per year for the first five years (representing slow growth until wide-spread confidence).

3.3 Scenarios and model analysis

3.3.1 Five world scenarios

First, five 'world' scenarios are created(see Table 3.7). The 'Base Case' world assumes the following: (1) a constant inflation-adjusted price of oil at its 2016 peak of \$55/bbl[130]; (2) CO_2 tax of \$25/tCO_2 starting in 2016 and growing by \$1/year (3) a learning rate $LR = 10\%$, (4) initial overnight capital cost is \$600 Million/$MtCO_2$/y. The 'Climate Action' world adopts a CO_2 tax of \$100/tCO_2 in 2016 which increases by \$2/year. The 'High Oil' world has a constant inflation-adjusted oil price of \$110/bbl (similar to 6DS scenario in[33]). In the 'Depleting Resources world', oil starts at inflation-adjusted price of \$55/bbl and increases at a rate of 2%/year. Finally, the 'Forward Learning' world assumes effective R&D for CCS so LR is 14%, similar to that of flue gas desulphurization[125–127].

Table 3.7: Key variables assumed for each of the five world scenarios

World Scenario	Price of oil in 2016 \$/bbl	Tax/credit on CO_2 in 2016 \$/tCO_2	Tax rate increase \$/tCO_2/year	Learning rate	Oil price growth rate (inflation adj.)
Base Case (BC)	55	25	+1	10%	0%/y
Climate Action (CA)	55	100	+2	10%	0%/y
High Oil (HO)	110	25	+1	10%	0%/y
Forward Learning (FL)	55	25	+1	14%	0%/y
Depleting Resources (DR)	55	25	+1	10%	2%/y

3.3.2 Single-parameter sensitivity analysis

A single-parameter sensitivity analysis to Base Case assumptions is performed. Cumulative CCS capacity investment achieved by 2050 is used as the comparison variable. Sensitivity parameters include: inflation rate, nominal discount rate, cost of electricity, initial capital cost of CO_2 capture, capital cost per CO_2-EOR pattern and CO_2 capture rate per power plant. Each of these are varied by $\pm 10\%$ to assess their impact. Assumptions of industry growth limitations are also explored as well as the use of near-site saline aquifer storage at \$60/tCO_2 or \$20/tCO_2, CO_2 tax/credit scheme, project debt-to-equity ratios and responsibility for the CO_2 transport system. Finally, the sensitivity of MIICE to the MATLAB randomization seed for EOR field generation is assessed.

3.3.3 Exploration of key variables

In addition to the single-parameter sensitivity analysis described above, we iterate through combined ranges of key parameters. These include initial oil price, a CO_2 credit/tax rate, learning rate, FOAK capital cost, and oil price growth rate. A total of 36,036 combinations are evaluated. Ranges of variables are:

- Initial price of oil from \$45/bbl to \$140/bbl.
- CO_2 tax from \$0/tCO_2 to \$200/tCO_2.
- Initial capital cost of capture from 714 M\$ to 200 M\$ for every 1 MtCO_2 captured/year.
- Learning rate from 0.00 to 0.20.
- Growth rates of oil at 0%/y, -2%/y, and 2%/y.

3.4 Results and discussion

3.4.1 Five world scenarios

Figures 3.3, 3.4, 3.6 and 3.5 present outputs from the five world scenarios. CO_2 storage and oil production values are given as cumulative values over a projects' 30-year duration and presented in the year that a project receives investment (see Appendix Figure A4).

Figure 3.3 shows the cumulative CCS capacity investment made in each of the five worlds (bottom) and the resulting CO_2 capture cost decrease (top). All five worlds have an initial annualized cost of capture of \$86.7/tCO_2 assuming the fixed charge factor of 0.1185. These worlds show similar slow rates of CCS capacity deployment in the first 10 to 15 years. After 2030 scenario settings cause divergence in investment. In the 'Climate Action' world, the CO_2 tax exceeds \$130/tCO_2 by the 2030s and the cost of CO_2 capture has decreased to \$61/tCO_2 (as shown on the top graph of Figure 3.3). Thus, in 'Climate Action' world, the projects with highest IRR are those that capture more CO_2 and target smaller oil resources (see Appendix Figure A5). Nevertheless, all world scenarios succeed in driving down the cost of CO_2 capture to below \$50/tCO_2 by 2045 given technological learning. The 'Climate Action', 'High Oil' and 'Depleting Resources' scenarios follow the same capture cost reduction trends to 2050. The 'Forward Learning' scenario drives the cost below \$50/tCO_2 by 2033 and to \$40/tCO_2 by 2045, which allows it to diverge away from the 'Base Case'. The steep reduction in CO_2 capture cost obtained in the 'Forward Learning' scenario makes up for a low CO_2 tax and a low oil price. It behaves as a high CO_2 tax by providing more incentive for larger CO_2 capture plant projects that were not previously lucrative and that are more economically favorable to storing CO_2 rather than producing oil. This explains the peak in cumulative investment observed after 2045.

Figure 3.4 presents the cumulative projects' net CO_2 stored from CO_2 EOR projects. The top graph excludes the CO_2 emitted from combustion of produced oil (i.e., *displacement* assumption), while the bottom subtracts the CO_2 emitted in the combustion of produced oil from the total CO_2 stored in each project (i.e., *additionality* assumption). Using the displacement assumption, cumulative storage by 2050 is in the range of 50 Gt in the 'Climate Action' world and 10-20 Gt in all other worlds. If we include end-use emissions from crude oil consumption, only the 'Climate Action' world results in net CO_2 storage. In this case, the 'Climate Action' world achieves net storage by 2035. The 'sub-worlds' presented in Figure 3.4 represent alternative 'Climate Action' worlds, with CO_2 taxes start-

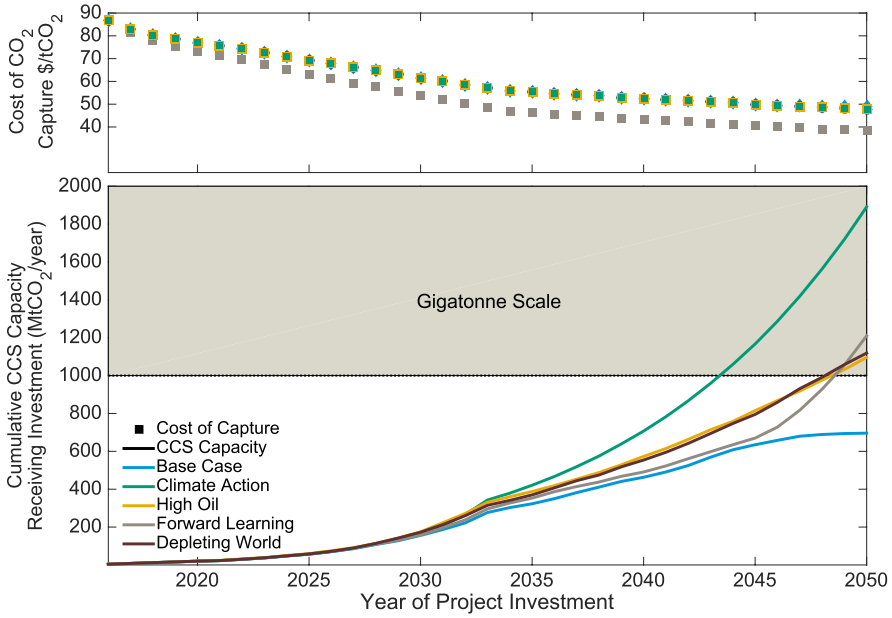

Figure 3.3: CCS capacity investment achieved as a result of each of the 5 world scenarios (bottom) and cost of CO_2 capture driven down as a result of technological learning (top).

ing at 60, 65, 70, 75, 80, 85, 90 and 95 \$/tCO_2 in 2016 and alternative High Oil worlds with oil prices of 60, 70, 80, 90, 100 and 120 \$/bbl. The alternative 'Climate Action' worlds show significantly different cumulative storage by 2050, while the effect of oil price variation is muted.

Figure 3.5 (top) shows revenues from oil and gas, illustrating that revenue from oil production dominates in all five worlds until 2030. Except in the 'Climate Action' world, oil revenue is ≈40 times CO_2 storage revenues. This is because the first projects that receive investment are those that have most favorable and known field characteristics for oil production and CO_2 storage and highest NPVs evaluated. In the 'Climate Action' world, CO_2 revenue exceeds oil revenue by 2030, and oil produced per tonne of CO_2 stored reaches 0 by 2050. In this case projects are built for the sole purpose of storing CO_2.

Figure 3.6 shows oil volumes produced per unit of CO_2 injected, captured or stored. The values plotted in Figure 3.6 align with other studies: Azzolina et al. 2015[111] found a range of oil production from CO_2-EOR of 1.7 - 6.3 bbl/tCO_2 used, while the IEA study that looked at the ability to store CO_2 through enhanced oil recovery found a range of 1.1 - 3.3 bbl/tCO_2 captured depending on whether an oil-driven or storage-driven EOR process was conducted[33].

The compound annual growth rate by 2050 in each world scenarios is compared against global and regional predictions for CCS deployment and oil production from CO_2-EOR in Table 3.8. As expected, the 'High Oil' and 'Depleting

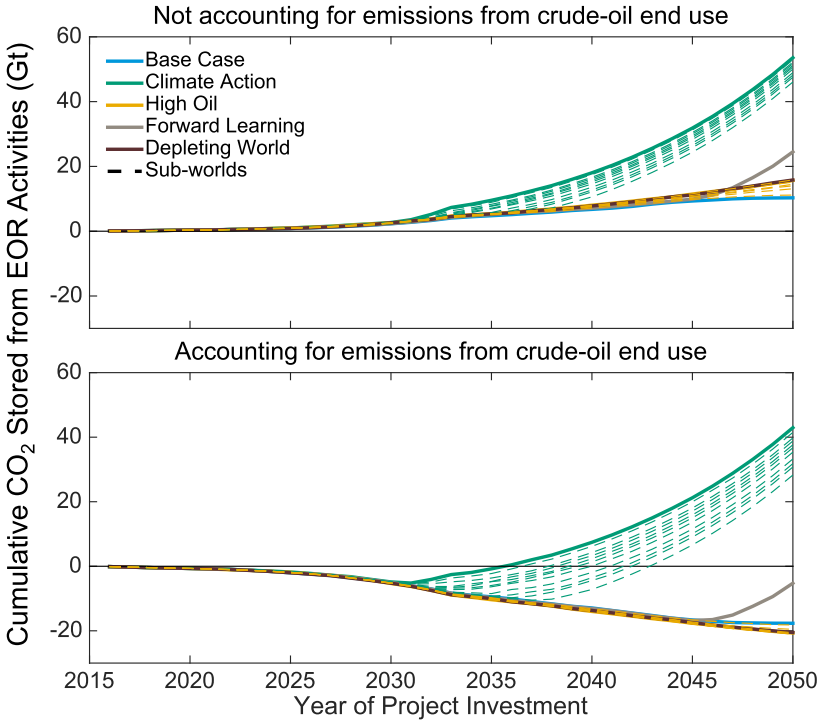

Figure 3.4: Net CO_2 stored as a result of CCS with CO_2-EOR project investment in all 5 world scenarios accounting for emissions from crude oil processing activities with (bottom) and without (top) crude oil end-use emissions including Sub-world scenarios describing 10 alternative 'Climate Action' world scenarios and 6 ' High Oil' world scenarios.

Resources' worlds are the ones to achieve the highest growth rates for the CO_2-EOR industry, exceeding those predicted for the U.S. by 2020. However, no scenario comes close to reaching the target growth required by the IEA for CCS deployment by 2050, though the 'Climate Action' world falls short by less than four percentage points. It is assumed that CCS with saline aquifer storage may also be deployed (not modeled here), once the cost of CCS has been driven down. This could contribute to a higher overall growth rate of CCS.

Table 3.8: Compound annual growth rate (CAGR) of the CCS industry and CO_2-EOR industry by 2050 in the five world scenarios compared with industry projections for CCS deployment needed by 2050 and U.S. CO_2-EOR industry expansion by 2020

World Scenario	CAGR CCS Industry	CAGR CO_2-EOR Industry
Base Case	9.73 %	8.12 %
Climate Action	12.91 %	5.17 %
High Oil	11.16 %	8.93 %
Forward Learning	11.48 %	8.31 %
Depleting Resources	11.23 %	8.93 %
Industry predictions (IEA 2050 CCS projection/ US CO_2-EOR 2020 Projection)	16.69 %	8.21 %

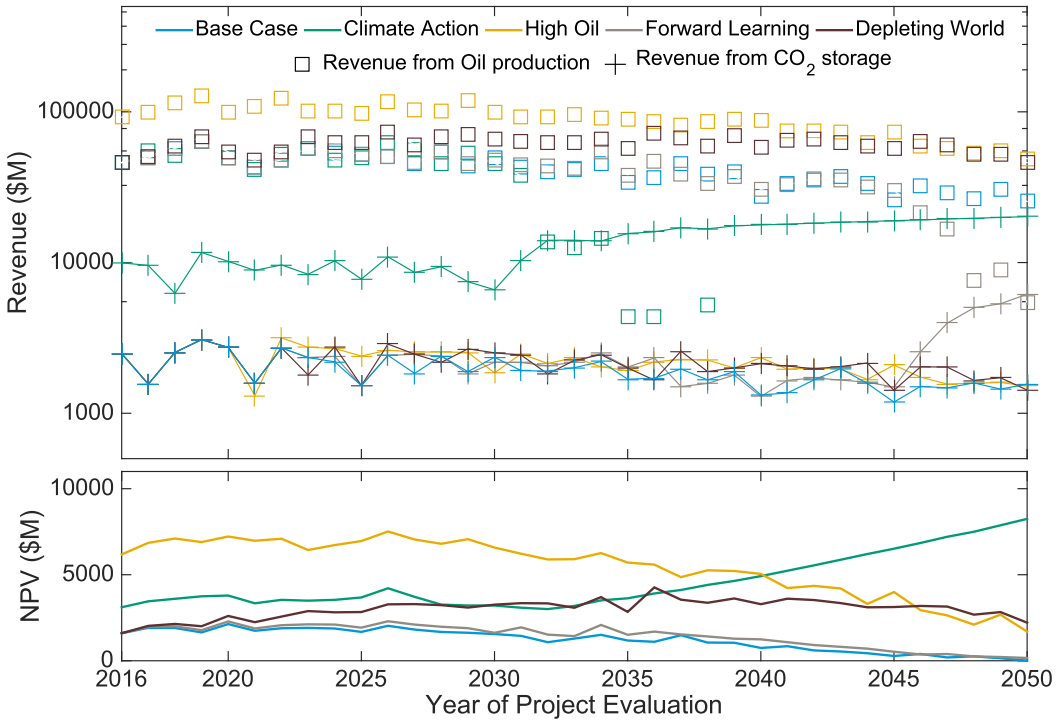

Figure 3.5: Proportion of revenue generated from oil production compared with that from CO_2 storage (top) and average NPV for successful projects assessed at a given year (bottom) in all 5 world scenarios

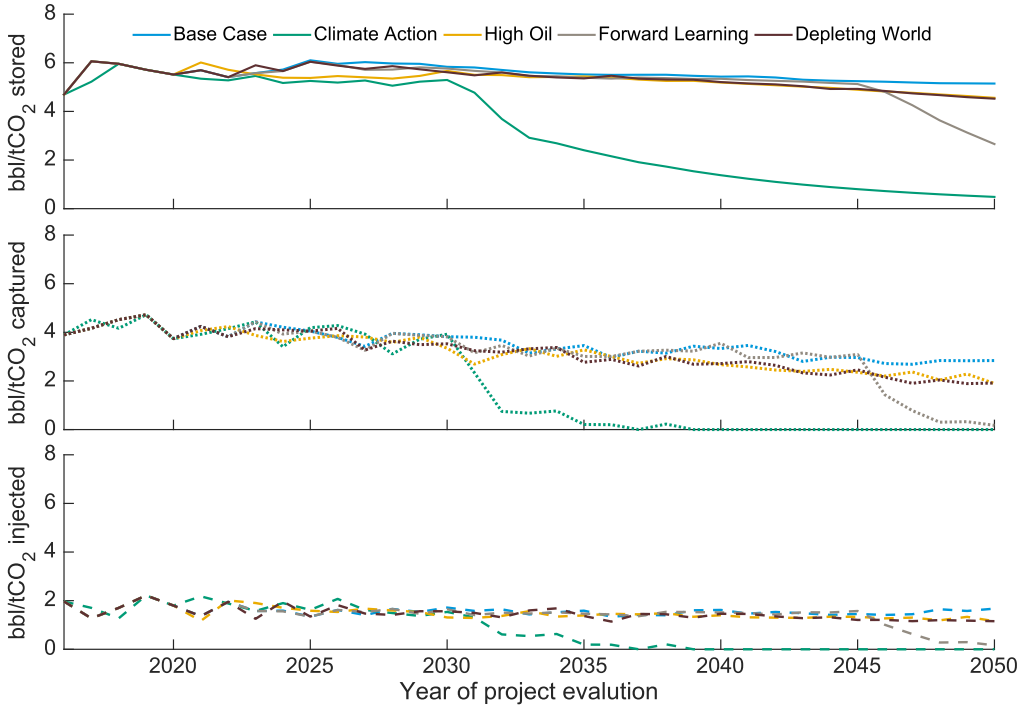

Figure 3.6: Rates of oil production per metric tonne of CO_2 stored, net used (total CO_2 captured) and gross used (total CO_2 injected) for all five world scenarios

3.4.2 Sensitivity to endogenous and exogenous model parameters

As highlighted in Figure 3.3, the 'Base Case' world scenario fails to reach the gigatonne scale of CCS capacity investment by 2050. Figure 3.7 demonstrates the sensitivity of this result to various assumptions.

First, by varying six parameter values by 10%, we find that the results are most sensitive to nominal discount rate and CO_2 capture rate. Each of these change the CCS capacity investment received during the period investigated by up to 15%. The initial capital cost of capture and capital cost of EOR per pattern significantly impact the investment choices made.

The impact of the industry growth limitations are also assessed. While a slower industry scenario sets back the growth rate of CCS, the fast industry growth ceiling does not enable many more projects to be built. The availability of "cheap" saline aquifer (SA) storage for residual produced CO_2 at \$20/tCO_2 results in 25% more projects receiving investment. Meanwhile, no CO_2 tax at all, reduces cumulative project investment by 19%.

The sensitivity to investment schemes is also investigated. A 40:60 debt:equity ratio at a 6% rate of interest does not strongly affect results. Including the cost of CO_2 transport infrastructure in the investment model has little effect on CCS investment. Finally, we conduct 1,000 realizations of our field generation process to explore the effects of generating candidate fields using a random number generator. Final project investment is affected by $\pm 5\%$ at the ± 1 SD level.

Note that all of these sensitivity studies fail to bring the Base Case scenario to gigatonne scale by 2050.

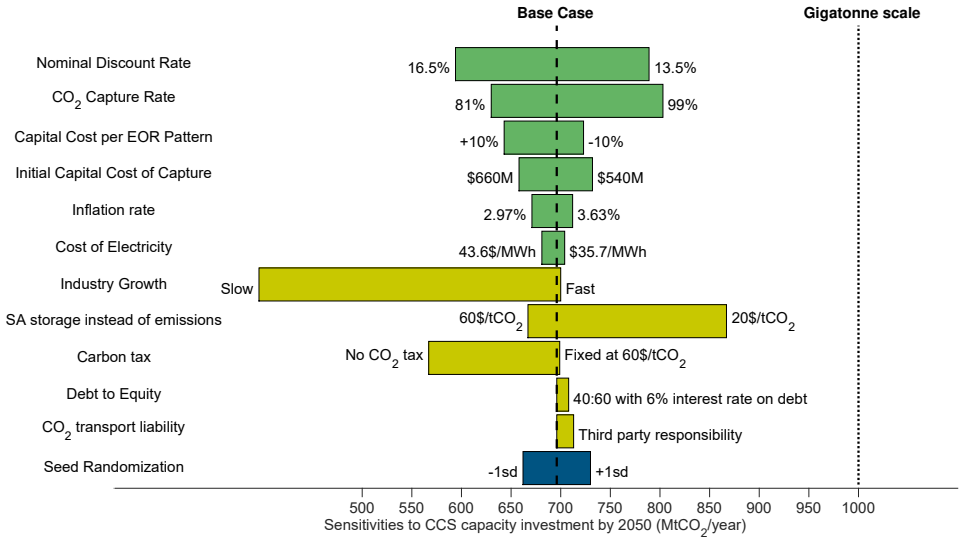

Figure 3.7: Effect of key parameters, variables, including the availability of saline aquifer (SA) storage at a cost, and randomization factors on 'Base Case' cumulative CCS capacity investment by 2050.

3.4.3 Sensitivity of CO_2 capacity, CO_2 storage and oil production to variations in 2 input parameters at a time

Lastly, we explore simultaneous variations in multiple key parameters across a range of conditions, resulting in $\geq$ 30,000 endpoint estimates for 2050 CO_2 capture capacity. Figure 3.8 shows two variable "slices" through the array of resulting CCS capacity investment by 2050. Values greater than 1,000 represent gigatonne-scale industry. Variables not shown in contour plot axes are set to Base Case values. Scenario worlds are plotted as red points (e.g., *CA* represents Climate Action world).

Contour plots show required shifts to push Base Case investment to gigatonne-scale by 2050. In the upper left we see that a 2050 CO_2 tax of $\geq$70 \$/t or an oil price of $\geq$85 \$/bbl are required to induce gigatonne scale by 2050. In the upper right, it becomes evident that beyond 70 \$/t the starting CO_2 tax in 2016 is more important than the learning rate in driving gigatonne emissions (note downward slope of isolines). However, at lower CO_2 tax rates, technological learning reduces the need for a high CO_2 tax at simulation start, though at 2015 observed carbon price levels of \$10-\$15/tCO_2 in EU and California carbon markets, the required learning rate for the first thousand projects must be at or above 18% (*i.e.* 18% cost reduction for every doubling of capacity deployed) to achieve gigatonne scale (a value for *LR* equivalent to that of small, modular technologies such as solar photovoltaics[125]). At the assumed base case CO_2 tax starting 25

$/tCO$_2$, which remains overly optimistic for most of the world, a doubling in technological learning rate (from 7% to 14 %) results in a near doubling of CCS deployment as well (from 597 MtCO$_2$/y CCS deployment to 1210 MtCO$_2$/y). Moving to the lower left, the initial cost of capture is surprisingly unimportant towards the likelihood of achieving gigatonne scale. The isolines are very steeply sloping, suggesting larger impacts from initial carbon taxes than capital cost. A challenge is evident in setting initial capital cost to that observed at real projects (i.e., 715 M$/Mt/y observed at Petra Nova). In that case, an initial CO_2 tax of almost 50 $/t is required to achieve gigatonne scale. Lastly, we see in the lower right that oil prices must return to recent historical highs of $\approx$ 100 $/bbl to induce gigatonne scale with Base Case initial costs of capture. This is perhaps unrealistic given recent developments and expansion of so-called "tight oil" driving oil prices to the 50 $/bbl range.

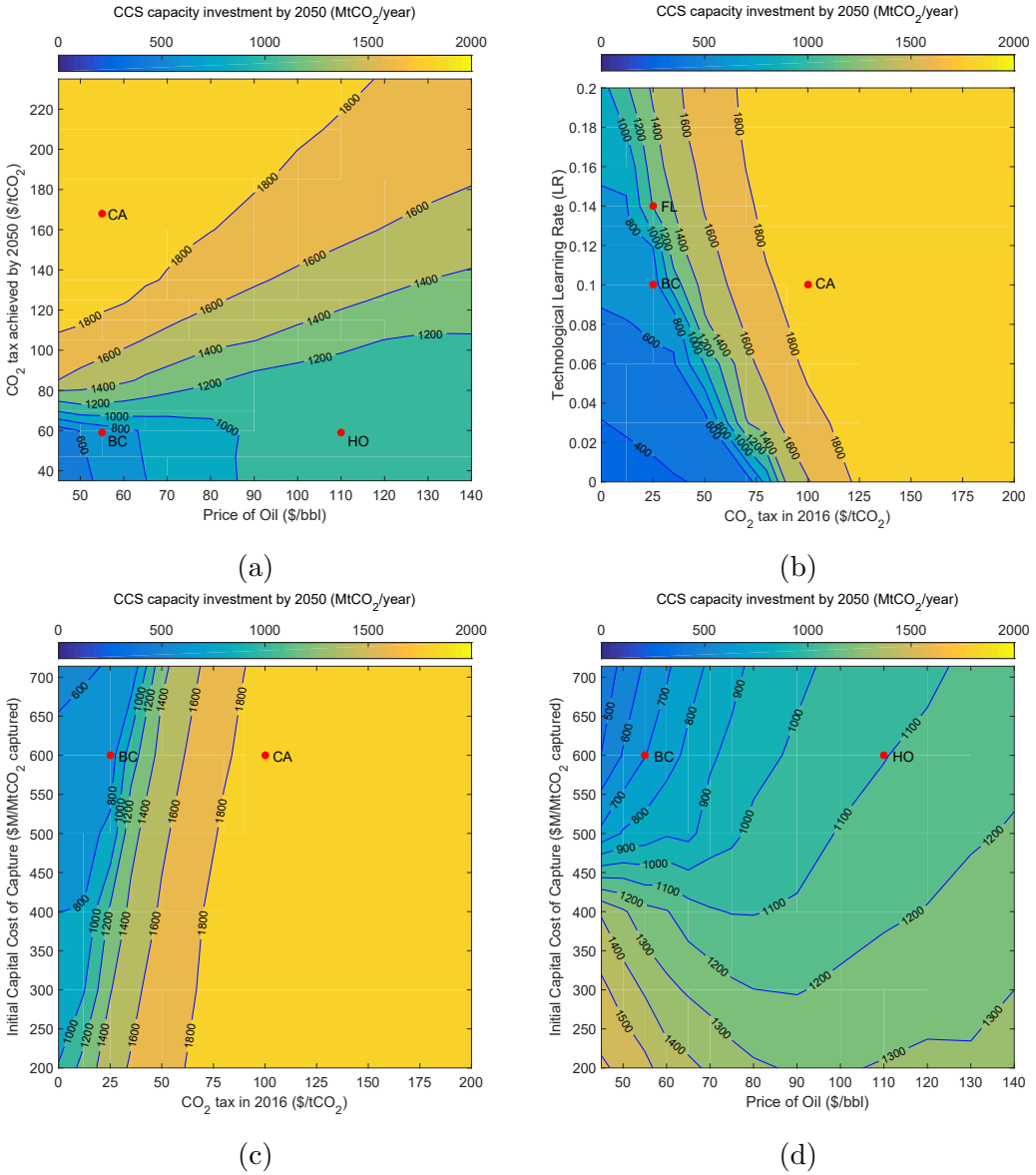

Figure 3.8: Heat maps showing contours of CCS investment achieved by 2050 in terms of CO_2 capture capacity ($MtCO_2$/y) as a function of (a) the CO_2 tax achieved by 2050 and the price of oil, (b) the CO_2 tax in 2016 and the amount of technological learning assumed, (c) the price of oil and the initial capital cost of capture assumed per $MtCO_2$ capture capacity in 2016, and (d) the price of oil and the initial capital cost of capture assumed per $MtCO_2$ capture capacity in 2016. Highlighted points of world scenarios include: BC ('Base Case'), CA ('Climate Action'), HO ('High Oil') and FL ('Forward Learning') described in Table 3.7.

3.5 Conclusions to chapter

As expected, today's low or non-existent CO_2 taxes and low oil prices are insufficient to trigger an upscaling of CCS to the gigatonne level. For the IRR-driven private sector, the revenue from EOR activities is currently too low to justify investment, as seen between 2014 and 2016 with a slow down of CO_2-EOR projects in the US. However, with higher CO_2 taxes or oil prices (or a combination of the two), CO_2-EOR does make CCS more attractive. Crucially, the revenue from oil in any CCS with CO_2-EOR project will initially provide the highest proportion of profit. This testifies to the benefit that CO_2-EOR brings to CCS when trying to portray it as a lucrative, investment-worthy endeavor, particularly when considering private sector involvement.

Although reservoir simulation for EOR operations in specific fields are not conducted here (as done by Dai et al. 2016[131] and Fukai et al. 2016[29]), this model incorporates a randomized selection of plausible fields and production profiles for CO_2-EOR and storage. This enables a general assessment of conditions under which gigatonne-scale CCS deployment can occur by 2050. This study extends the quantitative understanding to policy makers as to how much incentive is needed for CCS to become economically viable from an investment standpoint.

The specific trigger for investment matters. Whether EOR is induced by a CO_2 tax or a high oil price has clear effects on types of projects that are selected. High CO_2 taxes favor larger CO_2 capture projects and lower production rates of oil with smaller fields (in area and net pay thickness). High oil prices drive CCS capacity deployment but do not favor net carbon sequestration. As shown in Figure 3.8, given the base case assumptions considered here, gigatonne-scale of CCS deployment only becomes possible in regions where:

- CO_2 tax exceeds \$40/tCO_2 in 2016 and reaches over \$ 75/tCO_2 by 2050 or,
- Oil price is in excess of \$85/bbl or,
- The learning rate for every doubling is at least over 14%.

However, current EU Emissions Trading Scheme conditions give a market price for CO_2 of less than \$10/t[132]. Assuming this would increase gradually by 2050, this would require a learning rate in excess of 20% to reach gigatonne-scale of CCS deployment. With such low CO_2 taxes, recent oil prices fluctuating below \$ 50/bbl and a capital cost of CO_2 capture of over 700 \$M/MtCO_2/y only half-gigatonne CCS deployment is reached by mid-century, falling short of the gigatonne-scale expected.

The impact of recent US tax bill 45Q, that could provide the equivalent of a fixed 35\$/tCO_2 credit (non-increasing), when CO_2 is used for EOR, was also tested with MIICE and based on January 2018 values for oil price at 61\$/bbl and other 'Base Case' conditions. When compared to the equivalent conditions with no credit for CO_2 usage, the 45Q equivalent tax credit was found to improve CCS deployment achieved in 2050 by up to 10% and total CO_2 stored by 16%. These results remain optimistic compared to current conditions for the 45Q bill that state its duration to be 12 years and the credit reaching up to the product of 35\$/tCO_2 and the inflation adjustment factor by 2026. Nevertheless, these assumed conditions tested in MIICE still failed to reach a gigatonne of CCS deployed by 2050. Referring to Figure 3.8a this result lies directly below the x-axis at an oil price of 61\$/bbl, showing a CCS capacity investment below the 800 MtCO_2/year isoline.

3.6 Contributions made and future work

The development of MIICE, an open-source and detailed model that can be accessed and downloaded online (`http://doi.org/10.1039/C7EE02102J`), is one of the key contributions of the work described in this chapter.

The analysis that is drawn from MIICE is useful in answering the question posed as the title of this chapter and exploring quantitatively the conditions that may trigger gigatonne-scale CCS investment. CO_2-EOR can be a catalyst for CCS. The revenue from oil production, incorporating technological learning and a minimal CO_2 sequestration tax do suggest that CCS with CO_2-EOR can offer lucrative investments. However, without additional incentives such a government subsidy or a grant, a higher oil price or a higher CO_2 tax, investment in CCS capacity may not reach the gigatonne scale when considering only CCS with power plants. One should consider how CCS with other industrial sources will play a role in reaching this large-scale objective. Presumably while CCS with CO_2-EOR can help drive the costs of CCS down and trigger the development of CO_2 transport networks and storage infrastructure, it will become easier and more attractive for other industries such as cement, iron and steel producers for example, to invest in CCS at a lower capital cost. The results from MIICE's Climate Action world scenario also highlights a point beyond which revenue from CO_2-EOR is no longer needed for CCS deployment to be attractive to investors thanks to the cost reduction enabled early on. Coupling CCS with other industrial CO_2 sources, apart from power plants, are not included in MIICE and could be subject to further work. Furthermore, due to the nature of the data base for

oil fields and CO_2-EOR experience and costs being primarily from North America, the results are likely to differ when considering offshore CO_2-EOR fields and the cost implications of having to build CO_2 storage infrastructure from scratch as would be done in the North Sea for example.

Future work could also include adding scenarios with costs of various carbon capture technologies or technological breakthroughs (e.g., new solvents). The addition of regional parameters might be explored. This may strongly affect the extension of a transport network and development of infrastructure. Finally, the model could be extended to include actors with more or less stringent requirements on their returns and the risk they associate to such an investment (e.g., governments or government-corporate partnerships).

Chapter 4

Assessing the effect of UK CCS deployment and operation scenarios on storage sink response by simulating varying CO_2 injection rates into the Bunter Sandstone reservoir

We expect that CCS deployment rates may vary over the years and result in varying CO_2 supply rates. Hence, the work presented in this chapter takes a systems approach to looking at the interactions of the full CCS chain and poses the question: Will variations in CO_2 supply have a first order effect on the behavior of a CO_2 storage reservoir or not?

A reservoir model of the Bunter Sandstone Saline Aquifer was used to simulate CO_2 injection and demonstrate the effects of varying frequency and amplitude of injection rates on robustness and resilience of such a storage system. The Bunter Sandstone is particularly important to study as it is considered one of the main storage sinks for the UK and located in the Southern North Sea. The various injection rates tested here are informed by the outputs of energy systems models and conjectures on potential plans for UK CCS deployment. Results from this work can be fed back into models representing CO_2 storage supply in order to represent the interaction between CO_2 supply and storage appropriately.

The Bunter Sandstone reservoir model was obtained from and developed by the British Geological Survey (BGS) and described in Noy et al. 2012[133] and Williams et al. 2014[134]. This collaboration took place as part of the

MESMERISE-CCS project (https://www.imperial.ac.uk/a-z-research/mesmerise/what/) led by Niall Mac Dowell and Sam Krevor with Hayley Vosper, Gareth Williams (gwil@bgs.ac.uk) and John Williams (jdow@bgs.ac.uk) from the BGS. The work presented here was published in Kolster et al. 2018 (https://doi.org/10.1016/j.ijggc.2017.10.011) and also contributed to the publication of Agada et al. 2017 (https://doi.org/10.1016/j.ijggc.2017.08.014)[39].

4.1 Background to the need for modelling of CO_2 storage: example of the UK Bunter Sandstone

Under the 2008 Climate Change Act, the UK has committed to reducing its greenhouse gas emissions by 80% from 1990 levels by 2050 and according to the Committee on Climate Change, CCS is critical in reaching this target at least cost[135,136]. Evaluations for costs and deployment of low carbon energy systems are typically based on integrated assessment models that include the techno-economics associated with CCS development and risk. However, these typically assume a pressure vessel type description of CO_2 storage sinks, and do not include limitations that may be imposed by the storage reservoir as a result of sudden deployment or varying CO_2 injection rates[137]. In this work, reservoir simulation is used to evaluate some of the potential issues that may arise from regional large scale deployment of CCS in the UK in light of their commitment to reduce greenhouse gas emissions by mid-century.

The Bunter Sandstone Saline aquifer has been identified as having a significant CO_2 storage potential, particularly for the UK[133,134,138–140]. As a result, it has been subject to a number of numerical modelling studies evaluating the integrity of the reservoir seal and maximum safe overpressure (Heinemann et al. (2012)[139]), the effect of the reservoir's geological structure and heterogeneity on CO_2 storage efficiency (Williams et al. (2013)[141]) and the effect of large scale injection of CO_2 into the reservoir on brine displacement (Noy et al. (2012)[133]). A study conducted by Pale Blue Dot Energy for the Energy Technologies Institute found that injection into the Bunter saline aquifer will be key in providing the appropriate geographic spread and capacity to meet UK storage demand[142]. The Bunter Sandstone has the advantage of being in close proximity to the Eastern coast where the UK has a large concentration of industrial and power plants[135,142], including the largest coal firing power station in the UK: Drax

Power Station.

CO_2 storage reservoirs may be subject to dynamics across multiple time-scales. On a decadal time-scale, CCS capacity will be gradually deployed and ostensibly lead to an increase in target CO_2 injection rates. Meanwhile, the deployment of extensive amounts of intermittent renewable power could lead to displacement of thermal generation as well as an increased, hourly dependent, variability in storage demand for CO_2 from power[143–146]. The work presented in this chapter looks at investigating the effect these variable rates of CO_2 injection can have on regional reservoir behaviour and storage supply.

Studies have simulated varying rates of CO_2 injection over an extended period of time in order to understand the effects of large-scale CCS deployment. These have shown a clear link between reservoir injectivity and dynamic storage capacity, while showing no link between varying injection rate and overall plume migration or regional pressure build up [147–152]. In a study conducted by Wiese et al. (2010)[152] numerical simulations are used to look at the impact of temporal variations in CO_2 injection through a single well into a saline aquifer in order to mimic the impact of CO_2 capture variability. They find that in the long term such variability has little impact on storage capacity. Bannach et al. (2015)[149] conduct a dynamic simulation of large-scale industrial rates of CO_2 injection with seasonal variation into the Volpriehausen sandstone in North Germany. They find that varying CO_2 injection rates have the largest negative effect on overall injectivity within the first years of operation when compared to injection at a constant rate. In both cases, the study finds that the pressure build up is highest in the first few years of injection and decreases with time. The study also shows that reducing permeability by 50% generates a proportional decrease in the injection rate. Xie et al. (2016)[147] investigates injectivity of saline aquifer sites in the Ordos Basin of China and compares the storage capacity of sites within the Ordos Basin using analytical methods and numerical simulations. The study highlights that, when conducting numerical simulations, a lower injectivity is obtained, compared to injectivity obtained from an analytical solution for injection. This is because the numerical simulation incorporates the effects of reservoir heterogeneity and the evolution of relative permeability. Deng et al. (2012)[148] looks at the effect of industrial-scale CO_2 injection on injectivity over time of a model of the Weber Formation in Wyoming. This study finds that injectivity is limited by the safe injection pressure imposed and the heterogeneity of the reservoir model over 50 years of injection. Storage capacity of a reservoir over time will also depend on such reservoir conditions including boundary conditions, density and viscosity of the fluids, permeability and porosity distributions, reservoir thickness and depth[153,154].

This study focuses on these issues in the UK context of large-scale regional CCS deployment. The objective is to improve understanding of potential limitations to CO_2 storage by considering a variety of scenarios for CCS development. These scenarios are grouped into three categories designed to encompass the range of future potential CO_2 storage demand scenarios.

Firstly, the UK has seen a lot of change in its energy portfolio with increasing penetration of intermittent renewable energy sources and nuclear power. Hence, CCS with power and industry may become more or less important at different points in time, resulting in varying CO_2 storage demand. In addition, meeting storage demand may be conditional to reservoir properties around a selected and developed injection site. In an initial set of injection scenarios, the sensitivity of storage supply to varying and cyclical fluctuation in rates of demand and injection site selection are investigated, which will differ in local permeability and depth.

Secondly, between 2007 and 2015 the UK conducted two CCS competition projects intended to serve as a jumpstarter for the technology. The last one was canceled in November 2015 due to a lack of allocated budget[135]. The White Rose CCS project, led by a consortium company called Capture Power Limited, aimed to capture CO_2 by retrofitting a Drax Power Station coal firing unit with CCS and injecting the CO_2 into the Bunter Sandstone[155]. This demonstration project aimed at capturing 2 $MtCO_2$/year[156,157]. A future for CCS in the UK is envisioned, starting with a similar demonstration size project and eventual expansion to retrofit capture onto more power plant units. Each CCS plant may start development at different points in time and take several years to construct[158] adding to the imposed variability onto the storage system. In a second set of CO_2 injection scenarios, the impact of gradual industrial-scale CCS deployment on CO_2 storage supply is investigated.

Thirdly, energy systems models suggest deployment rates for CCS to meet emissions reduction targets while meeting electricity demand[145]. However, sufficient injectivity and reservoir pressurization will be key in this match between the capture system and storage needs[153,159,160]. The feedback between the energy system and the CO_2 storage demand is investigated here with a third set of injection scenarios based on previous energy systems modelling work[145].

4.2 Methodology

4.2.1 Bunter Sandstone geological reservoir model

The Bunter Sandstone is located offshore the East of England in the UK Southern North Sea and is part of a larger reservoir rock unit of which the onshore part is known as the Sherwood Sandstone Group. The geological and dynamic simulation model used in this work to represent the Bunter Sandstone regional aquifer was developed from the British Geological Survey (BGS) model presented by Noy et al.[133]. The model area chosen is bounded by an overlying seal of mudstones and evaporites that constitute the Upper Triassic Haisborough Group and the Bunter Shale Formation as an underlying seal, each with permeabilities of the order of microDarcies. The outer boundary of the model is also assumed to be impermeable as it consists of a series of discontinuous salt walls and erosional margins that result from major fault zones[133]. The presence of gas fields within the model area, including the Esmond, Forbes and Gordon fields as well as the Hewett Field Group just outside of the model boundary, suggest an effective reservoir seal[139]. However, uncertainty remains around the potential presence of an outcrop to the seabed[133,138,141]. An outcrop to the seabed could provide pressure relief as a result of expulsion of brine from the reservoir while posing a risk for CO_2 leakage into the seabed. However, the simulations scenarios run as part of this study showed that neither of these occur over the time periods considered i.e. 100 years.

The model covers an area of approximately 143 km East to West and 125 km North to South, and uses a grid of 250 (x) $\times$ 285(y) $\times$ 25 (z) elements sized 500m by 500m. The reservoir is divided vertically into 25 layers, of which layers 1-6 of the coarse grid model represent the impermeable caprock region. Well penetration data were used to obtain depth at different locations in the reservoir. The mean depth of the reservoir model is 1850m. A mean reservoir temperature of 65°C was assumed, while an average reservoir pressure of 19.5MPa, an average porosity of 20% and permeability of 100mD was used. Brine salinity was set to 130,000 ppm and rock compressibility to 4.5×10^{-10} Pa^{-1}. These values were the same as those used in Noy et al.[133]. Dissolution of CO_2 in the formation pore-water was also included in the model as done by Noy et al.[133].

Using the reservoir simulator ECLIPSE 100, the model is set up as a CO_2-brine black oil model with pressure, volume and temperature (PVT) data computed using the method described by Hassanzadeh et al.[161]. Relative permeability data tables for water and gas were based on core-flood experiments on a water-wet Bunter sandstone sample[162]. Recognizing the importance of capillary

trapping in safe CO_2 sequestration[154,163,164], a Killough hysteresis model[165] was implemented to account for hysteresis in the gas relative permeability[166].

4.2.2 Simulation parameters and constraints

The reservoir model includes 12 injection sites with a minimum distance from site to site of 30km and a large site diameter (0.3048m or 1 foot). It is assumed that, in practice, each injection site could represent several wells. The number of wells deployed at a given injection site will typically depend on the trade off between the cost of adding a well and the amount of CO_2 that can be safely injected into one well without overpressure[167]. In practice, this may also depend on the permeability of the targeted field. The Sleipner project for example only needed one injection well, while the In Salah project, with the same targeted injection rate (1 $MtCO_2$/year) but lower permeability, required 3 injection wells[168,169]. The locations of the 12 injection sites were based on proximity to existing infrastructure in place from gas fields in the area. The injection sites are completed in every layer of the reservoir (layers 6-25). The fluid injection into the sites modelled is limited by a bottom hole pressure (BHP) constraint. This is set at 75% of the estimated lithostatic pressure at each injection site, which also represents the lower bound of reported leak-off tests at depths greater than 1000m[133]. Leak-off tests are carried out in order to give a good indication of the fracture pressure of a formation. The lithostatic pressure gradient assumed is 22.5kPa/m, which implies that the deeper the site, the higher its bottom-hole pressure limit will be[133]. Other studies use more or less stringent pressure build up limits ranging from 60% to 90% of lithostatic pressure[133,139,154]. Reduced uncertainty with regards to pressure gradients in the reservoir may lead to less stringent limits on the bottom hole pressure and quicker injection.

In simulation studies aimed at representing CO_2 injection on a regional scale and due to the coarseness of such a model (i.e. having grid blocks of the order of 10s or 100s of metres), modelling injection of CO_2 with one large injection site is customary and captures the key reservoir behaviour[153,170]. In this study the grid resolution is of 500m $\times$ 500m, which is similar to other studies looking at injection over large regions[160]. Simulations that focus on a single injection site with several wells will use a more refined grid resolution of the order of 10s m^2[171]. Here, the grid cells that include an injection site and the three grid cells in each x-direction and y-direction of the grid cell with the injection site are refined. These are refined by a factor of 11, bringing the grid resolution to 45.5m $\times$ 45.5m in the grid cells surrounding and including each injection site.

Table 4.1: Depth and bottom hole pressure (BHP) limit of 12 base case injection sites obtained from the BGS Bunter Sandstone reservoir model

Injection site	Depth (m)	BHP limit (MPa)
1	1751	29.54
2	2007	33.87
3	1742	29.39
4	1743	29.42
5	2564	43.26
6	2020	34.09
7	1971	33.26
8	2311	39.00
9	1517	25.60
10	1729	29.18
11	1738	29.33
12	1795	30.30

In this study, a timeline of CO_2 injection and monitoring that commences in year 2030 is considered, which would be operated for under 100 years. Within this timeline closed lateral and vertical boundaries are imposed, providing a conservative estimate of reservoir pressurization given that greater pressure increase will occur. The results of CO_2 injection obtained from ECLIPSE 100 simulations are evaluated and analysed in Petrel. In this study a base case scenario of 24 $MtCO_2$ injection per year in the field is considered, which is split evenly between the 12 injection sites. While studies by Noy et al.[133] and Farhat et al.[150] consider higher rates of injection per site at 5 $MtCO_2$/year, on average, industry practice in the North Sea would suggest an injection rate per site to be 1-2 $MtCO_2$/year[168,172,173]. The model parameters are summarized in Table A5 in Appendix A1.

4.2.3 Injection rate scenarios and injection site selection

Three sets of reservoir simulations were conducted based on three sets of injection scenarios summarized in Table 4.2. The first set of injection scenarios covers highly fluctuating cyclic variation of CO_2 storage demand rate regimes. This includes a sensitivity analysis that highlights key injection rate differences that may stem from variation in permeability and depth at different injection site locations. The second set of injection scenarios describes injection demand from gradually increasing potential UK CCS deployment rates. These first assume

that a demonstration plant of the same size as White Rose CCS is deployed and then CCS is retrofitted onto some of the remaining Drax Power Plant units. The third set of injection scenarios is based on the output and extension of an energy systems model for CCS deployment on coal fired power plants in the UK.

Table 4.2: Three sets of injection scenarios based on storage demand for the field: 1) Four high amplitude cyclic fluctuations of target injection rates (rates given as: starting rate/2nd cycle rate) compared with a Base Case Scenario of target field total 24 $MtCO_2$/year injection, 2) Storage demand for five CCS deployment scenarios based on hypothetical CO_2 capture rates obtained from Drax power plant and number of units, demonstration (DEM) or large-scale (LS) deployed, 3) Three UK CCS with coal deployment and displacement scenarios determining storage demand rates for the Bunter Sandstone

Set	Scenario	Target Injection rate(s) ($MtCO_2$/year)	Variation	Inj. Time (years)	Unit Deployment
1	Base Case	24	Constant	50	6 x LS
	+/- 80%	43.2/4.8	Every 5 years	50	6 x LS
	-/+ 80%	4.8/43.2	Every 5 years	50	6 x LS
	+/- 80%	43.2/4.8	Every 2.5 years	50	6 x LS
	-/+ 80%	4.8/43.2	Every 2.5 years	50	6 x LS
	Sensitivity	1.0	Constant - one site at a time	50	Injection Site 1, 5, 9.
		Target Peak Inj. ($MtCO_2$/year)	Peak Inj. Year	Inj. Time (years)	Unit Deployment
2	Drax 1	14	2045	85	1 x DEM, 3 x LS
	Drax 2	14	2040	75	1 x DEM, 3 x LS
	Drax 3	14	2045	55	1 x DEM, 3 x LS
	Drax 4	14	2060	70	1 x DEM, 3 x LS
	Drax 5	22	2050	60	1 x DEM, 5 x LS
		Target Peak Inj. ($MtCO_2$/year)	Peak Inj. Year	Inj. Time (years)	Variation Level
3	E-system 1	12	2030	50	High-low-end
	E-system 2	12	2050	50	Low-high-low-end
	E-system 3	11	2030	50	Constant

Sensitivity of plume migration and pressure to varying injection rates, depth and permeability - Set 1

In a first set of reservoir simulation scenarios of dynamic CO_2 injection, the impact of cyclic variations in CO_2 injection was investigated. This enables understanding from a theoretical standpoint why variation in CO_2 injection may have an effect on reservoir behaviour and storage efficiency. Hence, in these scenarios, represented in Figure 4.1, the amplitude of target injection per site (by 80% above and below the average) and the cycle period (2.5 years and 5 years) were varied. These were compared to a constant rate of CO_2 supply over the same total duration of operation, 50 years. The average rate of CO_2 supply and target injection was set at 24 $MtCO_2$/year for the whole reservoir and split evenly between the 12 injection sites.

The effect of permeability and depth on injectivity of the reservoir is highlighted by considering the injection of 1 $MtCO_2$/year for 50 years in three distinct sites, 1, 5 and 8. The near-well bore horizontal permeability, depth and lithostatic pressure at each site is summarized in Table 4.3. Compared to the average reservoir permeability and depth, injection site 1 and 8 are in low permeability

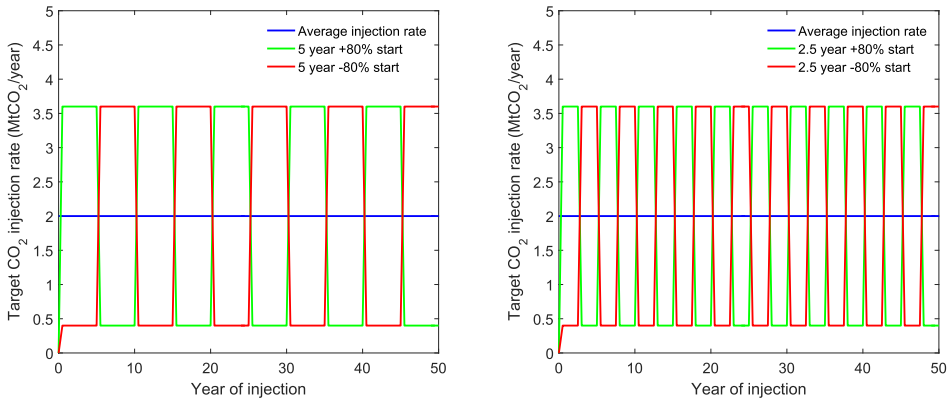

(a) (b)

Figure 4.1: Target injection rates varying every 5 years(a) and every 2.5 years (b) at 80% above and below an average target injection rate of 2 $MtCO_2$/year starting at the higher or lower amplitude of injection

shallow and deep zones respectively, while injection site 5 is in a high permeability, deep zone. The lithostatic pressure at a given site is proportional to the depth at the injection site. The horizontal permeability distribution is shown in Figure 4.2. Here, while injecting into one site at a time, all other sites are closed.

Table 4.3: Horizontal permeability, depth, and lithostatic pressure near injection sites 1, 5 and 8 compared with average reservoir characteristics.

Site	Permeability (mD)	Depth (m)	Lithostatic pressure (MPa)
Injection Site 1	21	1751 (Shallow)	39.39
Injection Site 5	283	2564 (Deep)	57.68
Injection Site 8	36	2311 (Deep)	52.00

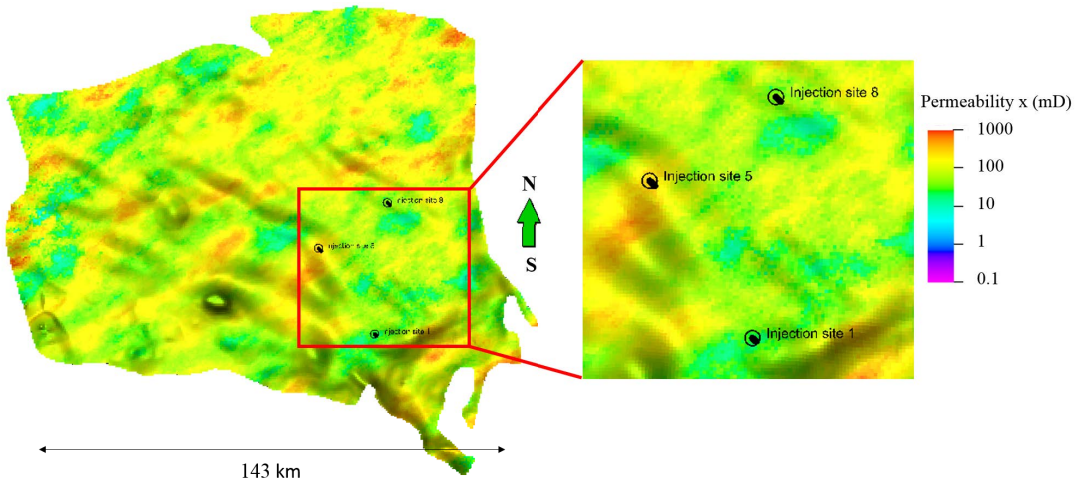

Figure 4.2: Horizontal permeability surrounding injection sites 1 and 5 in the heterogeneous Bunter Sandstone reservoir field model.

Injection scenarios envisioned for UK government led regional CCS deployment - Set 2

Based on the UK government's past CCS deployment strategy we consider five scenarios for CO_2 storage demand from the Bunter Sandstone, summarised in Table 4.2. The first four scenarios of CO_2 storage demand assume that CCS deployment peaks at 14 $MtCO_2$/year in 2045, 2040, 2045 and 2060, which is equivalent to one demonstration plant and three Drax Power Plant units retrofitted with CCS. In a fifth scenario, it is considered that CO_2 storage demand peaks at 22 $MtCO_2$/year in 2050. Each scenario is initiated in 2030 with target injection rates equivalent to the capture rate of 2 $MtCO_2$/year, referred to as the demonstration plant (DEM) and subsequent plants correspond to a rate of capture at 4 $MtCO_2$/year, referred to as the large-scale plant (LS).

In considering these scenarios trade offs between an expansive deployment strategy, where all 12 sites are in place for the start of injection (injection is split evenly across all sites), and limited site deployment strategies that split injection in the field into a maximum of 6 selected sites are investigated. The oil and gas industry in North America is used as an example to describe storage developers, who are likely to build injection sites progressively in response to short term demand[174]. This minimizes upfront capital cost. Hence, four improved injection strategies with a reduced number of total sites targeted are assumed. These are summarized in Table 4.4. In a first site deployment strategy splitting target injection into sites 1-6 throughout the full injection period ('6 sites') is considered. In a second strategy targeting injection into sites on a need-only basis with a maximum of 6 injection sites in use at any given time ('Need base deployment') is considered. Third, targeting injection into 2 first sites then splitting the CO_2 supply into four more sites pre-empting that storage demand will increase in a few years ('Progressive deployment') is considered. Finally, strategically choosing the deepest sites in which to target injection ('Deep sites'), which will have the highest limits on bottom hole pressure is looked at. The 'Deep sites' injection strategy assumes that the deepest sites, 5 and 8 (see Table 4.1) are first deployed to meet capture rates from the demonstration plant (2$MtCO_2$/year), then, before the 1st large scale CO_2 capture plant is deployed, injection is split into the next four deepest sites, 2, 6, 7 and 12. The choice of site as a function of depth is based on the information provided in Table 4.1.

Table 4.4: Injection site deployment strategies to meet the storage demand scenarios for the UK government CCS deployment strategy (Set 2, Table 4.2)

Strategy name	Characteristic Deployment/ Shut Down	Description
12 sites	Expansive/Immediate	Reservoir target injection rate from storage demand is split evenly in all 12 sites at the start of CCS deployment and for the whole simulation period.
6 sites	Limited/Immediate	Reservoir target injection rate from storage demand is split evenly in sites 1-6 at the start of the CCS deployment period.
Need base deployment	Limited/Gradual	Injection in demonstration years (2 $MtCO_2$/year) is targeted and split evenly at injection sites 1 and 2, and then targets sites 1-6 when large-scale capture units add to CO_2 storage demand. Sites are then closed down one by one as target demand for storage decreases step-wise.
Progressive deployment	Limited/Gradual	Starting with injection targeted to sites 1 and 2, half way through the demonstration period with 2 $MtCO_2$/year storage, injection is split evenly to sites 1-6. Sites are then closed down one by one as target demand for storage decreases step-wise.
Deep sites	Limited/Gradual	Sites 5 and 8 are targeted first when demonstration plants are providing demand, then half way through the demonstration period, injection target is split evenly between the 6 deepest sites in the field 2, 6, 7 and 12. Site shut down is also conducted progressively in response to decreasing demand.

Impact of varying storage demand based on a systems model output of UK coal power with CCS - Set 3

In a third set of injection scenarios (see Figure 4.3), we take the deployment rates for CCS based on previous energy systems modelling work[145]. This earlier work uses a UK based electricity market model that integrates UK emissions reduction plans with a portfolio of clean energy options in order to establish the role that coal with CCS may play in the future energy mix. It shows 'coal CCS' starting with a high capacity factor and thus a high CO_2 storage demand in 2030, which slowly decreases over the 50-year timeline as a result of increasing market penetration of renewable energy (E-system 1). This target injection into the reservoir model is simulated and the injectivity with two injection scenarios of identical average target injection rate over the 50 years considered is compared. The first comparative scenario (E-system 2) assumes a ramp up of 30 years before reaching a peak of 12 $MtCO_2$/year storage demand in 2060 followed by a sharp decline in demand. Meanwhile the second comparative scenario (E-system 3) assumes a constant CO_2 storage demand rate.

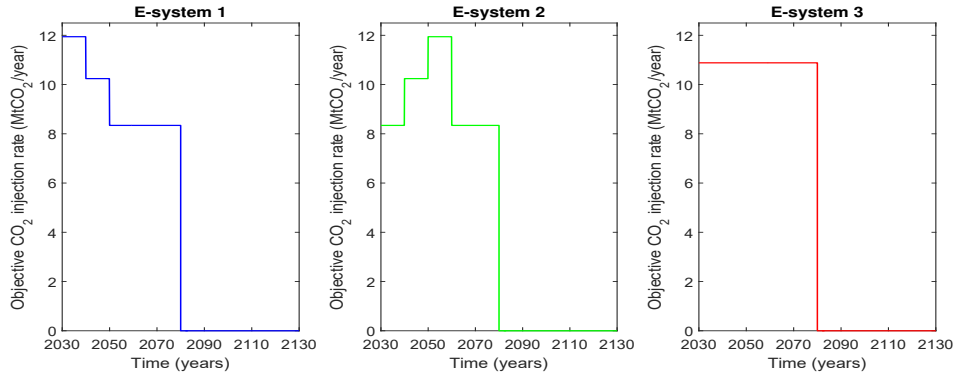

Figure 4.3: Objective (target) injection rates for three CO_2 capture rate deployment scenarios[145]

4.3 Results and discussion

4.3.1 Sensitivity of plume migration and pressure to varying injection rates, depth and permeability - Set 1

Figure 4.4 shows the CO_2 plume distribution and pressure development in the reservoir as a result of constant injection over 50 years and varying CO_2 injection by 80% every 2.5 years starting at the highest rate. The gas saturation and pressure development distribution maps for the other scenarios in set 1 are shown in A2. The static image of reservoir behaviour after 50 years of CO_2 injection are presented in these figures at the 15th layer of the reservoir model. The plume migration differs because of variable injectivity across sites (Figures 4.4a and 4.4b). This is because the geology around certain sites is more favourable to higher initial injection rates than others. We observe that after 50 years of injection, all scenarios have a similar plume extent.

Similarly, the pressure distribution in the reservoir after 50 years of injection for all 5 injection rate scenarios are alike (Figures 4.4c and 4.4d). Pressure in the reservoir is higher around the same South-Eastern area reaching pressure up to 350 bar, while remaining lowest in the North-West boundary of the model, between 100 and 150 bar. Average pressure build up in the reservoir is highest for the case of constant site injection, at 23% above original pressure, because cumulative CO_2 injection is highest. Meanwhile, the lowest pressure build up is 20% higher than original pressure, found at 50 years of the 5-year cycle injection starting at the higher bound rate (+/- 80%). In all varying rate scenarios, the average reservoir pressure, limited by injectivity in the early years of injection, remains 1-3% lower than that of constant injection throughout the total injection period. This is because lower total volumes of CO_2 were injected throughout the simulation period as a result of lower injectivity at the start of injection. This,

however, is an artefact of artificially low injectivity at the beginning of the simulations[175] and will not be a feature of real injection projects.

The analysis shows that the simulated reservoir dynamics associated with injecting at periodically varying rates of CO_2 is similar to injecting at constant rates of CO_2 over the periods considered. This shows that high amplitude rate fluctuations are not important to take into account when evaluating large volume injection over decade-long timescales. Hence, assuming a constant average rate of injection can prove to be sufficient in representing CO_2 storage in first-order systems models so long as the total volume of CO_2 injected over that time period is properly represented.

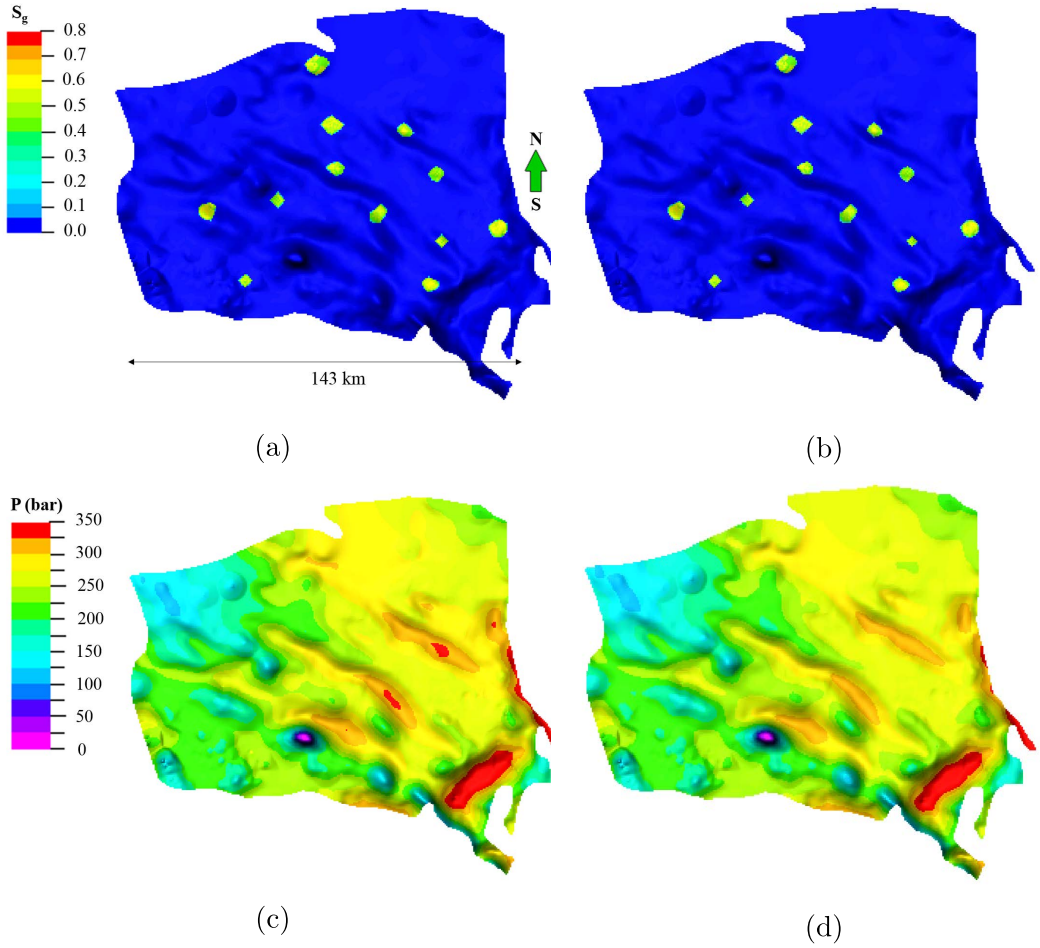

Figure 4.4: Gas saturation S_g and reservoir pressure P after 50 years of constant CO_2 injection in all 12 sites at 2 $MtCO_2$/year (a), (c) and after 50 years of varying CO_2 injection rate by 80% above and below the average 2 $MtCO_2$/year every 2.5 years (b), (d)

Figure 4.5a shows the sensitivity of injectivity to near-site permeability and depth. Early time spikes in pressure, followed by subsequent decreases in pressure, are discounted as gridding artefacts. Pickup et al. 2012[176] and Mathias et al. 2012[175] found that similar early-time injection rate delays are a result of

the grid scale used for the simulation model. The bottom hole pressure at each injection site is appropriately represented following the early-time evolution in Figure 4.5b. The bottom hole pressures are bounded by the maximum allowable pressure limit at each injection site. After 10 years, the pressure evolution in the wells is free from gridding artefacts. All three sites exhibit pressure well below the limiting threshold. Site 5, at a depth of over 2,500 m and near-site horizontal permeability over 280 mD, is farthest from the limit. This sensitivity analysis suggests that at higher rates of injection, near-well bore permeability and depth can become key drivers for injectivity due to the effect of the bottom hole pressure limit as shown in our earlier work[39]. Deeper sites however will require higher drilling and completion costs for wells. It is found that at such rates of injection, there will not be a problem reaching sufficient injectivity in time to meet storage demand.

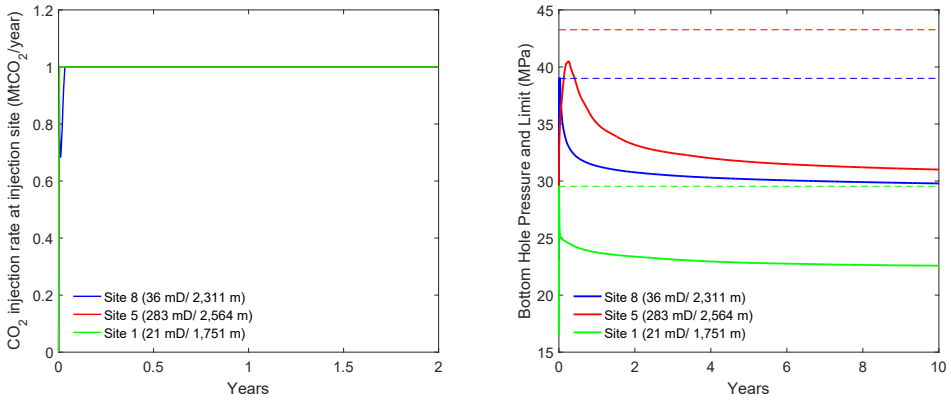

(a) (b)

Figure 4.5: CO_2 injection rate in the first 2 years of injection (a) and bottom hole pressure in the first 10 years of injection (b) at the respective site in response to the targeted injection of 1 $MtCO_2$/year in each site. The dotted lines in Figure (b) refer to the bottom hole pressure limit for each site.

4.3.2 Injection scenarios envisioned for UK government-led regional CCS deployment - Set 2

Figure 4.6 presents actual injection rates achieved for deployment scenarios Drax 1 and Drax 4 and for all five deployment strategies (summarized in Table 4.4). Scenarios Drax 2, 3 and 5 are described in more detail in Supplemental Materials A3. These results show that splitting injection into all 12 sites in the field and initiating injection at 2 $MtCO_2$/year results in target injection rates being met for the majority of the simulation period. This is the case whether the

target peak injection rate is 14 $MtCO_2$/year or 22 $MtCO_2$/year, reflecting that limitations are imposed by injectivity constraints, not volumetric constraints. The expansive, '12 sites' deployment strategy to injection strategies with different levels of limited site deployment are compared. It is found that in Scenarios Drax 1 and 4, the other injection strategies result in a small shortfall in injection rate, compared to the target injection rate, at their peaks of ramp up, in 2055 and 2070 respectively. This difference however is very small with a reduction in injectivity of 3.4% to 3.9% for Drax 1 and 3.9% for Drax 4 in all reduced injection strategies. In rapidly increasing storage demand scenario Drax 1, the 'deep sites' injection strategy shows slightly better injectivity than '6 sites', 'Need base' and 'Progressive' deployment strategies, with a 3.4% reduction in injectivity compared to 3.9% for the latter three by year 2055. In slowly increasing deployment scenario Drax 4, the injection strategies do no have an effect on the ability to ramp up the CO_2 injection rate in response to an increasing storage demand and all have a 3.9% reduction in injectivity by 2070 compared to the '12 sites' strategy. Such a small difference, however, is well within the uncertainty of the outcomes. These results suggest that there is no substantial benefit to deploying large infrastructure upfront to achieve initially low injection rates equivalent to one or two demonstration units ('12 sites' and '6 sites' strategies), but rather adopt a deployment strategy that meets storage demand as it increases progressively ('Need base deployment', 'Progressive deployment' and 'Deep sites' strategies). Meanwhile, there may be a trade off in deploying higher cost injection sites earlier rather than later (i.e. deep sites requiring more costly drilling and completion work).

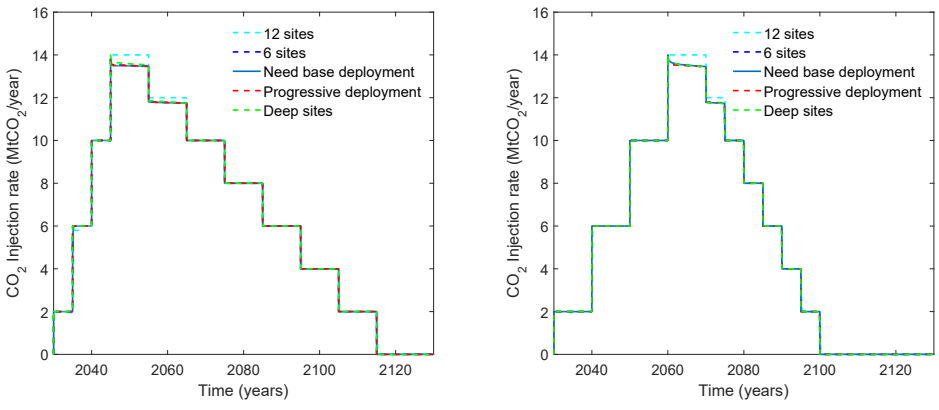

(a) (b)

Figure 4.6: Graph showing CO_2 injection rates obtained as a result of 5 injection site deployment options for storage demand scenario Drax 1 (a) and Drax 4 (b)

In all 5 Drax CCS deployment scenarios considered here, the total targeted

CO_2 injection over the project lifetime is less than or equal to 1 $GtCO_2$. This is in agreement with studies assessing the dynamic storage capacity of the Bunter Sandstone Formation. Heinemann et al. (2012)[139] assesses the dynamic storage capacity of the Bunter Sandstone to be between 3.8-7.8 $GtCO_2$ for thirty years of injection, while Noy et al. (2012)[133] finds a more stringent estimate of 0.75 - 1 $GtCO_2$ for a 50-year injection period.

From a systems level perspective these results suggest that the reservoir behaviour at these levels of injection is indifferent to the rate at which target injection increases to meet increasing demand and the rate at which injection sites are deployed to meet it.

4.3.3 Impact of varying storage demand based on a systems model output of UK coal power with CCS - Set 3

Energy systems models describing the UK's future energy mix still consider a proportion of coal consumption, which remains one of the main drivers for an imminent need for CCS. Figure 4.7 shows the difference between the daily target injection rate and the actual injection rate for the 3 scenarios considered in set 3 (E-system 1-3) within the first five years of injection. It is important to recall that injection is split evenly between all twelve sites described in the Bunter Sandstone reservoir model. The results show that there is an insignificant difference in reaching the target injection rate in each of these scenarios. This is regardless of whether injection is initiated at a high rate with progressive ramp down associated with a reducing 'coal CCS' capacity factor (E-system 1), a lower initial target rate with progressive ramp up of injection associated with increasing the capacity factor for 'coal CCS' (E-system 2) or at a constant average rate of target injection over a 50-year project scope (E-system 3). The early time limits on injection are gridding artefacts that do not impact later time pressure evolution[175,176]. Hence, these results suggest that varying the rate at which injection takes place in the reservoir does not have an effect on the ability to meet storage demand. Therefore, CCS deployment rate predictions that result from energy systems models should be able to consider, that, within the pressure limitation range of each injection site, injection rate variations including ramping up or down will not have an effect on storage capacity and reservoir injectivity.

Considering that the UK could phase out of coal, it is important to note that this result applies for these CO_2 supply rates that can be from any type of source; coal with CCS is just an example used here.

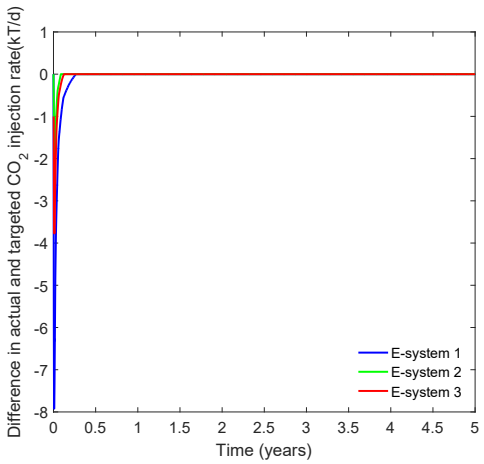

Figure 4.7: Graph showing the difference between the CO_2 injection rate achieved and the target CO_2 injection rate for scenarios E-System 1-3 of Set 3 as described in Table 4.2

4.4 Conclusions to chapter

In this study potential limitations to subsurface storage capacity over yearly and decadal time scales that could result from time-varying storage demand were evaluated. Three sets of scenarios were considered: a theoretical scenario set to explore the effect of time varying rate amplitude, frequency and site location, a set based on the past UK government deployment strategy in the Southern North Sea, and a set based on deployment predictions from an energy systems model of the UK for coal power with CCS.

As a result of a first set of injection scenarios, it was shown that varying amplitude and frequency of CO_2 storage demand has little effect on reservoir pressure response and plume migration. Hence, as long as the total amount of CO_2 injected over several decades is represented in the storage system model, there is no need to include granular variation in injection rates for first order modelling of the type used in systems models. By investigating the pressure build up and injection rate at different injection sites in the reservoir model, it was shown that injectivity does not vary with time, and injection rate per site will be dominated by near-well bore permeability and depth.

In a second set of injection scenarios, UK government led CCS development for different storage infrastructure deployment strategies was envisioned. It was found that reduced injection site deployment, to meet increased storage demand, has no substantial effect on the ability to store CO_2 in the reservoir. In addition, it was shown that this is the case regardless of the rate at which injection is ramped up. Therefore, from a storage infrastructure perspective, it is suggested that injection sites can be deployed as needed and progressively instead of incurring a large upfront cost of deployment to meet future storage demand. Also

highlighted: there may be a trade-off when choosing the sites to deploy first as deeper sites for example will be more costly but may allow for higher injection rates later on.

In the final set of injection scenarios the reservoir response to CO_2 storage demand based on energy systems models predicting the UK coal power with CCS deployment was investigated. It was found that such energy systems models that include CCS do not need to take into account any effects related to the initial response to variation in CO_2 storage demand other than the usual effects related to reservoir permeability and injection.

4.5 Contributions made and future work

The results from this work are very broadly applicable to this reservoir's behaviour in response to the deployment of CCS capacity on any type of point source. While in this work the example of CO_2 from coal firing power is taken, the same result can be drawn from considering CO_2 supply from gas fired power, natural gas processing or heavy industry sources. A reservoir with similar characteristics to those of the Bunter Sandstone (permeability of reservoir and caprock, porosity, average pressure and depth), can expect similar conclusions to be drawn in terms of the ability to provide for varying rates of CO_2 supply. This work also provides a suitable systems framework and example to follow in order to understand the effects and interactions of wider scale CCS deployment on the full CCS chain, from CO_2 supply to CO_2 sequestration.

If investigating timelines of hundreds or thousands of years it may be worth considering the effects of other trapping mechanisms such as CO_2 dissolution and CO_2 mineralization. These are not included here as the timeline considered is only over several decades.

Chapter 5

The role of flexible operations, transport networks and shared infrastructure in reducing the cost of CO_2 capture

This chapter presents a holistic and systems approach to reducing the cost of the CO_2 capture process. The work draws on the flexible operations of multiple capture plants, their interactions with the CO_2 transport system and cohesion of CCS stakeholders in sharing of infrastructure in the aim of reducing overall investment cost in CCS.

This work draws on process models of the CO_2 compression and purification (CO_2-CPU) process in oxy-combustion capture presented by Posch and Haider 2012 (`https://doi.org/10.1016/j.fuel.2011.07.039`)[177] and earlier Pipitone and Bolland 2009 (`https://doi.org/10.1016/j.ijggc.2009.03.001`)[178]. Both looked at designing the process for minimum compression work and cooling duty. Reproducing and modifying these in ASPEN HYSYS, this work presents the first full account and breakdown of the cost of this process and its variations. This is particularly important because the CO_2-CPU accounts for at least half of the cost of oxy-combustion CO_2 capture.

Three key results are presented here. The first is in identifying a significant trade off between the purity of captured CO_2 and cost of the modelled CO_2-CPUs. The second, is a novel approach to using pipeline transport networks to minimize the cost of capture through a multi-source to sink CO_2 transport system. The third is a proposed process model that exhibits that the cost of sharing capture infrastructure could be highly beneficial to large-scale CCS deployment.

The bulk of this work is published in Kolster et al. 2017 (`https://doi.org/`

10.1016/j.ijggc.2017.01.014) and was presented in the Early Stage Assessment report of this thesis. This work was conducted with supervisors Niall Mac Dowell and Sam Krevor and with inputs on the modelling from Evgenia Mechleri. The cost values and metrics have been adjusted from the aforementioned publication (to 2016 USD) in order to maintain consistency throughout the thesis. An open-source financial model, CPU-INVEST, used to calculate the price of CO_2 needed to meet an investor's required rate of return for investing in a CO_2-CPU, is developed in MATLAB and can be accessed and downloaded here: https://doi.org/10.5281/zenodo.1230482.

5.1 Background to the link between CO_2 purity, capture, transport and storage

Purity requirements for CO_2 in transport and storage have been set at high levels, between 95% and 99.9% purity in most instances and with strict limits on moisture and oxygen content. The precise requirements on purity have varied with region and protocol. The EU CCS directive for example says that a CO_2 stream for subsurface storage needs to "overwhelmingly consist of CO_2" [179], which has been associated with a widespread requirement of at least 95% CO_2 content [180–182]. The first industry to have dealt with CO_2 on a scale of hundred millions of tonnes, is the oil and gas industry and most CO_2-centered regulations have been inherited from this industry [183]. The CO_2 used in the oil and gas industry has been predominantly from high purity and cheap sources of CO_2 such as natural CO_2 reservoirs or from natural gas processing and used for enhanced oil recovery (described in Chapter 3) [56,69,103,184]. Also, when discussing purity requirements of CO_2 transport via pipeline, these have generally been set by final storage requirements. However, although currently operating large-scale CCS plants such as the Boundary Dam plant in Saskatchewan and Petra Nova CCS in Texas, are single-source to single-sink systems, the same is unlikely to be true once multiple CCS plants are in operation and in close proximity, with transportation networks being more cost-effective [185–187].

With oxy-combustion and membrane CO_2 capture processes, the level of purity required for the final CO_2 stream is largely what drives the high cost of capture. This is not the case in adsorption-based post-combustion capture technologies which, by virtue of their high selectivity, inherently produce a high purity stream of CO_2 [188]. In oxy-combustion capture, the raw exhaust gas exiting from an oxy-combustion boiler is around 80% CO_2 with the balance composed of N_2,

O_2 and Ar (non-condensables), and H_2O and other trace elements[1]. A capital and energy intensive CO_2 compression and purification unit (CPU) is then used to dehydrate the stream, strip it of the non-condensables and compress it.

Table 5.1 shows the typical CO_2 composition recommendations for CO_2 transport and storage whilst only considering a source-to-sink approach where both recommendations - for transport and storage - are one. Certain impurities however may have a negative effect on transport and none on storage and vice versa. While the final CO_2 storage destination imposes a hard constraint on CO_2 purity, it is possible to safely transport CO_2 containing some impurities such as N_2, O_2 or Ar, as long as the amount of water is limited to the parts per million (ppm) level[189]. The presence of H_2O in the CO_2 stream, for example, is detrimental to transport and injection material as it can cause corrosion, but has no effect on storage efficiency as it is already present in geological reservoirs[190]. High contents of water in the pipeline can result in hydrate formation which causes plugging [191].

Large volumes of CO_2 (on the scale of 1 $MtCO_2$/year[192]) are best transported as a supercritical/dense phase fluid[193] and phase changes associated with pressure or temperature changes should be avoided for safe operation of the pipeline. It must further be recognized that the pressure to which the CO_2 stream needs to be compressed to ensure safe operation of the transport element is a strong function of the composition of that stream [192,194]. This pressure requirement increases in proportion to the fraction of impurities in the stream as they bring the mixture's two phase region above that of pure CO_2.

Yan et al.[180] studied the effect of a change in inlet stream composition on the pipeline inlet pressure requirement and have shown that an inlet stream of 87 vol% CO_2 requires a 17% increase in inlet pressure compared to an inlet stream of 96 vol%. Wetenhall et al.[195] has shown that a higher content of non-condensable gases in the inlet stream increases the pipeline inner diameter and thus the relative cost per km of pipeline. However, Yan et al.[180] demonstrated that over a short pipeline distance of 30km, there is no change in pipeline cost with product purity and transporting lower purity CO_2 streams is reasonable over these distances. Hence, in a context in which transport networks are considered - with multiple pipelines joining into a trunkline linking to a storage sink - lower purity CO_2 streams can be inserted into the network before joining higher purity CO_2 streams and when mixed in the pipeline will reach desired purities.

Other studies, such as Mahgerefteh et al.[196], modeled the likelihood of propagating fractures in pipelines as a function of the content of non-condensable

[1] SO_x and NO_x

Table 5.1: Typical oxy-combustion flue gas composition from a coal fired power plant (a.), typical CO_2 composition for EOR (b.) and Dynamis CO_2 stream quality recommendations (c.)

	a.Flue gas composition range by mass (volume) from coal fired oxy-combustion plants[177]	b.Weyburn EOR project CO_2 composition by volume[5]	c.Dynamis recommendations for CO_2 quality by volume[177]
CO_2	0.793-0.824 (0.724-0.764)	>0.960	>0.955
N_2	0.078 - 0.099 (0.113-0.142)	<300 ppm	<4%
O_2	0.061-0.076 (0.078 - 0.095)	<50 ppm	<4% (saline aquifers) 100-1000 ppm (EOR)
Ar	0.028 - 0.031 (0.028 - 0.031)		<4%
SO_2	200 ppm (100 ppm)		<100 ppm
H_2O	0.048 - 0.059 (0.010 - 0.014)	<20 ppm	<500 ppm

gases in the CO_2 stream. This theoretical study implied that, if a crack occurs in a pipeline containing an oxy-combustion derived CO_2 stream of 88.4% purity, the crack would propagate creating a long running fracture, whereas a pure CO_2 stream in the same pipeline would not cause the crack to propagate. It is important to note that fracture propagation is a strong function of the pipeline external temperature, this phenomenon is ultimately driven by the fact that the saturation pressure of an impure CO_2 stream is greater than that of a pure CO_2 stream. Hence, de-pressurisation of the pipeline results in rapid phase change (dense phase to vapour phase) and subsequent cooling, which makes the pipeline prone to fracture propagation [196]. However, it is important to note that these conclusions have not been corroborated by experimental data[197].

The design of the transport system is then a function of the final storage sink chosen: saline aquifers [2] or depleted hydrocarbon reservoirs and the potential to use the stream for enhanced oil recovery (EOR). A CO_2 stream suitable for EOR is commonly regarded as needing to be of very high purity, with limits on O_2 concentration at about 100ppm[92]. High levels of oxygen in the CO_2 stream used for EOR risks causing overheating at the injection point, oxidation and biological growth in the reservoir [178]. However, a number of studies have pointed out that there is a lack of fundamental research and industrial experience with anthropogenic CO_2. The actual level above which a 'high level' of oxygen is reached and

[2]Saline aquifers are likely to provide the largest storage capacity with an estimated global storage potential of 10,800 Gt_{CO_2} [198] while depleted hydrocarbon reservoirs provide an estimated storage capacity of up to 1,000 Gt_{CO_2} [116]

associated risks become plausible remains highly uncertain[178,199]. This is linked to that fact that most of the regulations and common practices for CO_2-EOR are based on North-American experience[192]. An example of a naturally occurring CO_2 stream used for EOR is from the Sheep Mountain CO_2 reservoir in the US that contains 97 vol% CO_2, 0.6 vol% N_2, 2.4 vol% CH_4 and trace amounts of water. This stream of natural CO_2 is typically delivered to the oil producers at a pressure of 97 bar and at a temperature below 24°C [200].

The presence of impurities in CO_2 is also found to have an impact on storage and was demonstrated as part the EU's IMPACTS project[182]. The IEA GHG R&D Programme [190] studied the reduction in storage capacity as a result of higher fractions of non-condensables in the CO_2 stream. This study showed that in a saline formation at a depth of 895m, 92 bar and 33°C a high impurity CO_2 stream with 15% non-condensables reduces the storage capacity by 39% compared with a pure stream of CO_2. It is, however, important to note that the quantity of storage available would be sufficient to provide storage for several centuries [3] and therefore should not be considered a limiting factor.

Under the EU's 7th Framework Programme for research, the IMPACTS project, initiated in 2014, set out to improve the understanding of effects of CO_2 quality on transport and storage in order to to establish appropriate regulations for CCS projects[182,183,202]. As part of this, Eickhoff et al. 2017, used a simple cost function approach to show increasing purity at CO_2 capture point sources shows a linear increase in operating cost and a step-wise increase in capital cost and is not specific to a particular capture process[182]. In contrast to the IMPACTS project, this work has identified and examined the potential trade off between the cost of capturing CO_2 in oxy-combustion and the purity at which the final CO_2 product is produced with a detailed techno-economic modeling methodology.

Furthermore, a large number of studies continue to consider a source-to-sink approach, particularly for CO_2-EOR[92,200]. Although several studies have alluded to the benefits of having CO_2 transport networks[185,186,195,203], these have yet to demonstrate economic benefits that could stem from having such networks.

This work is novel in that it considers the combination of CO_2 streams from various point sources into a transport network that leads to one major trunkline stream ready for injection. This study demonstrates the benefits of a flexible capture system, the oxy-combustion CO_2-CPU, and how shared infrastructure, beit on the transport or capture side can reduce the cost of CO_2 capture for wider CCS network.

[3] 2017 CO_2 annual emissions rate is at ~37 $GtCO_2$ [201]

5.2 Oxy-combustion CO_2 capture

As described in Chapter 1, oxy-combustion capture is one of three main promising and well understood CO_2 capture technologies. However, the trends in large-scale CCS projects so far have all used post-combustion capture[4]. Reducing the cost of oxy-combustion capture, could improve the incentives for oxy-combustion capture versus post-combustion and increasingly drive down the cost through 'learning by doing'. Oxy-combustion capture does allow for improved combustion efficiency[17] and can in principle be applied to any type of fuel used for thermal power generation[181].

The oxy-combustion capture process, as illustrated in Figure 5.1, consists of separating oxygen from air, using an energy intensive Air Separation Unit (ASU), mixing the oxygen (and some excess nitrogen) with recycled flue gas and thereby providing a high-oxygen environment in which to burn the fuel of choice. This part of the system produces a saleable product, electricity, and a waste product, flue gas. The flue gas produced is rich in CO_2 but still requires further purification and compression (see Table 5.1). While when retrofitted to a power plant, the ASU may be an added piece of equipment, employing oxy-combustion capture for industrial CO_2 capture, where ASUs are already in use could prove most viable.

The flue gas then goes through a CO_2 compression and purification unit (CO_2CPU) with a high energy demand and produces a dehydrated, high purity, high pressure CO_2 product ready for transport and a waste product made up of impurities (H_2O, O_2, N_2, Ar, SO_2) and lost CO_2.

Both the CO_2CPU and ASU impose approximately the same energy penalty on the power plant - each reduce the overall power plant efficiency by approximately 5% relative to the base plant efficiency [17]. Owing to the relatively impure raw exhaust gas which is produced from the oxy-combustion boiler, the CO_2CPU is crucial to providing a CO_2 stream that is suitable for transport and subsequent sequestration. Thus far, work has been done on maximising the economic revenue of the ASU[204] and minimizing the energy penalty caused by the ASU[17,205–207], while relatively little focus has been given to the cost of the CO_2CPU and how to drive this down. A few studies, however, have looked at modeling the purification and compression process of oxy-combustion derived flue gas for usage in EOR and for its sequestration [177,178,208]. In this work, the CO_2CPU part of the oxy-combustion capture process is modeled in Aspen HYSYS, considering four different designs each with a different product gas purity, and looks at how this process can be manipulated to reduce the costs associated with oxy-combustion CCS.

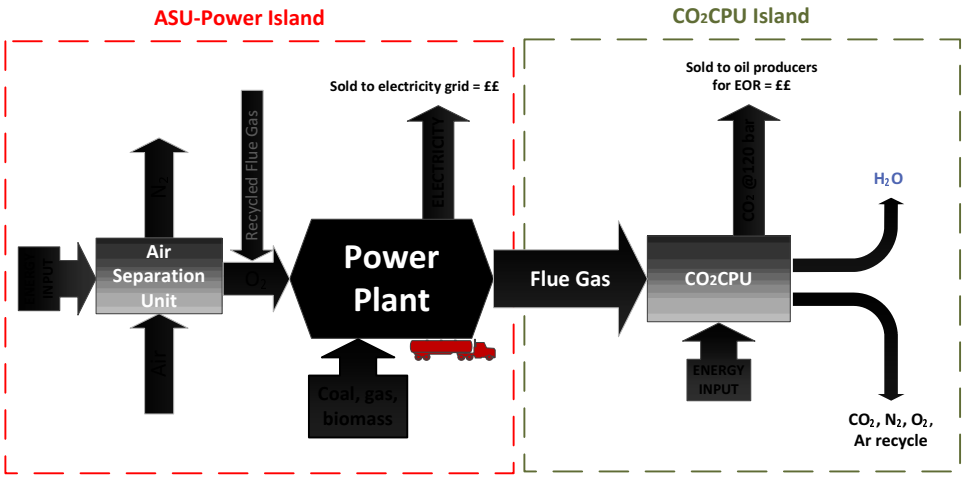

Figure 5.1: Illustrative diagram of the oxy-combustion capture process highlighting the main energy intensive units and potential revenue sources and outputs for each island: the ASU island and the CO_2CPU island.

5.3 Techno-economic modelling of four variations of the CO_2 compression and purification unit (CO_2-CPU) for oxy-combustion capture

5.3.1 Process modelling methodology

The flue gas produced by oxy-combustion will vary in purity depending on a number of factors, including the type and quality of the fuel burnt, the amount of flue gas recycled for combustion and the water content (see Table 5.1). Therefore, the flue gas still requires dehydration, further purification and compression in order to be suitable for transport and storage. As discussed, the latter is performed by means of a CO_2CPU.

In view of the importance of the CO_2CPU within the oxyfuel combustion capture process, four variations of this process were modelled in Aspen HYSYS following previous work by Posch et al. [177]. These different models analyse the trade-offs that exist between purity of the CO_2CPU product and its cost, and are all based on typical phase separation techniques [177,178,208] widely used in carbon capture processes. The first CO_2CPU model is the most simple, consisting

of a 6-stage compression and dehydration system only. As compression and dehydration is also required in post combustion capture, this model is applied to both scenarios: oxy-combustion flue gas and post-combustion CO_2 product (see Figure 5.2). The three remaining models are built on the compression and dehydration model with increased complexity and different product purities. The first, in order of complexity, consists of a low purity double flash system without heat integration (see Figure 5.5), followed by a double flash system with heat integration (see Figure 5.4) and a high purity product and finally a CPU process with a 6-stage distillation column with incorporated heat integration (see Figure 5.6). As these models increase in complexity, they increase in product purity and energy penalty while decreasing in separation efficiency.

These models use the Peng-Robinson equation of state[209] and mixing parameters of Kopke et al. 2008 [210]. This property method is suitable for the simple, non-associating fluids considered in the flue gas (CO_2, H_2O, N_2, Ar, O_2, SO_2) and the range of temperatures (-60°C to 250°C) and pressures (1 bar to 120 bar) relevant to this study. Each plant was assumed to have 8460 working hours per year and a plant lifetime of 35 years. The flue gas inlet composition and flow rate are based on a pulverized coal firing power plant at nominal load [177]. These values are outlined in Table 5.2.

Table 5.2: Example of flue gas properties from an oxy-combustion pulverised coal firing power plant at nominal load generating 347 MWe from Posch et al. 2012[177].

Flue Gas Porperty (CPU inlet)	
Temperature (Celsius)	13.2
Pressure (bar)	1
Flow Rate (tonne/hour)	342.7
Composition (mass fraction/mole fraction)	
CO_2	0.824/0.764
O_2	0.061/0.078
N_2	0.080/0.113
Ar	0.031/0.031
H_2	0.006/0.013
SO_2	200(ppm)/100 (ppm)

5.3.2 Process model 1: The 6-stage CO_2 compression and dehydration model

The 6-stage CO_2 compression and dehydration model is the least complex of the CO_2CPU models. The flue gas enters the system at 1 bar and 13°C and goes through a 3 stage pre-compression train with an inter-stage cooling and flash system. After each compression stage the flue gas exits at 10 bar, 20 bar and 30 bar in that order. All compressors are centrifugal with a polytropic efficiency of 85%. This applies to all compressors in the CO_2CPU models presented in this chapter. Each inter-stage cooler, which uses cooling water at 20°C reduces the flue gas temperature to 25°C in order to avoid overheating of the system as the gas is compressed. The fluid then goes through a flash after each compression-cooling stage. Once the flue gas has reached 30 bar, it is sent through a dehydrator. After each 3 stage pre-compression the flue gas is then taken through a dehydration system, which is described in more detail later on. Finally, the dry fluid exiting the dehydrator is compressed to 60 bar, cooled to 25°C compressed again to 80 bar, cooled to 15°C using refrigerant propane and compressed a final time to 120 bar - a fluid pressure suitable for pipeline transport[192]. Here, it was assumed that at 120 bar and above, the CO_2 streams considered are all supercritical (well above the critical point).

This process gives a CO_2 product at 82.9 wt% purity. It is important to note that the composition of the CO_2 product stream obtained will vary with the composition of the inlet stream.

In post combustion CO_2 capture a compression and dehydration unit is also required to eliminate the remaining water in the stream and obtain a pressure adequate for transport. This process model is represented in figure 5.2 and its respective inlet and outlet conditions are highlighted. The characteristics of the CO_2 stream entering the system are shown in Table 5.3. The wet CO_2 stream enters the CO_2CPU at 98.5wt% CO_2 and exits at 99.97wt.% purity.

Table 5.3: CO_2 product stream characteristics from an amine-based post combustion capture process [24]

CO_2 (wt%)	H_2O (wt%)	N_2 (wt%)	O_2 (wt%)	Temperature (°C)	Pressure (bar)
98.5	1.5	200 ppm	100 ppm	35	2

The post combustion stream entering the CO_2CPU is at a pressure of 2 bar - as opposed to 1 bar in the oxy-combustion system - which is the typical pressure

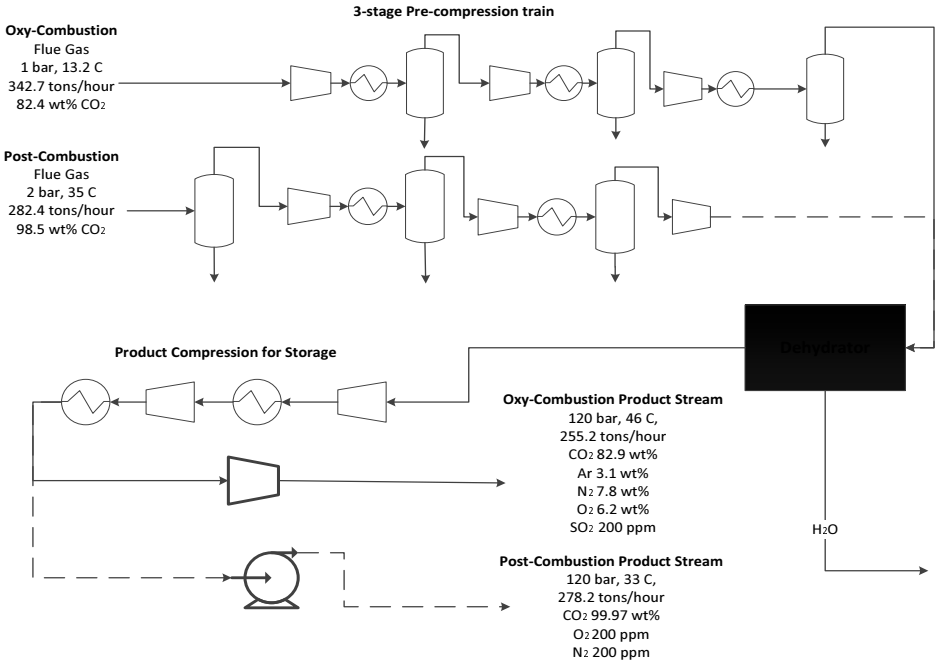

Figure 5.2: Flow diagram of a compression and dehydration process consisting of a three-stage pre-compression train, a dehydration unit and a final product compression train applied to both a post combustion product stream and an oxy-combustion derived flue gas stream

for the stripper/solvent regeneration column in amine-based post combustion [17,24]. In the model, the post-combustion stream first enters into a flash prior to the first compressor and cooler. This is due to the fact that a fraction of the stream entering the system is in aqueous phase. The rest of the pre-compression train then follows the same pattern - the first compressor takes the stream up to 10 bar, the next to 20 bar and the third to 30 bar - with the exception of the last cooler and flash combination. The installed cost per tonne of CO_2 captured yearly for different process units (compressors, pump and coolers) and the electricity cost per tonne of CO_2 captured are illustrated in Figure 5.3. Cooler 3 referenced in Figure 5.3 only applies to the 3-stage pre-compression train in an oxy-combustion CO_2CPU and is not present when applied to post-combustion (see Figure 5.2).

Two versions of the CO_2CPU pre-compressions train needed for post combustion capture were modeled, in order to establish the proportion of system cost allocated to the difference in inlet pressure and stream composition when compared to a CO_2CPU for oxy-combustion capture. An additional \$ 4.1/tCO_2 processed would be added to the installed cost of compressor 1 if the inlet stream

pressure were at 1 bar rather than 2 bar. An additional \$ 2.9/tCO_2 captured yearly would be added to the annual electricity costs if the inlet stream of the post combustion CPU were at 1 bar as opposed to 2 bar. This implies that the remainder of the difference in electricity costs between the post combustion and oxy-combustion CO_2CPUs (\$ 3/tCO_2 captured yearly) is due to the higher amount of impurities in the oxy-combustion process streams. A study by the IEA GHG R&D Programme explains that the larger presence of non-condensable gases with critical temperatures and pressures below that of CO_2 shift the two phase region upwards[190]. These non-condensable gases then take up a larger volume of the fluid and more work is required for compression. The use of a pressurized combustion process for oxy-combustion could therefore substantially reduce both the capital and operating costs associated with the first compressor of the CO_2CPU. However, compressing high purity oxygen for combustion in turn has very high cost implications due to the special materials that would be required for the compressor and piping to avoid oxidation[211]. A number of operational and safety issues would also need to be considered when designing a combustion chamber for oxy-combustion as described in the IEAGHG report on Oxy Combustion Processes for CO_2 Capture from Power Plant[212]. The remaining difference in installed cost of compressors for each system results from the difference in density between the two streams.

Furthermore, coolers 4 and 5 have higher installed cost per tonne of CO_2 captured in the post combustion system. This is due to the molar enthalpy of the stream going through coolers 4 and 5 being much lower in the post combustion system than it is in the oxy-combustion system thereby requiring more heat exchange surface. Finally, coolers 1 and 2 have very small installed costs per tonne of CO_2 captured (between \$ 0.08/tCO_2 and \$ 1/tCO_2), while cooler 3 is only present in the oxy-combustion version of this CO_2CPU.

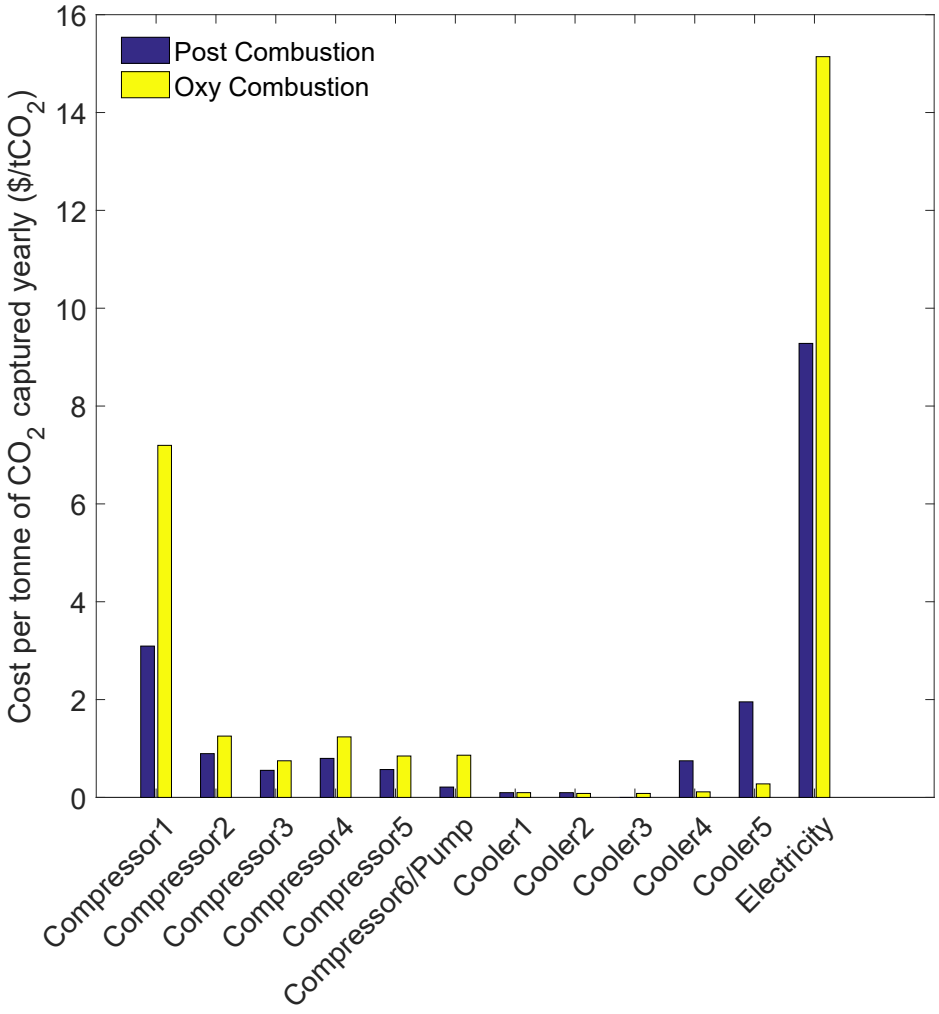

Figure 5.3: Bar chart comparing installed equipment cost and electricity costs of the oxy-combustion and the post combustion 6-stage compression and dehydration CPU systems

5.3.3 Process model 2: High purity double flash CO_2-CPU with heat integration

The high purity double flash CO_2-CPU with heat integration, a second model of the CO_2CPU, is developed with increased complexity. This model brings in the same flue gas as described in Table 5.2 and takes it through a 3 stage pre-compression train with an inter-stage cooling and flash system. As in the previous model, the flue gas is compressed to a pressure of 30 bar and the flue gas is sent through a dehydrator.

The dehydrated and compressed flue gas is cooled down to -27°C via multi stream heat exchanger 1 and then goes into flash 1 (see Figure 5.4). Out the bottom of flash 1, a CO_2 rich stream is expanded in an adiabatic throttle and is used as a cooling agent in multi stream heat exchanger 1. The top product

from flash 1 is the CO_2 poor stream with a CO_2 mass fraction of 0.67. This stream is recycled and cooled in multi stream heat exchanger 2 to -54°C before going through flash 2. The CO_2 product out the bottom of flash 2 remains at approximately -54°C and is used as a cooling agent in multi stream heat exchanger 2. This stream is then expanded through an adiabatic throttle to 8 bar and recycled through multi stream heat exchanger 2 and again through multi stream heat exchanger 1. The cooling potential of the top gaseous products of flash 1 and flash 2 are also recycled through multi stream heat exchangers 1 and 2 as illustrated in Figure 5.4.

Finally the bottom products from flash 1 and flash 2 are mixed together, forming a high purity CO_2 stream at 8 bar and -10°C. The product stream then goes through a two stage compression (60 bar then 80 bar) with inter-stage cooling, bringing the stream down to 25°C after each compression, then pumped up to 120 bar. The final product stream achieves a CO_2 purity of 97.5 wt.%.

The waste stream from the CO_2CPU system is the top product of flash 2 with remaining cooling potential at 30 bar and -35 °C . At appropriate temperature and pressure, this waste stream could be used as a flue gas recycle into the combustion chamber.

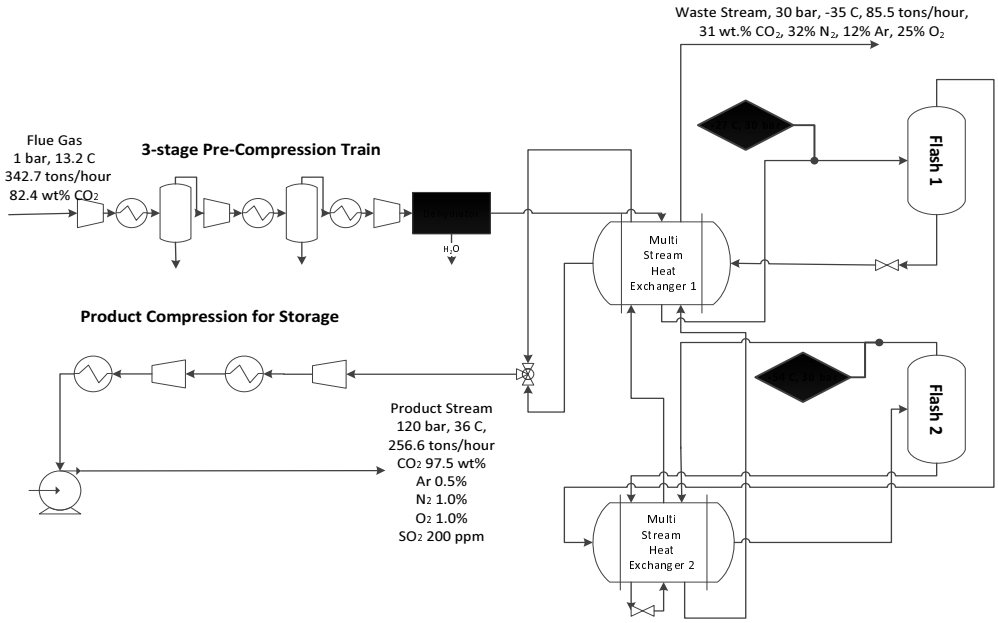

Figure 5.4: Flow diagram of a double flash CO_2CPU system model with heat integration consisting of a 3-stage pre compression train, a double flash separation system and dehydrator and a final product compression train resulting in a high purity CO_2 product stream

A range of temperatures and pressures were tested for the system bearing in

mind that the triple point of CO_2 is at 5.19 bar and -56.6°C[213]. The temperature and pressures outlined above were found most suitable for obtaining a high purity CO_2 stream whilst minimizing compression and cooling duty as described in the work by Posch et al.[177].

5.3.4 Process model 3: Low purity double flash CO_2CPU without heat integration

The low purity double flash CO_2CPU without heat integration, a similar double flash CO_2CPU system, was also modeled in Aspen HYSYS using much higher pressure (68 bar after the upstream compression train) and higher temperature (-18°C stream coming into Flash 1). The operating pressure of 68 bar was chosen because at that pressure and very low temperatures (between -55°C and -44°C) a mixture of CO_2, N_2 and O_2 was separated into a liquid and a vapour phase with most of the CO_2 in the liquid phase and most of the N_2 and O_2 in the gas phase [214]. Since Ar behaves very similarly to N_2 and O_2 at such pressure and temperature [190], the same operating pressure and temperature is used in the Aspen HYSYS model.

Once the flue gas is compressed to 68 bar in the pre-compression train, dehydrated then cooled to -18°C it then goes through a first flash with a CO_2-rich bottom stream at 92.7wt.% purity. The top product, still containing 15% of the CO_2 in the system, is cooled to -55°C and taken through a second flash that produces a CO_2 rich bottom product at 91.3 wt.% CO_2 and a waste stream top product with some remaining CO_2. Each of the bottom product CO_2 streams are taken through adiabatic throttles and expand to 10 bar at which point they mix and form a stream of 92.6wt.% CO_2 and are compressed up to 120 bar in the final compression stage.

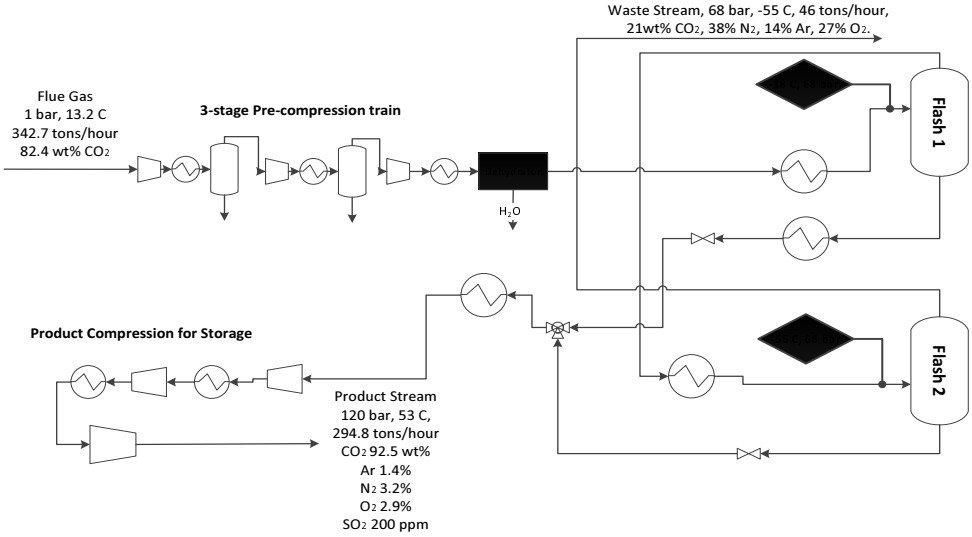

Figure 5.5: Flow diagram of a double flash CO_2CPU system model without heat integration producing a low purity CO_2 product, consisting of a 3-stage pre-compression train, a double flash separation system and dehydrator and a final product compression train

5.3.5 Process model 4: CO_2CPU with a 6-stage distillation column

The CO_2CPU with a 6-stage distillation column, the third viable CO_2CPU model, represents the most complex system. The 3-stage pre compression train shown in Figure 5.6 is identical to that in the 6-stage compression and dehydration unit (see Figure 5.2) with the exception of the third compressor that brings the flue gas to a pressure of 28 bar. After going through the pre-compression stage, the flue gas is sent to a dehydrator as for all the other process models. Once the stream is dry it goes through the multi-stream heat exchanger where it is cooled to -35°C . This stream then goes through the 6 stage distillation column, comprising of a partial condenser with flash 1 at the top and a partial reboiler with flash 2 at the bottom. Flash 1 splits the top product into a vapour fraction of 0.45, whereas flash 2 splits the bottom product into a vapour fraction of 0.75. Six stages for the distillation column was found to be optimum in giving a good trade-off between the high purity of the CO_2 stream coming out as the liquid bottom product and the higher flow rate of CO_2 coming off the top of the distillation column[177].

The top vapour product passes through the multi stream heat exchanger and

is cooled to -55°C and then the vapour-liquid mixture is separated in flash 3. The CO_2-rich bottom product from flash 3 passes through an adiabatic throttle where it is expanded and cooled to -55.5°C and its cooling capacity used through the multi stream heat exchanger, then compressed back up to 28 bar and cooled down to -35°C before being recycled back into the inlet stream of the distillation column. The top product of Flash 3 (the waste stream) is expanded and cooled through another adiabatic throttle to -66°C and its cooling capacity used through the multi stream heat exchanger. This stream contains only 25mol% CO_2 and the remainder is a combination of O_2, N_2 and Ar. Due to the very low freezing points of the latter components, -219°C -210°C and -189°C respectively, the freezing point of the mixture is well below -66°C [215].

The CO_2-rich distillation column's bottom liquid stream then passes through an adiabatic throttle where it is expanded and cooled to -54°C and is used for its cooling potential through the multi-stream heat exchanger, before being sent through to the final compression stages and pumped up to 120 bar, 36°C and achieving a final CO_2 product purity of 99.98 wt.%.

The choice of temperature and pressure going into the distillation column were based on minimising compression duty whilst maximising cooling capacity circulated in the system. Posch et al. [177] found that entering the distillation column at 28 bar was best in satisfying cooling agent demand and entering at a temperature of -35°C was optimal for minimising compression duty in the system.

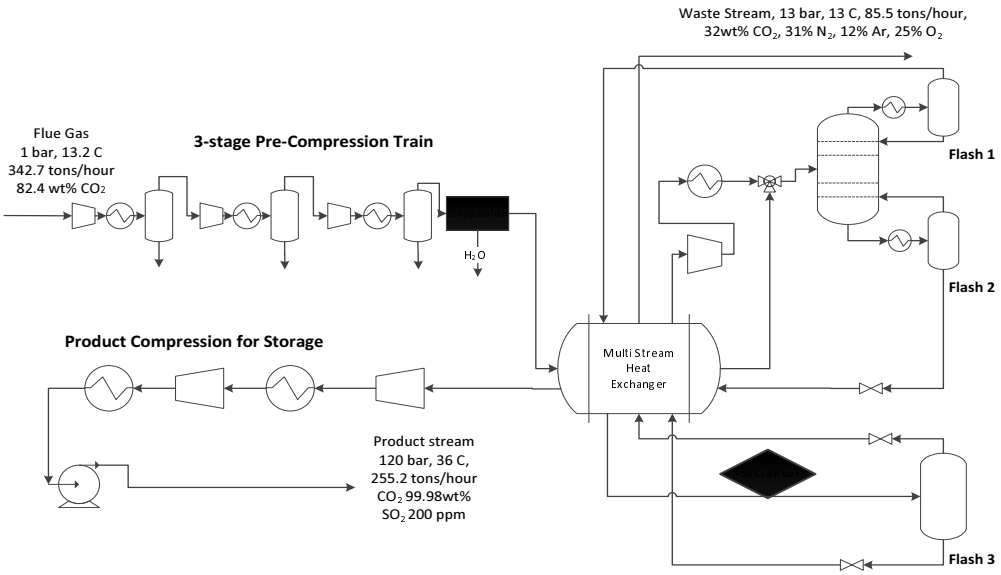

Figure 5.6: Flow diagram of a CO_2CPU system model with a 6-stage distillation column separation process using heat integration, a dehydrator and pre & post processing compression

5.4 CO_2CPU System Performance

5.4.1 Product Purity, System Efficiencies, Capital and Operating Costs

For each CO_2-CPU process model presented in section 5.3.1, economic evaluations were conducted using the Aspen HYSYS economics tool in order to obtain detailed system cost and performance. These are summarized in Table 5.4. The default utility assumptions used in Aspen HYSYS are presented at the end of this Chapter A1. Given the extensive ASPEN Tech database on unit operations and cost, it was assumed that these are at the nth of a kind stage (NOAK). The economic evaluations and financial analysis that follows were converted from constant 1st quarter 2013 GBP (as given in Aspen[216,217] and presented in the aforementioned publication of this work) to 2016 USD. Conversion to USD was based on average currency exchange rate on January 31st 2013 (1 GBP = 1.5826 USD) and adjusted to 2016 USD with a consumer price index of 102.88%[218].

The results in Table 5.4 show that as the models increase in complexity and product purity (descending order of complexity: Distillation, Double Flash with

Table 5.4: System performance and economic evaluation of all CO_2CPUs modeled (*separation efficiency only applies to the CO_2CPU of the post combustion system)

Property of CPU	Distillation CPU	Double Flash CPU		Compression and Dehydration Unit	
		High Purity	Low Purity	Oxy-Combustion	Post Combustion
CO_2 product stream Mt/year	2.16	2.25	2.49	2.88	2.35
Separation Efficiency	90%	92%	97%	100 %	100%*
CO_2 Purity	99.98 wt.%	97.54 wt.%	92.55 wt.%	82.91 wt.%	99.97 wt.%
Oxygen Content	0.4 ppm	1.03 wt.%	2.89 wt.%	6.18 wt.%	150 ppm
Total Capital Cost	$ 83M	$ 55M	$ 68M	$ 54M	$ 38M
Total Yearly Operating Cost	$ 55M	$ 52M	$ 59M	$ 46M	$ 28M

Heat Integration, Double Flash without Heat Integration, Compression and Dehydration), the capital costs (CAPEX) and operational costs (OPEX) incurred increase as well. This is due to an increase in energy requirement per tonne of CO_2 captured and an increase in power plant net efficiency loss with increased complexity and product purity.

Notably, the 6-stage Distillation CPU model with a capital cost of $ 83 million presents a much higher cost burden than the other CO_2CPU models. This is primarily due to the presence of the distillation column. Unsurprisingly, the double flash system without heat integration (low purity output) was found to have the second highest capital cost at $ 68 million, which is mainly due to the larger compressors required upstream (compression to 68 bar) and the large heat exchange areas required for the interstage cooling upstream. In addition, the operating costs incurred for the distillation CPU and the double flash *with* heat integration (high purity) CPU systems are substantially higher than for the CO_2 compression and dehydration unit, $9 million and $6 million higher, in spite of starting and ending at the same pressures.

In addition, the power plant net efficiency loss (in percentage points) caused by each type of CO_2CPU was calculated assuming that the power plant output without the capture plant was 347 MWe and that the average efficiency of a pulverized fuel coal fired power plant is of 40% (LHV basis) [219].

The main process results, capital and operating costs for all process models, including the CPU for a post combustion derived flue gas are presented in Table 5.4. These results are compared with other oxy-fuel purification process models with similar product streams presented in literature. White et al. [208], for example, finds that for an oxy-fuel CO_2 purification system taking a CO_2 stream from 1 to 110 bar and achieving a purity of 99.97 mol% CO_2, requires 177 kWh/tCO_2 captured. Similarly, the Distillation CPU process model consumes 172 kWh/tCO_2 captured at a purity of 99.98% (see Table 5.5).

The separation efficiency is the amount of CO_2 that is captured in the product stream over the amount that comes into the CPU system and calculated here:

$$\eta_{sep} = \frac{\dot{m}_{CO2,product}}{\dot{m}_{CO2,inlet}} \tag{5.1}$$

where:

η_{sep} = Separation efficiency of CO_2 from the initial flue gas into the system

$\dot{m}_{CO2,product}$ = Mass flow rate of CO_2 out of the system (after product compression for storage)

$\dot{m}_{CO2,inlet}$ = Mass flow rate of CO_2 into the system (before pre-compression stage)

As the separation efficiency increases the amount of work required per tonne of CO_2 captured decreases with it. This is because lower purity product streams, lose less CO_2 in the separation process as it becomes increasingly difficult to separate CO_2 from non-condensable gases with similar properties. This is consistent with the results presented by White et al.[208]. Hence, while the systems decrease in product purity and complexity, they increase in separation efficiency. The compression and dehydration system captures 100% of the CO_2 in the system, whereas the Double Flash without heat integration and with heat integration capture 97% and 92% of the CO_2 entering the system as a raw flue gas. The 6-stage Distillation CPU process captures only 90% of the CO_2 entering the system. Hence, with decreased system complexity, less CO_2 would be vented to the atmosphere and indeed more of the CO_2 coming into the system would be captured. In a context in which unabated CO_2 would be penalized, a lower separation efficiency may also imply a higher system cost.

These results indicate that a trade off will need to be made between purity and capture efficiency. Also, a higher purity product may bare the risk of a high capital cost investment while a lower purity product obtained at lower capital cost may have a smaller investment risk, but less suitable for transport or storage. Similarly, achieving higher product purity requires more energy and electricity costs, and if assumed to contribute to the power plant's energy output, it would reduce power plant efficiency by higher percentage points.

The system costs for the compression and dehydration unit applied to a typical amine-based post combustion stream are significantly lower than that of the same process model used for an oxy-combustion derived stream, with a capital cost of $ 38 million and $ 54 million respectively and an $ 18 million difference in yearly operational costs. As portrayed in Figure 5.3, this is a result of the difference in inlet pressures as well as the larger amount of non-condensable gases

present in the oxy-combustion derived stream causing additional compression work.

Table 5.5: Power plant net efficiency losses and CO_2 separation efficiencies resulting from all of the CO_2CPUs modeled (*separation efficiency only applies to the CO_2CPU of the post combustion system)

Property of CPU	Distillation CPU	Double Flash CPU		Compression and Dehydration Unit	
		High Purity	Low Purity	Oxy-Combustion	Post Combustion
Separation Efficiency	90%	92%	97%	100 %	100%*
CO_2 Purity	99.98 wt.%	97.54 wt.%	92.55 wt.%	82.91 wt.%	99.97 wt.%
Unit Energy (kWh/tCO_2 captured yearly)	172	150	158	103	96*
Power Plant Net Efficiency Loss Breakdown	5.7% CPU	5.1% CPU	6.0% CPU	4.5% CPU	3% CPU
	5% ASU[17]	5% ASU[17]	5% ASU[17]	5% ASU[17]	6% Regeneration 1% Solvent Transport

5.4.2 Investing in a CO_2-CPU

While system performance and upfront costs, as described above, are key measures to inform decision makers and process optimization, investors will look for a measure of rate of return on investment and hence a market for the service or product provided. Assuming therefore, that there is a market for captured CO_2, *e.g.* in its use in EOR or in receiving a credit for sequestration, the process model costs are translated into a price on CO_2, *i.e.* what the value of CO_2 on a metric tonne basis needs to be for investment in a CO_2CPU to be lucrative.

The CO_2CPU is assumed to be an entity independent of the power plant and the ASU, as represented in Figure 5.1. This implies that the cost of the ASU will impact the cost of electricity output from the power plant, but the cost of the CO_2CPU will not. It was assumed that the CO_2CPU has two inputs - a raw material/waste by-product (flue gas from the power plant) and a set of expenses (energy cost) - and two key outputs - a product/revenue stream (CO_2 at high pressure and purity) and two waste streams: a gas mixture (CO_2, N_2, O_2 and Ar) and water. A price for the CO_2 product from each of the CO_2CPU process options was then derived assuming that the investments in the CO_2CPU would only be made if a set rate of return post tax is met. A minimum required rate of return of 15%-20% is deemed appropriate for an early-stage project, which is typically how CCS has been perceived. In theory, as CCS becomes more widespread, investor confidence would increase and minimum required rate of return could be reduced to 5%-10% [203]. This analysis assumes that a lower purity CO_2 stream would have the same market share as a higher purity CO_2

stream.

Using the results produced by the Investment Analysis function in Aspen HYSYS, which includes capital cost, cost of goods sold, general & administrative costs and tonnes of CO_2 captured per year, a net present value (NPV) model is formulated for each CPU model and presented at the end of this chapter. Assumptions include, a debt to equity ratio of 40:60, an interest rate of 6%, an inflation rate of 3.3%, a tax rate of 30% and an investment span of 30 years with depreciation. The minimum CO_2 price is then derived based on the condition that the internal rate of return (IRR) on the CO_2CPU is greater or equal to the minimum required rate of return or hurdle rate. CO_2 prices are obtained for each CPU model and four distinct hurdle rates: 5%, 10%, 15% and 20%. It is assumed that as long as the hurdle rate is met, the investment will go through. The results from this analysis are presented in Figure 5.7.

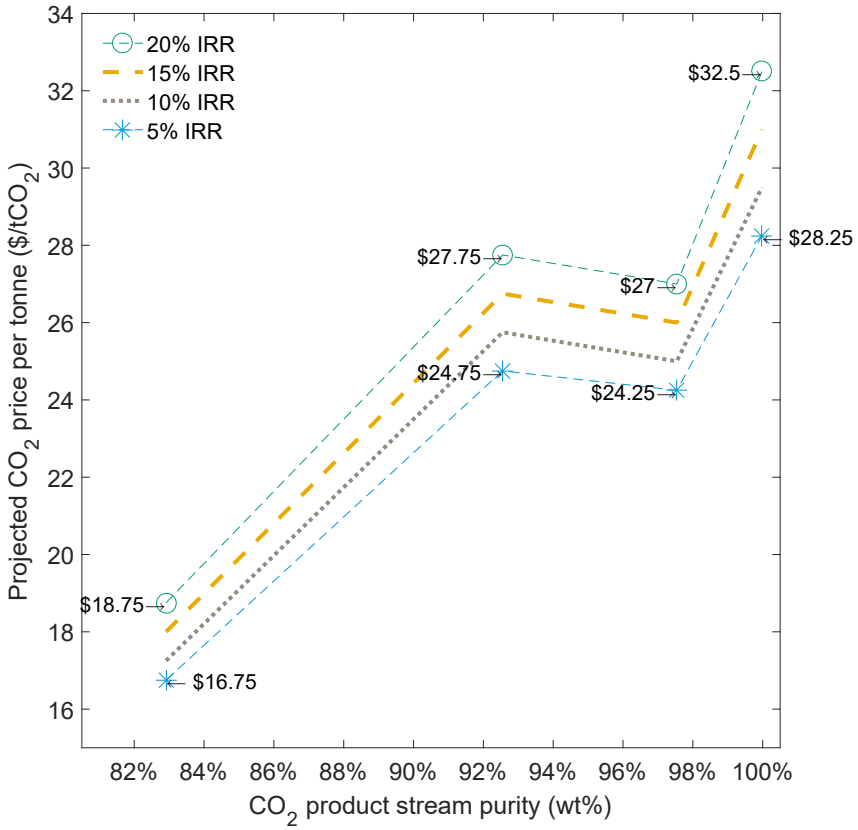

Figure 5.7: Graph showing the price value required per tonne of CO_2 for minimum rates of return on investment in the CO_2CPU of 20%, 15%, 10% and 5%, as a function of CO_2 stream purity.

Figure 5.7 demonstrates that the relationship between CO_2 price and stream purity is non-linear and non-monotonic. The non-monotonicity is due to the fact that the double flash system without heat integration is highly inefficient

and requires a much higher pressure state in order to obtain a separation that gives a 92.6wt.%purity. The CO_2 price resulting from this CO_2CPU would also decrease if heat integration were applied. The non-linearity observed is entropically driven: the higher the purity the more costly it becomes for an incremental increase in purity [177,208]. From this point on, the double flash 'low purity' CPU without heat integration will be excluded since it is more costly than alternative systems with higher product purities.

The same NPV analysis is also applied to the CPU used for post combustion and, assuming that the CPU is an independent entity in which to invest - separate in this case from the post combustion amine-based process - a CO_2 price of \$13 - \$14.75/tCO_2 for a product stream of 99.97 wt.% purity will match a minimum required rate of return of 5% - 20%. It is important to note that the CPU needed for post-combustion capture is only a part of a cost intensive capture process (1/3 of the energy penalty resulting from post-combustion capture [17]) and hence the CO_2 price here does not reflect the rest of the process.

It is assumed in a first instance that investment would only take place as long as a 20% rate of return is achieved. The results show that for the highest purity achievable from the CO_2CPU, a saleable CO_2 stream at a price of \$32.5/tCO_2 would make the investment worth-while whereas a CO_2 stream that is saleable at a purity of 82.9 wt.% would only need to be sold for \$18.75/tCO_2 for a lucrative investment. This difference represents a 42% decrease in product price. However, none of these results are meaningful unless a market for CO_2 exists. If targeting oil producers who could provide a market for CO_2 in its use for EOR, it is critical to be able to offer a low CO_2 price [203]. Although CO_2-EOR offshore has yet to be done in the North Sea, studies have shown the feasibility and benefits that could be brought on by its deployment [86,87,220,221].

However, if CO_2 for EOR maintains its strict requirements in terms of CO_2 purity, particularly with regards to the oxygen content (limited to 100 ppm), this eliminates the market for all product streams with the exception of the 99.98 wt.% purity stream at and upper bound price of \$32.5/tCO_2. Nevertheless, given the history behind the requirement settings for CO_2 purity in EOR, there may be leverage to relax CO_2 requirements for use in EOR and thereby consider a lower purity and cheaper CO_2 stream. In addition, if a combination of the cheaper lower purity sources of CO_2, at 82.9 wt.% and 97.5 wt.% for \$18.75/tCO_2 and \$27/tCO_2, were to be mixed with inherently higher purity sources of CO_2 (e.g. from post combustion capture or natural gas processing) in a transport network system, the aggregation of streams could produce a stream suitable for injection and EOR at a much lower overall cost. This potential for cost reduction through the use of transport networks is assessed in the next section.

The minimum CO_2 price value when assuming minimum rates of return of 15%, 10% and 5% are shown in dashed and dotted lines in Figure 5.7. As expected, the CO_2 price decreases as the minimum rate of return required decreases. However, the reduction in price is greatest for the streams with highest capital cost: the 6-stage Distillation CPU and the Low Purity Flash CPU. These prices are compared to studies of the cost of CCS summarized in the review paper by Rubin et al. 2015[15]. The latter study quotes oxy-combustion capture cost to be between \$37/tCO_2 and \$69/tCO_2 and assume a discount rate of approximately 10% [4]. Considering that the CO_2CPU accounts for approximately half of the oxy-combustion capture costs, the prices presented here are in line with the Rubin et al. range for cost of CO_2 captured.

5.4.3 Triethylene Glycol Dehydration System

The models and cost analysis described above include a dehydration system that acts as a 'black box' separation system comprising only of operating costs involved in stripping the respective streams of water and is not associated with an equipment cost. For completeness of this analysis, a triethylene (TEG) glycol CO_2 absorption system is modeled separately. This was done in Aspen HYSYS using the HYSYS glycol property package and its cost assessed using the Aspen HYSYS economic evaluation tool. Absorption was chosen over adsorption as adsorption dehydration plants typically have higher installation costs and glycols (used in absorption) are cheaper than adsorbents and easier to replace than an adsorber bed [222–224]. Furthermore, triethylene glycols are chosen amongst other glycols as these are best for gas dehydration as they can be regenerated at high concentration without degradation at high temperatures due to their high degradation temperature (260°C) [223,225,226]. The dehydration system (illustrated in Figure 5.8) consists of an absorber that pumps in TEG to the pressure of the inlet flue gas stream (either 30bar or 28 bar depending on the CPU model described in section 5.3.1) at the top and water-rich flue gas entering at the bottom of the column. The dry flue gas then exits the absorber as the top product (with less than 10ppm H_2O) and water-rich TEG as bottom product. The TEG stream expands through a throttle valve to atmospheric pressure and through a flash vessel then splits off a small amount of waste flue gas. The TEG stream is then heated up to 150 °Cand enters the stripper for regeneration of the TEG stream. The dry TEG stream leaves the bottom of stripper and is cooled using propane as

[4]Rubin et al. 2015 quotes a fixed charge factor ranging from 9.3% to 10.9%, which refers to the capital recovery factor (CRF) used derived from the discount rate and investment period assumed.

a refrigerant before being recycled back into the dehydration system. The costs associated with this dehydration system are shown in Table 5.6. It is assumed that fresh TEG is purchased once yearly given a usage rate of 2000 kg/hour and at \$ 2/kg [227]. Due to the pressure at which the absorption occurs, this TEG dehydration system is not applied to the low purity double flash CPU model and is henceforth excluded from the analysis as it is not considered economically advantageous.

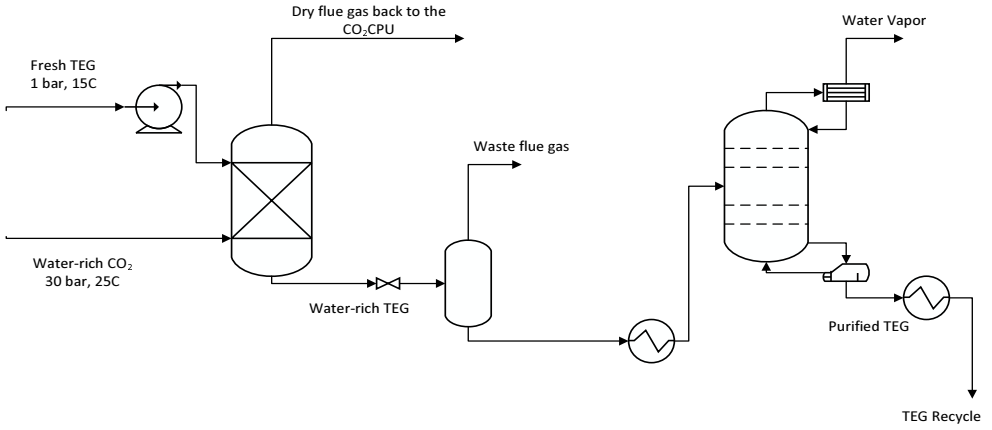

Figure 5.8: Flow diagram of the triethylene dehydration system used to dehydrate pressurized flue gas, consisting of an absorber-stripper system

Table 5.6: Capital and operating costs of the triethylene glycol dehydration system compared with overall costs for the compression & dehydration CPU (CD CPU), the high purity double flash CPU (HPDF) and the distillation CPU (Dist CPU).

	TEG Dehydration	% of total CD CPU	% of total HPDF CPU	% of total Dist CPU
Yearly Operating Costs	\$289,515	0.6%	0.6%	0.5%
Total Installed Equipment Cost	\$1,185,167	2.2%	2.1%	1.4%

5.5 A CO_2 transport network system can reduce the cost of capture

The next part of this work demonstrates how a mutually informed decision on CO_2 capture, transport and storage can reduce capture costs for a wider CCS network.

5.5.1 Transport network scenario

This section uses an example of a transport network based on UK conditions and data. However, the methodology is applicable to any country/region with any number of point sources within reasonable proximity to one another.

Having a number of purification options at different costs is worth exploiting when applied to a number of sources with various capture technology options to drive down overall costs of capture in a given region. In order to demonstrate this benefit, a CO_2 transport network system was assumed based on capture rates from real UK power and industrial plants inputting CO_2 from different sources and with varying product purities. A UK-based case study by Prada et al.[228] was used to obtain representative flow rates from 10 combined cycle gas turbine (CCGT) plants, 10 coal fired power plants and 1 steel plant. The flow rates from these CO_2 outputs and their hypothetical capture plants are shown in Table 5.7. Each plant is then coupled with a type of capture plant which will in turn give the purity of the CO_2 stream extracted from a given power or industrial plant. CCGT plants are constrained to exclusively adopt post-combustion capture. This is due to the current absence of gas turbines designed for oxy-combustion. The flue gas composition resulting from post combustion capture, prior to entering the CPU, is given in Table 5.3. The coal power plants and the steel plant are assumed to adopt oxy-combustion CO_2 capture. In the case of CO_2 capture from a steel production plant, oxy-combustion - as opposed to post-combustion - provides the flexibility needed to make up for the varying compositions of flue gas from the blast furnace as well as the high temperature flue gas [5]. Each of the CO_2 sources considered are assumed to join at a central hub from which a trunkline of CO_2 brings the combination of streams to the Bacton terminal and sent through for storage in the Southern North Sea. This scenario is illustrated in Figure 5.9.

Each point source's capture plant cost is associated with the cost of a CO_2CPU and can choose from three process configurations. Each will determine the re-

Figure 5.9: Illustration of a UK based CO_2 transport network scenario [229]

sulting level of cost and purity prior to entering the transport network. This choice is informed by the process models and cost analysis of CPUs presented in sections 5.3.1 and 5.4.2. In combining multiple streams, of different cost and purity, transport network scenario then seeks to minimize cost while maximizing purity of a final trunkline stream. It is formulated as a bi-objective optimization problem with a mixed-integer linear programming model (MILP). The resulting MILP model was solved using the GAMS CPLEX solver as this is well suited for solving problems of this type[230]. The objective here is to show that for a minimum purity required at the injection point mixing high purity sources of CO_2 with lower purity sources of CO_2 within the transportation network can significantly reduce the cost of the final CO_2 product stream for injection and thereby improve the economic viability of the system as a whole.

Table 5.7: UK case study: flow rates of gas CCGT plants, coal plants and steel plant.

Gas Plant (J)	Flow rate ($MtCO_2$/yr.)
Keadby	1.5
Didcot B	2.6
South Humber Bank	2.6
Barking	2.4
Killingholme A	1.3
Sutton Bridge	1.8
Damhead Creek	1.7
Spalding	1.7
Coryton	1.5
Little Barford	1.3
Coal Plant (K)	Flow rate ($MtCO_2$/yr.)
West Burton	7.8
Cottam	8.4
Drax	19.4
Kingsnorth	6.3
Ratcliffe	7.7
Rugeley	3.8
DidcotA	4.7
Ferrybridge C	6
Eggborough	6.5
Tilbury	3.8
Steel Plant (L)	Flow rate ($MtCO_2$/yr.)
Corus	5.8

5.5.2 Formulation of the optimization problem

The optimization problem is expressed has the following objective functions:

$$\min[y(i)],\ subject\,to\ x(i) \geq 0.96, \tag{5.2}$$

$$\min[z(i)],\ subject\,to\ x(i) \geq 0.96, \tag{5.3}$$

where y is the capital cost incurred per tonne of CO_2 captured and z, the operating cost incurred per tonne of CO_2 captured. These are subject to a constraint on x, the final product purity at the trunkline ready for injection. Constraint x is varied to obtain the pareto front.

The optimization variables are the choices of CO_2CPU systems i and include a post-combustion CPU option (PostC) in subset v, and three oxy-combustion CPU options in subset u: a distillation unit (Dist), a high purity double flash

unit (HPDF) and a compression and dehydration unit (CD). It is assumed here that all gas plants will apply post-combustion capture and that the $CO2_2$CPU processes a typical amine-based post combustion captured CO_2 stream at 90% capture efficiency of purity of 99.97 wt.%[228]. The composition of the final post combustion CO_2 stream coming out of the CPU is provided in Table 5.4.

Each optimization parameter and variable is described in the appendix at end of this chapter (see Section A3). In this work, only the capital and operating costs that stem from the CO_2CPU needed for oxy-combustion capture and the compression and dehydration unit needed in the final stage of post combustion capture are considered. Hence, when talking about an oxy-combustion option or a post combustion option this refers solely to the choice of CO_2CPU. With each category of capture and subset of CO_2CPU option several optimization parameters are given. These include: CO_2 product purity resulting from each oxy-combustion option *A1(u)* and resulting from the post combustion option *A2(v)*, capital cost in \$/tCO_2 captured per year for oxy-combustion options *CAP_oxy(u)* and for post combustion *CAP_post(v)*, operating costs \$ /tCO_2 captured per year for oxy-combustion options *OP_oxy(u)* and for post combustion *OP_post(v)*.

Each plant is separated into the three categories as described in section 5.5, with j referring to the gas plants, k the coal plants and l the industrial plant (one steel plant only in this example). The flow rate for each of the plants is given by the following optimization parameters: *Flow_gas(j), Flow_coal(k), Flow_ind(l).*

Two binary variables are introduced in order to allow for the plants to choose among the different discrete CO_2CPU options. These binary variables are decision variables that take integer values only, hence the use of a mixed-integer linear programming (MILP) solver. Equations 5.4 and 5.5 present the constraints on each binary variable limiting the selection of each plant to a single CO_2CPU option:

$$\sum_u binary1(u,k) = 1 \quad \forall k \tag{5.4}$$

$$\sum_u binary2(u,l) = 1 \quad \forall l \tag{5.5}$$

These binary variables are used to calculate the product purity, the capital and operating costs for the sum of all coal streams and for the product resulting from the capture of CO_2 from the industrial plant. The equations used calculate the final product purity, capital cost and operating cost per tonne of CO_2 in the trunkline ready for injection are presented in Appendix A3. The constraint set

on this problem is for the final trunkline purity, x, of at least 96 wt.% for injection with ppm levels of water. As a result of this study we obtain the quantitative trade off between the two conflicting objectives: minimum cost and maximum purity.

5.5.3 Transport network optimization: Pareto front

Figure 5.10 shows the bi-objective optimization pareto front for these competing objectives: minimum cost and maximum purity. It is clear that when increasing the purity requirement, cost increases as well. The purity of the CO_2 stream in the trunkline, x, has a lower bound set at 0.96 mass fraction. The first solution, to the far left represents a scenario in which the West Burton coal plant (see Table 5.7) uses the CD CO_2CPU and the rest of the coal plants and the steel plant use the HPDF CO_2CPUs. As explained in section 5.5, the gas plants are assumed to adopt the post combustion capture method and therefore contribute a fixed cost and purity in all scenarios.

This first result gives a minimum capital cost of \$22.51/tCO_2 and a minimum operating cost of \$20.42/tCO_2 for minimum acceptable mass fraction of CO_2 in the trunkline of 0.96. As the minimum purity requirement at the storage injection point (or trunkline) is increased, the capital cost increase follows a non-linear trend. At a minimum requirement of 0.98 wt% CO_2 the slope starts increasing, representing a scenario in which all coal and steel plants use an HPDF CPU and Tilbury, a coal plant, has just switched from an HPDF CPU to a Dist CPU. This scenario gives a capital cost of \$23.52/tCO_2 and operating cost of \$21.15/tCO_2. Once the minimum mass fraction of CO_2 in the trunkline reaches 99.2 wt% purity, the slope of the CAPEX curve sees a sharp increase before reaching a 'plateau' at a 99.95 wt% CO_2 purity requirement. The 'plateau' represents a scenario in which all coal and industrial plants have switched to a Dist CPU system reaching a capital cost of \$34.24/tCO_2 and operating cost of \$23.06/tCO_2.

The pareto front highlights that above a certain purity requirement (98 wt.% CO_2) the capital investment cost increases drastically, increasing the investment risk and CO_2 price. This steep increase in cost when aiming for a purity above 98 wt.% CO_2 is also reflected in the CO_2 price curve shown in Figure 5.7 as the above design point of the CO_2CPU is set at a much higher capital cost to achieve 99.98 wt.% CO_2. Using the investment analysis presented in section 5.4.2 and the prices that reflect the cost of each CO_2CPU with a different product stream - applied both to oxy-combustion and post combustion - a final trunkline product

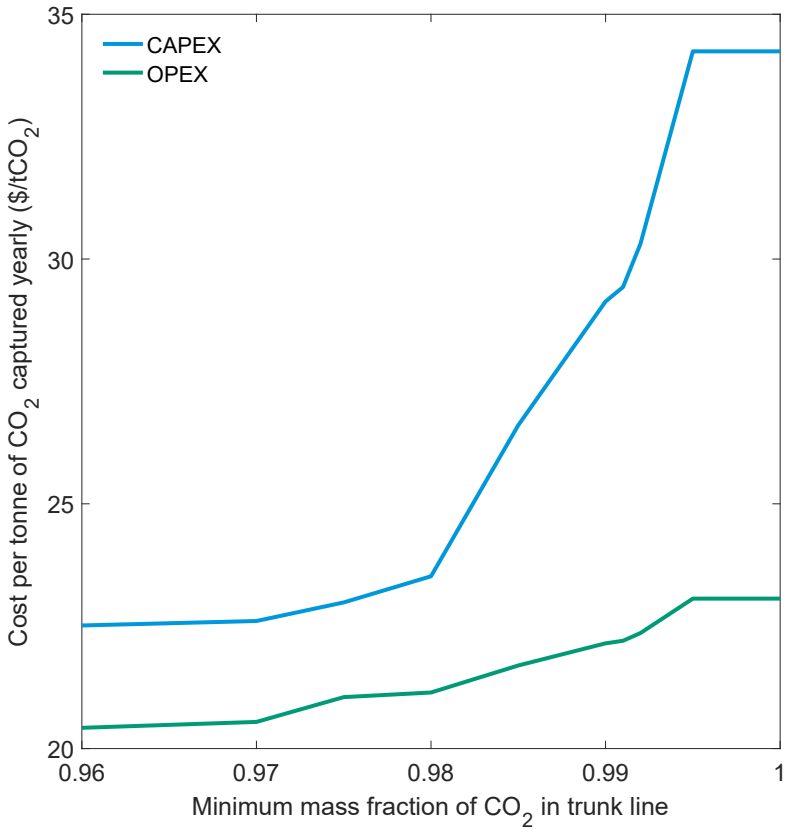

Figure 5.10: Graph Showing Network Capture System CAPEX and OPEX per tonne of CO_2 Captured as a Function of Minimum Trunkline Purity - Pareto Front

stream price is derived. The trunkline CO_2 price will differ based on the minimum required rate of return for each CPU and these are plotted in Figure 5.11 for a 20%, 15%, 10% and 5% IRR. Assuming a 20% minimum rate of return on investment is required, minimizing cost results in a final trunkline CO_2 stream at 96.8wt.% purity for a price of \$24.06/tCO_2. Meanwhile, maximizing purity results in a final trunkline stream of 99.98wt.% purity at a price of \$29.19/tCO_2. This difference represents a 17.6% saving in CO_2 product price.

Assuming an entity wants to purchase CO_2 above 96 wt% purity, the savings that result from combining streams of different purity and costs are plotted against the minimum rate of return required from the investor(s) in Figure 5.12. The lower the minimum require rate of return or IRR, the less substantial the savings will be. Hence, as the maturity of the technology increases and the minimum required rate of return decreases, the trade-offs between having a high purity stream at higher cost versus a lower purity stream at lower cost will be less significant. These results are valuable both on the capture side as well as

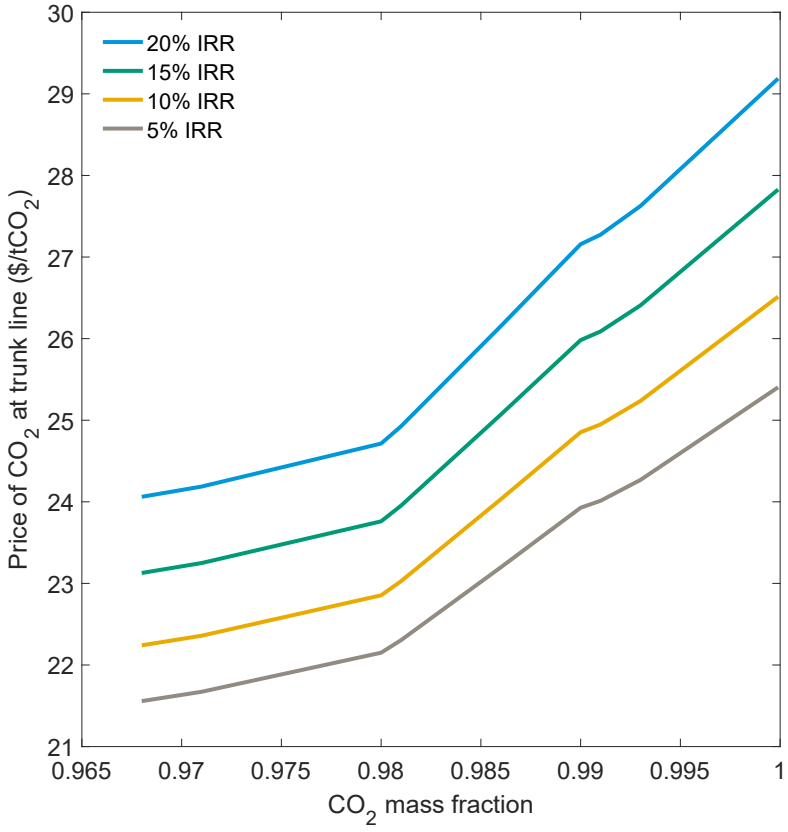

Figure 5.11: Graph showing the price of CO_2 received at the trunkline end in order for all CPU investors to achieve at least 20%, 15%, 10% and 5% rate of return on investment as a function of CO_2 purity requirement at injection point.

the CO_2 market side. For iron, steel and cement production, it is crucial to be able to provide a low cost CO_2 capture option in order to provide such plants with a low-carbon option that is more worthwhile than relocating to a region with less stringent emissions reduction policies. In being able to mix low purity CO_2 streams with higher purity ones, producing a final stream suitable for injection, this low cost scenario is rendered possible for such industries. This study, however, does not include transportation costs and therefore does not take into account the fact that having a cheap, low purity CO_2 stream will increase the required pipeline diameter and thereby increase the transportation costs incurred[195]. Nonetheless, this has been shown to have little or no effect on pipeline costs over short distances (30km), and this is one of the key advantages of using a multi-hub transport network as in this study[180].

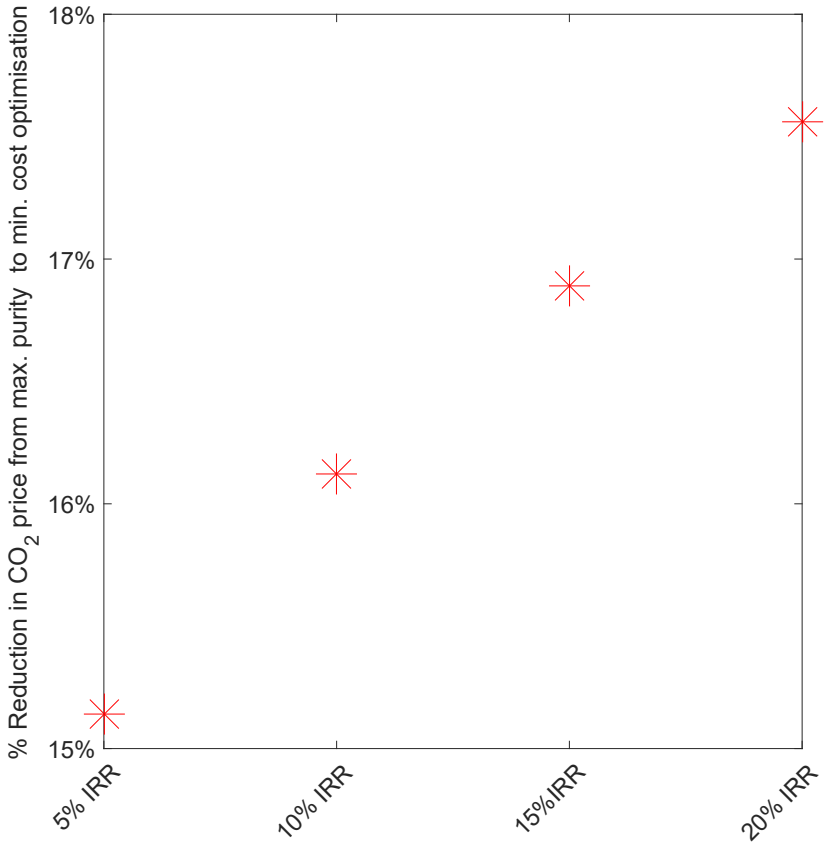

Figure 5.12: Graph showing the percentage reduction in CO_2 price when choosing a minimum cost scenario as opposed to a maximum purity scenario for minimum required rates of return of 20%, 15%, 10% and 5%.

5.6 Shared compression and dehydration unit infrastructure

Economies of scale will dictate that building larger infrastructure will prove to be less costly than several smaller scale infrastructures. In that vein, this work has shown that sharing capture infrastructure for several point source emissions could prove to be less costly than having a lot of the same infrastructure at a smaller scale at different capture plants. This could be sensible for large point source emissions that tend to be clustered in industrial areas, outside large cities, in low density areas and in close proximity to a water basin. This would imply that very short large diameter pipes or trucks could transport flue gas from these point sources to one larger CO_2 compression and purification facility, for example, instead of having one at each site and reducing the volume of infrastructure and materials required overall. In the UK, for example, coal plants, Kingsnorth and Tilbury, and gas CCGT plants, Damhead Creek and Coryton, are situated in a 50km by 50km square grid[228] and together would require a CO_2CPU plant

of total capacity 14.8 $MtCO_2$/year.

Here, the capital and operating costs of four CO_2CPUs each of yearly capacity 5 $MtCO_2$ was compared against that of one CO_2CPU of the same overall capacity of 20 $MtCO_2$/year. The CD (compression and dehydration) CO_2CPU process, presented in section 5.3.1, was modeled in Aspen HYSYS at these two scales. The same inlet flue gas composition and characteristics presented in Table 5.2 were used with flow rates scaled accordingly and results are presented in figure 5.13. This analysis, does not take into account the costs that would incur from transporting the flue gas streams over short distances in the shared infrastructure scenario. Transportation costs, however, over short distances are negligible compared to capture costs: the cost of CO_2 transported via onshore pipelines over 50km long is 25-30 times less costly per tonne of CO_2 than the cost of capturing [228].

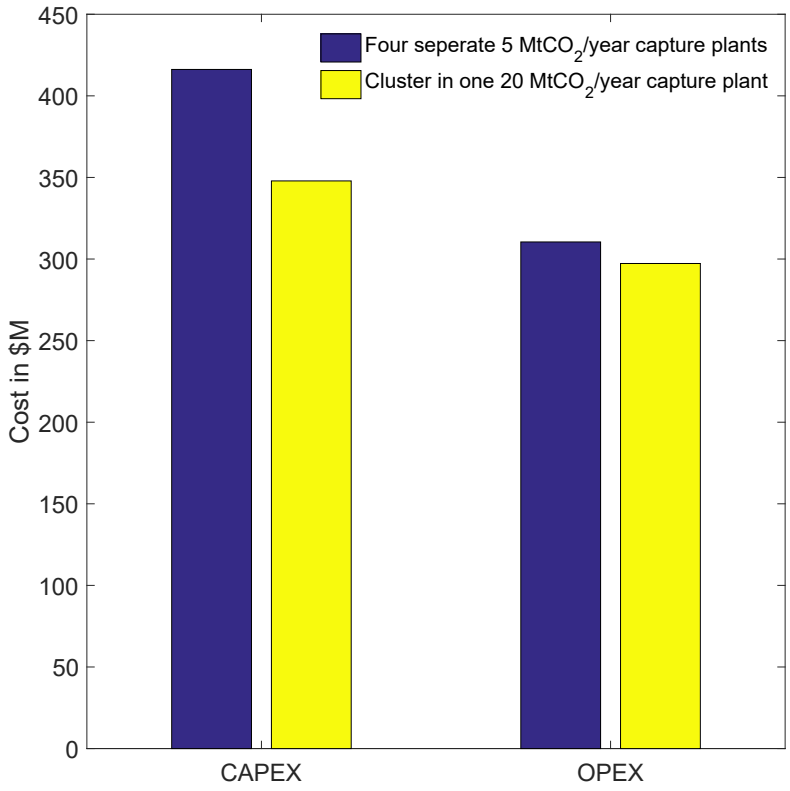

Figure 5.13: Bar chart showing the CAPEX and OPEX for one large CO_2CPU processing 20 $MtCO_2$/year compared with four smaller CO_2CPU plants with the capacity to process up to 5$MtCO_2$/year each

Having one large CO_2CPU of 20 Mt/year capacity instead four capture plants of 5 Mt/year capacity, could save $ 68.3 million in capital expenditure and $

13.2 million/year in operating costs. This equivalent to a 16% reduction in total CAPEX and 4% reduction in annual operating costs. In providing a method for the decarbonisation of industries such as iron, steel and cement production, CCS needs to take advantage of all cost effective solutions in order to avoid reducing competitiveness, which could be the case if the cost of decarbonisation is passed on to the consumer [231]. Adopting shared CO_2 capture infrastructure can further reduce the capital investment risk that is assimilated with CCS. Furthermore, the Zero Emissions Platform reported in their study "The Costs of CO_2 Capture, Transport and Storage" [232] that pipeline costs per tonne of CO_2 are also reduced by at least 3 fold if considering a large volume of CO_2 (20 Mt/year) as opposed to a small volume of CO_2 (2.5 Mt/year), justifying the added benefit of having a larger product stream from a shared capture infrastructure.

5.7 Conclusions to chapter

The results presented in this chapter provide a novel way of addressing CO_2 capture deployment plans. In literature, a focus on the cost of CCS and particularly the cost of capture are often addressed with a myopic view on future deployment needs. This work has shown that it is in looking at widespread and future deployment scenarios for CCS that increased cost efficiency can be obtained.

Through a detailed study of four CO_2 compression and purification units applicable to oxy-combustion capture, this work has shown that higher CO_2 purity is associated with higher costs of capture and lower capture efficiencies. This was translated into a minimum price on CO_2 that would offer suitable return on investment assuming that the CO_2CPU is a entity independent of the rest of the power plant (and excluding the air separation unit). If all else is equal, investing in a unit that gives a compressed, low purity dehydrated CO_2 stream (82.9 wt.% CO_2) could offer the same return to an investor as a unit producing the highest purity CO_2 (99.98 wt.% CO_2) and be sold at a price that is reduced by as much as 42%. However, the cheaper, lower purity CO_2 product stream may not be deemed suitable for injection into storage or use in EOR for example. Meanwhile, assuming the only compound really worth excluding for transport is water, that same low purity, low cost CO_2 stream would be suitable for transport.

In addition, this work has shown that transport network infrastructure can help drive down the cost of capture by being able to combine lower cost and lower purity streams with higher purity streams coming from different CO_2 capture systems and point source emissions (e.g. gas plants, coal plants, heavy industrial

plants). Hence, minimizing overall system cost of multiple CO_2 capture plants and streams. This was demonstrated assuming that the transport network can mix multiple CO_2 streams and feeds into a final trunkline CO_2 stream with a composition that is suitable for CO_2 injection for storage. The costs considered only pertained to the CO_2 compression and purification units. Using a UK-based transport network optimization problem example, it was found that up to 18% reduction in the final price tag on CO_2 at the trunkline can be achieved by combining CO_2 at different purities and cost. Reducing the minimum required rate of return on investment in CO_2 capture is also found to reduce the savings achieved in this transport network example. This is because as higher investor confidence is achieved, the risk associated with the investment is also reduced reflecting a reduction in associated cost and thereby narrowing the gap between the maximum purity high cost system and minimum purity lower cost result.

The compression and purification unit models and cost analysis was taken one step further here in assessing the impact shared capture infrastructure would have on total costs. Similarly, a 16% reduction in capital and 4% reduction in operating costs per Mt of CO_2 captured was found to result from a four fold scale up in infrastructure size.

The results from this work would suggest that there are clear benefits to draw from a cohesive policy on CCS, particularly on the national level, where land is shared (for transport network deployment) and CO_2 storage sinks targeted are similar in their properties. Furthermore, providing incentive for collaborative deployment and investments, in shared capture plants and common transport infrastructure, rather than that of individual market leaders could lead to a significantly better return over just a few decades (30 year investment outlook considered here).

5.8 Contributions made

This work has provided the first detailed account of the cost purity trade offs involved in the CO_2 compression and purification process. This has highlighted the very high cost of capture that results from seeking to achieve a 99.98% purity CO_2 stream and the subsequent reduction in capture efficiency. This has led to questioning the justification and history behind CO_2 purity requirements as they are given today. In particular, the recurring source-to-sink approach of CCS deployment to date has led to equating CO_2 purity requirements for transport with those for storage. The analysis here suggests that these requirements result from prior experience with naturally occurring CO_2 sources used in the CO_2-EOR industry in North America. Demonstrated through the lens of the

oxy-combustion CO_2-CPU process, relaxing these purity requirements is shown to lead to substantial reduction in the cost of capture and increased capture efficiency. This result suggests a high value in further research to quantify the tradeoff in cost and risk of a lower purity CO_2 stream on transport and storage operations. The business model developed for investment in a standalone CO_2-CPU - where an investor will go ahead with a project if the required rate of return is met for a certain price on CO_2 - is presented and can be accessed here: `https://doi.org/10.5281/zenodo.1230482`.

Leaning on the cost purity tradeoff highlighted with the CO_2-CPU, this work has demonstrated the value for multiple point sources to make a collective decision on their choice of capture process in view of minimizing overall system cost. This was done by developing a transport network optimization model based on 21 point sources in the UK with joining CO_2 streams at different individual purities to meet a final trunkline purity of 96%; suitable for storage. This approach and optimization problem can and should be assessed for regions looking at the deployment potential for CCS since the collective cost of CO_2 capture is found to be lower than multiple individually assessed capture plants. This work has clearly demonstrated the benefit of shared infrastructure both in capture and transport and the sunk cost that would otherwise result from isolated assessments of deployment.

This work confirms the benefit of aligning policy with an outlook on systems needs *i.e.* for future CCS deployment based on energy systems changes and industrial resource needs. It is important to consider relaxing CO_2 purity requirements in view of reducing capture costs particularly for industries that are at risk of delocalization as a result of more or less stringent emissions policies in different countries.

Chapter 6

Conclusions

6.1 Key Conclusions

This thesis is built on the notion that CCS is a well understood, technologically developed and needed technology. It has nonetheless failed to be deployed at a scale large enough to contribute a significant or sufficient amount of carbon dioxide abatement to meet climate change mitigation needs[1]. Hence, the work described here has identified key bottlenecks to overcome for achieving large-scale CCS (*i.e.* of the order of gigatonnes of CO_2 captured and stored per year) through a systems analysis of the various interactions (*i.e.* between the energy system, capture plants, transport networks and storage sites) and stakeholders involved in the CCS deployment process.

A key barrier to CCS deployment has been its cost and particularly the cost of capital it represents to investors. Chapter 2 of this thesis presents a method developed to highlight the way the cost of CCS is calculated from an investor standpoint. This takes into account the riskiness of the asset in which to invest *i.e.*, CCS, as perceived by the investor, the investment period and the level of technological learning gained for the CCS process as it is deployed. Using the capital asset pricing model (CAPM) to relate asset risk and required rate of return on investment, this analysis is among the first to demonstrate quantitatively the cost reduction that can be achieved for CCS as a result of reducing financial risk. Public policy can play a key role in targeting financial risk by underwriting all or part of the investment's sequestered CO_2, insuring the large capital cost and ensuring the availability of infrastructure for transport and storage. Mitigating financial risk to reflect a reduction in required rate of return from 20% to 10% is shown to reduce levelized cost of CCS by up to 47%.

Financial incentives for CCS, including oil revenue from using CO_2 for EOR, credit for sequestering CO_2, subsidies or grants to aid the high capital cost in-

vestment and technological learning through learning by doing, are all expected to boost the deployment of CCS. From an investor standpoint, this is because these incentives will allow them to meet their required rate of return. With reduced financial risk of investing in CCS, this required rate of return and the incentives needed to meet it would also be lower. Chapter 3, presents MIICE, an open-source iterative investment model developed within this thesis (accessed here: `http://doi.org/10.1039/C7EE02102J`), that is able to quantify the value of these incentives on CCS deployment levels. The results from a combination of over 36,000 of these variables are output with MIICE. At an initial price of oil of 55$/bbl, a CO_2 storage credit of 25$/t$CO_2$ and learning rate for large infrastructure type plants, MIICE suggests that CO_2-EOR can play a key role in boosting the deployment of CCS. Using the required rate of return as a decision metric for each potential investment, coupling CCS with CO_2-EOR can bring a sufficient number of projects forward to trigger CCS cost reduction of up to 40%. However, MIICE also highlights that an oil price of over 85$/bbl or a CO_2 credit reaching 75$/t$CO_2$ within 35 years would be needed in order to expect a gigatonne of CCS deployment when considering only CCS with power.

While projections for CCS deployment are made on a regional or global scale, individual CCS projects are often regarded in isolation of one another with purity requirements based on a source to sink approach. Chapter 5 presents developed process models for the CO_2 compressions and purification unit (CO_2-CPU), a key part of all types of CO_2 capture processes and accounting for 50% of the cost of oxy-combustion capture. The process models are based on earlier models developed by Posch et al. 2012[177] and Pipitone et al. 2009[178]. Three of these models demonstrate the variation between final CO_2 product purity and process cost. Taking an investor's approach, CPU-INVEST (accessed here: `https://doi.org/10.5281/zenodo.1230482`) was developed to obtain the price at which CO_2 would need to be sold for to an off-taker in order for an investment in one CO_2-CPU to match the required rate of return. This assumes there is a market for CO_2 utilisation or credits for its sequestration. A 43% reduction in CO_2 price required results from relaxing the final product purity requirement from 99.98 wt% CO_2 down to 83 wt% CO_2. The literature behind CO_2 purity requirements has suggested that a dehydrated CO_2 stream, to avoid corroding transport materials and limiting the risk of hydrate formation in the presence of oxygen, does not need to equate to a very costly 99.98% purity stream. Purity requirements for CO_2 injection into a storage reservoir suggest a CO_2 purity requirement of 96% CO_2 instead. A systems approach is adopted to include each of these CO_2-CPU options, with their respective price points and purities, into a transport network optimization problem that considers a UK case study of

21 point sources. By combining these CO_2 sources to obtain a final trunkline purity of 96% instead of requiring each individual source to meet the final purity requirement, the final price on CO_2 required can be reduced by up to 18%. This is analogous to an 18% reduction in the levelized cost of CCS. Chapter 5 also demonstrates significant capital cost reduction potential of up to 16% when considering one large shared CO_2-CPU infrastructure site equivalent to four individual standalone plants.

Results from MIICE that demonstrated the gradual deployment of CCS and the possibility of a growing transport network of CO_2 sources targeting one storage sink, suggested the importance of assessing reservoir behavior in response to the possibility of varying CO_2 storage demand on yearly and decadal time scales. Chapter 4 presents results from simulating CO_2 injection into a reservoir model of the UK's main storage sink, the Bunter Sandstone saline aquifer, located in the Southern North Sea. The geological reservoir model used to conduct the simulation was obtained from the British Geological Survey and based on Noy et al. 2012[133]. This work showed that the reservoir is resilient to variations in CO_2 injection. This work also demonstrates that frequency variations in CO_2 storage demand can be modelled as an average constant CO_2 storage supply rate when incorporated into energy systems models with CCS since such variations will not have a differing effect on reservoir behavior.

6.2 Key Contributions

The work presented in this thesis demonstrates that with three key actions described above, on financial risk, CO_2 utilization incentives through EOR, and shared transport infrastructure the value of levelized cost of CCS can be reduced by 47%, 40% and 18% respectively. Considering an initial levelized cost of CCS at 100\$/tCO_2 avoided, these results combined can achieve at least a 74% reduction in levelized cost down to only 26\$/tCO_2 avoided, at which point CCS would become highly cost competitive.

The models (MIICE and CPU-INVEST) and the systems analysis frameworks presented in this thesis are among the key contributions of this work. While some of these have drawn on geography specific examples, the methodologies and approaches can be tailored to, arguably, all regions considering the deployment of CCS in the next few decades. These have highlighted and quantified the effects of key policies and actions on CCS. These include:

- Providing insurance on cost and liability of CO_2 in the aim of reducing

financial risk is key to boost investment by reducing levelized cost.

- CO_2-EOR is valuable in initial plans for CCS deployment, but other financial incentives particularly a CO_2 storage credit and technological learning are key to favoring sequestration.

- Providing incentives for large and shared CCS infrastructure is key to reducing overall system costs of CCS deployment in the long term and avoiding impractical costs related to very high CO_2 purity requirements.

6.3 Thesis Extension

MIICE, model of iterative investment in CCS with CO_2-EOR (accessed here: `http://doi.org/10.1039/C7EE02102J`), is the first of its kind to include: detailed EOR production profiles, a detailed account of CCS and EOR costs, a yearly updating set of input variables and parameters to reflect a changing economic climate and the relevant levels of CCS deployment. The following is a list of elements to consider for further work on MIICE:

- Oil field characteristics currently included in MIICE are geographically biased to North American oil fields due to the nature of the input data obtained on existing conventional EOR fields in this region. MIICE can easily be extended to include a pool of oil field characteristics that pertain to offshore oil fields as well.

- Cost correlations for CO_2 transport and storage included in MIICE are most relevant to onshore CO_2-EOR and sequestration. MIICE can be extended to include offshore costs in the event that investment in offshore CO_2 storage and EOR meets the required rate of return on an iteration. This would be particularly relevant for considering CCS with CO_2-EOR in the North Sea for example.

- MIICE assumes capture costs for CO_2 with amine-based post combustion technology on a pulverized coal firing power plant. MIICE can easily be extended to include different CO_2 capture options and their relevant costs as well as different CO_2 point source types. This would be an extended selection pool to iterate through on each year of potential investment and coupled with each field option. This would be particularly relevant in considering CO_2 capture for industrial sources such as cement, iron and steel production.

Furthermore, the analysis of the CO_2 compression and purification unit model costs and their relevant CO_2 product purity highlighted the following: a strict CO_2 purity requirement is the main driver for high CO_2 capture cost. The literature analysis presented in Chapter 6 shows the lack of clear and quantifiable justification of CO_2 purity requirements for transport or storage. Particular points of uncertainty that are worth investigating include:

- Quantifying the value of additional compression work needed to have a single phase CO_2 stream in the presence of inert gases such as N_2, O_2 and Ar.
- The trade off of having low concentrations of O_2 and H_2O from a lower cost capture process and the additional investment needed for less corrosive and more resistant materials for transport compared with a higher cost of capture for very high purity, dehydrated CO_2.
- Further qualifying and quantifying the assumed risk of having over 100 ppm of O_2 in a CO_2 stream injected into a depleted oil or gas reservoir.

The transport network optimization problem presented in Chapter 6, considers 21 point sources based on a UK case study of which 10 are gas power plants, 10 are coal fired power plants and 1 is a steel plant. Based on a minimum purity requirement set at the final trunkline, each point source is coupled with a CO_2-CPU such that the overall cost is minimized. This optimization network can be extended to include more industrial sources that can provide additional low cost CO_2 capture options to meet a final purity requirement at a set trunkline and CO_2 injection point. Furthermore, the network optimization problem can be extended to include distances between point sources and their relevant costs, which would add additional constraints to the model. These would affect the objective function for minimizing cost and the resulting decision on the combination of capture technologies to choose from and point sources to target.

Bibliography

[1] Climate Change 2014: Synthesis Report. Contribution of Working Groups I, II and III to the Fifth Assessment Report of the Intergovernmental Panel on Climate Change. Technical report, IPCC, 2014. [Core Writing Team, R.K. Pachauri and L.A. Meyers(eds.)]. IPCC, Geneva, Switzerland, 151 pp.

[2] United Nations Framework Convention on Climate Change. Paris Agreement 2015. `https://tinyurl.com/y75g5pqb`, 2015.

[3] Bui, M. and Adjiman, C. S. and Bardow, A and Anthony, E. J. and Boston, A. and Brown, S. and Fennell, P. S. and Fuss, S. and Galindo, A. Hackett, L. A. and Hallett, J. P. and Herzog, H. J. and Jackson, G. and Kemper, J. and Krevor, S. and Maitland, G. and Matuszewski, M. and Metcalfe, I. S. and Petit, C. and Puxty, G. and Reimer, J. and Reiner, D. M. and Rubin, E. S. and Scott, S. A. and Shah, N. Smit, B. and Trusler, J. P. M. and Webley, P. and Wilcox, J. and Mac Dowell, N. Carbon capture and storage (CCS): The way forward. *Energy and Environmental Science*, In press.

[4] Global CCS Institute. The Global Status of CCS: 2017. Technical report, Australia, 2017.

[5] IPCC Special Report on Carbon Dioxide Capture and Storage. Technical report, Prepared by Working Group III of the Intergovernmental Panel on Climate Change [Metz, B. and Davidson, O. and de Coninck, H. C. and Loos, M. and Meyer L. A. (eds.)], Cambridge University Press, Cambridge, United Kingdom and New York, NY, USA, 442 pp., 2005.

[6] Rogelj, J. and Elzen, M. and Hohne, N. and Fransen, T. and Fekete, H. and Winkler, H. and Schaeffer, R. and Sha, F. and Riahi, K. and Meinshausen, M. Paris Agreement climate proposals need a boost to keep warming well below 2°C. *Nature*, 534:631–639, 2016. Perspective.

[7] Energy Technology Perspective 2014: Harnessing Electricity's Potential. OECD/IEA 2014, International Energy Agency, Paris, France, 2014.

[8] MIT Energy Initiative. Cancelled and Inactive Projects. `http://sequestration.mit.edu/tools/projects/index_cancelled.html`, 2016. Accessed on February 14, 2016.

[9] UNEP. The Emissions Gap Report 2017. Technical report, United Nations Environment Programme (UNEP), 2017. Nairobi.

[10] IRENA. Renewable Power Generation Costs in 2017. Technical report, International Renewable Energy Agency, 2018. Abu Dhabi.

[11] KPMG International. Taxes and incentives for renewable energy. Technical report, KPMG, 2015. `https://assets.kpmg.com/content/dam/kpmg/pdf/2015/09/taxes-and-incentives-2015-web-v2.pdf`.

[12] IEA Coal Industry Advisory Board. The Role of Coal for Energy Security in World Regions. Technical report, 2016. `https://www.iea.org/ciab/The_role_of_coal_for_energy_security_in_world_regions.pdf`.

[13] Qi, Y. and Stern, N. and Wu, T. and Lu, J. and Green, F. China's post-coal growth. *Nature Geoscience*, 9:564566, 2016.

[14] Shearer, C. and Ghio, N. and Myllyvirta, L. and Yu, A. and Nace, T. Boom and Bust 2017: Tracking the Global Coal Plant Pipeline. Technical report, CoalSwarm, GreenPeace USA, Sierra Club, 2017.

[15] E. S. Rubin, J. E. Davison, and H. J. Herzog. The cost of CO_2 capture and storage. *International Journal of Greenhouse Gas Control*, 40:378–400, 2015.

[16] Simpson, J. and McConnel, C. and Matsuda, Y. Economic Assessment of Carbon Capture and Storage Technologies: 2011 update. Technical report, Worley Parsons and Schlumberger, 2011.

[17] M. E. Boot-Handford, J. C. Abanades, E. J. Anthony, M. J. Blunt, S. Brandani, N. Mac Dowell, J. R. Fernández, M.C. Ferrari, R. Gross, J. P. Hallett, R. S. Haszeldine, P. Heptonstall, A. Lyngfelt, Z. Makuch, E. Mangano, R. T. J. Porter, M. Pourkashanian, G. T. Rochelle, N. Shah, J. G. Yao, and P. S. Fennell. Carbon capture and storage update. *Energy & Environmental Science*, 7:130 – 189, 2014.

[18] Lipponnen, J. and McCulloch, S. and Keeling, S. and Stanley, T. and Berghout, N. and Berly, T. The politics of large-scale CCS deployment. *Energy Procedia*, 114:7581 – 7595, 2017.

[19] Herzog, H. Financing CCS demonstration projects: Lessons learned from two decades of experience. *Energy Procedia*, 114:5691 5700, 2017.

[20] Watson, J. and Kern, F. and Gross, M. and Gross, R. and Heptonstall, P. and Jones, F. and Haszeldine, S. and Ascui, F. and Chalmers, H. and Ghaleigh, N. and Gibbins, J. and Markusson, N. and Marsden, W. and Rossati, D., and Russel, S. and Winskel, M. and Pearson, P. and Arapostathis, S. Carbon Capture and Storage: Realising the Potential? Technical report, UKERC, April 2012.

[21] Leigh Hackett. Commercialization of CCS - "What needs to happen?". Technical report, IChemE Energy Center: carbon capture and storage, December 2016.

[22] Amec Foster Wheeler. *UK Costs for a Range of CCS Technologies*, Imperial College London, September 2017.

[23] Global CCS Institute. The Global Status of CCS: 2011. Technical report, Australia, 2011.

[24] N. Mac Dowell, N. Florin, A. Buchard, J. Hallett, A. Galindo, G. Jackson, C. S. Adjiman, C. K. Williams, N. Shah, and P. Fennell. An overview of CO_2 capture technologies. *Energy & Environmental Science*, 3(11):1645–1669, 2010.

[25] Advanced Resources International and Melzer Consulting. Optimization of CO_2 Storage in CO_2 Enhanced Oil Recovery Projects. Technical report, Department of Energy & Climate Change (DECC) Office of Carbon Capture and Storage, 2010.

[26] Blunt, M. Carbon dioxide storage. *Grantham Institute for climate change: Briefing Paper no. 4, December 2010*, pages 1–12, 2010.

[27] U.S. Department of Energy. Length of large-scale CO_2 pipelines in the United States in 2015, by region (in miles). https://www.statista.com/statistics/615063/length-of-the-large-scale-carbon-dioxide-pipelines-in-the-united-states-by-r 2015. Accessed on January 31, 2018.

[28] McConnell, C. and Toohey, P. and Thompson, M. Strategic Analysis of the Global Status of Carbon Capture and Storage, Report 5: Synthesis Report. Prepared for the Global CCS Institute, Worley Parsons and Schlumberger, 2009.

[29] Fukai, I. and Mishra, S. and Moody, M. Economic analysis of CO_2-enhanced oil recovery in Ohio: Implications for carbon capture, utlization, and storage in the Appalachian Basin region. *International Journal of Greenhouse Gas Control*, 52:357–377, 2016.

[30] Gale, J. Geological storage of CO_2: What do we know, where are the gaps and what more needs to be done? *Energy*, 29(9-10):1329–1338, 2004.

[31] Celia, M.A. and Bachu, S. and Nordbotten, J. M. and Bandilla K.W. Status of CO_2 storage in deep saline aquifers with emphasis on modeling approaches and practical simulations. *Water Resources Research*, 51(9):6846–6892, 2015.

[32] OECD/IEA 2004. Prospects for CO_2 Capture and Storage. In *Energy Technology Analysis*. Paris, 2004.

[33] Heidug, W. and Lipponen, J. and McCoy, S. and Benoit, P. Storing CO_2 Through Enhanced Oil Recovery: Combining EOR with CO_2 storage (EOR+) for profit. OECD/IEA 2015, International Energy Agency, 2015.

[34] IEA Greenhouse Gas R&D Program (IEA GHG). CO_2 Storage in Depleted Oilfields: Global Application Criteria for Carbon Dioxide Enhanced Oil Recovery. 2009/12 December, 2009.

[35] Gale, J. and Abanades, A. C. and Bachu, S. and Jenkins C. Special Issue commemorating the 10th year anniversary of the publication of the Intergovernmental Panel on Climate Change Special Report on CO_2 Capture and Storage. *International Journal of Greenhouse Gas Control*, 40:1–5, 2015.

[36] H. deConnick and S. Benson. Carbon Dioxide Capture and Storage: Issues and Prospects. *The Annual Review of Environment and Resources*, 39:243–270, 2014.

[37] Kolster, C. and Agada, S. and Mac Dowell, N. and Krevor, S. The impact of time-varying CO_2 injection rate on large scale storage in the UK Bunter Sandstone. *International Journal of Greenhouse Gas Control*, 68:77–85, January 2018.

[38] Kolster C. and Masnadi, M. S. and Krevor, S. and Mac Dowell, N. and Brandt, A. R. CO_2 enhanced oil recovery: a catalyst for gigatonne-scale carbon capture and storage deployment? *Energy & Environmental Science*, 10:2594–2608, 2017.

[39] Agada, S. and Jackson, S. and Kolster, C. and Mac Dowell, N. and Williams, G. and Vosper, H. and Williams J. and Krevor S. The Impact of Energy Systems Demands on Pressure Limited CO_2 Storage in the Bunter Sandstone. *International Journal of Greenhouse Gas Control* , 65:128–136, 2017.

[40] C. Kolster, E. Mechleri, S. Krevor, and N. Mac Dowell. The role of CO2 purification and transport networks in carbon capture and storage cost reduction. *International Journal of Greenhouse Gas Control*, 58:127–141, March 2017.

[41] R. T. J. Porter, M. Fairweather, C. Kolster, N. Mac Dowell, N. Shah, and R. M. Wooley. Cost and performance of some carbon capture technology options for producing different quality CO_2 product streams. *International Journal of Greenhouse Gas Control*, 57:185–195, 2017.

[42] Barkatullah, N. and Ahmad A. Current status and emerging trends in financing nuclear power projects. *Energy Strategy Reviews*, 18:127 – 140, 2017.

[43] Sharpe, W. F. Capital Asset Prices: A Theory of Market Equilibrium under Conditions of Risk. *Journal of Finance*, 19:425–442, 1964.

[44] J. Lintner. The Valuation of Risky Assets and the Selection of Risky Investments in Stock Portfolios and Capital Budgets. *Review of Economics and Statistics*, 47:13–37, 1965.

[45] YCharts. S&P 500 Annual Total Return Historical Data. `https://ycharts.com/indicators/sandp_500_total_return_annual`. Accessed on May 1, 2018.

[46] SignalTrend Inc. FTSE 100 Stock Market Index Historical Returns. `http://www.forecast-chart.com/historical-ftse-100.html`. Updated February 6, 2018.

[47] 2018 Reuters. Markets: Indices. `https://www.reuters.com/finance/markets/indices`. Accessed on February 6, 2018.

[48] Chretien S. and Coggins, F. Cost of Equity for Energy Utilities: Beyond the CAPM. *Energy Studies Review*, 18(2):17–43, 2011.

[49] International Monetary Fund, International Financial Statistics and data files. Lending interest rates (%). https://data.worldbank.org/indicator/FR.INR.LEND, 2017. Accessed on February 4, 2018.

[50] Recommended Project Finance Structures for the Economic Analysis of Fossil-Based Energy Projects. Technical Report September, National Energy Technology Laboratory (NETL), 2008.

[51] DOE-NETL. Cost and Performance Baseline for Fossil Energy Plants Volume 1a: Bituminous Coal (PC) and Natural Gas to Electricity, Revision 3. Technical Report 2015/1723, July 2015.

[52] 2018 CNBC LLC. US 10-YR (US10Y:U.S.). https://www.cnbc.com/quotes/?symbol=US10Y. Data for December 20, 2017.

[53] Carbon Capture & Sequestration Technologies at MIT. Petra Nova W.A. Parish Fact Sheet: Carbon Dioxide Capture and Storage Project. https://sequestration.mit.edu/tools/projects/wa_parish.html, 2016. Accessed on January 20, 2017.

[54] Carbon Capture & Sequestration Technologies at MIT. Boundary Dam Fact Sheet: Carbon Dioxide Capture and Storage Project. https://sequestration.mit.edu/tools/projects/boundary_dam.html. Accessed on January 18, 2017.

[55] Kolster, C. and Masnadi, M. S. and Krevor, S. and Mac Dowell, N. and Brandt, A. R. MIICE - Model of Iterative Investment in CCS with CO_2-EOR (Open-Access). http://doi.org/10.1039/C7EE02102J, 2017.

[56] Melzer, L. S. Carbon Dioxide Enhanced Oil Recovery (CO_2-EOR): Factors Involved in Adding Carbon Capture, Utilization and Storage (CCUS) to Enhanced Oil Recovery. Technical Report National Enhanced Oil Recovery Initiative Resource, Melzer Consulting, Midland, Texas, 2012.

[57] Lord Ron Oxborough. Lowest Cost Decarbonisation for the UK: The Critical Role of CCS. Technical report, Parliamentary Advisory Group on CCS, September 2016. Report to the Secretary of State for Business, Energy and Industrial Strategy from the Parliamentary Advisory Group on Carbon Capture and Storage (CCS).

[58] MIT Energy Initiative. Kemper County IGCC Fact Sheet: Carbon Dioxide Capture and Storage Project. https://sequestration.mit.edu/tools/projects/kemper.html, 2016. Accessed on February 14, 2018.

[59] House of Commons - Energy and Climate Change Committee. Future of carbon capture and storage in the UK: Second Report of Session 201516, 2016.

[60] Jacobsen, R. Federal Budget Bill Includes Massive Tax Credits for Carbon Capture. https://www.triplepundit.com/2018/02/federal-budget-bill-includes-tax-credits-carbon-capture/, 2018.

[61] 115th Congress (2017-2018). S.1535 - FUTURE Act. https://www.congress.gov/bill/115th-congress/senate-bill/1535.

[62] Ms. Heitkamp. Bill to amend Section 45Q of the Internal Revenue Code of 1986, 2017. 114th Congress: 2nd Session.

[63] Scott, V. and Gilfillan, S. and Markusson, N. and Chalmers, H. and Haszeldine, R. S. Last chance for carbon capture and storage. *Nature Climate Change*, 3:105–111, 2012. Perspectives.

[64] NRG. News Release: NRG Energy, JX Nippon Complete World's Largest Post-Combustion Carbon Capture Facility On-Budget and On-Schedule. http://investors.nrg.com/phoenix.zhtml?c=121544&p=irol-newsArticle&ID=2236424, 2017. Accessed on February 6, 2017.

[65] U.S. Department of Energy, National Energy Technology Laboratory (NETL). Recovery Act: Petra Nova Parish Holdings: W.A. Parish Post-Combustion CO_2 Capture and Sequestration Project. https://www.netl.doe.gov/research/coal/project-information/fe0003311, 2016. Accessed on February 6,2017.

[66] U.S. Office of Fossil Energy. Petra Nova - W.A. Parish Project. https://energy.gov/fe/petra-nova-wa-parish-project, 2017. Accessed on January 17, 2017.

[67] Carbon Capture & Sequestration Technologies at MIT. Kemper County IGCC Fact Sheet: Carbon Dioxide Capture and Storage Project. http://sequestration.mit.edu/tools/projects/kemper.html, 2016. Accessed on February 16, 2017.

[68] Howard Herzog. Lessons Learned from CCS Demonstration and Large Pilot Projects: An MIT Initiative Working Paper. In *MIT Energy Initiative*. Massachusetts Institute of Technology, 2016.

[69] M. Verma. Fundamentals of Carbon-Dioxide-Enhanced Oil Recovery (CO_2-EOR) - A Supporting Document of the Assessment Methodology for Hydrocarbon Recovery using CO_2-EOR associated with Carbon Sequestration. Technical report, U.S. Geological Survey, 2015.

[70] Fred I. Stalkup, Jr. *Miscible displacement*. Society of Petroleum Engineers of AIME, Henry L. Doherty Series, 8 edition, 1984.

[71] Krevor, S. and Muggeridge, A. Introduction to Enhanced Oil Recovery Processes for Conventional Oil Production. In *The Imperial College Lectures in Petroleum Engineering*, Part 2 of Volume 3. World Scientific, 2017.

[72] OPEC & IEA. Average annual West Texas Intermediate (WTI) crude oil price from 1976 to 2018 (in U.S. dollars per barrel). `https://www.statista.com/statistics/266659/west-texas-intermediate-oil-prices/`, 2018. Accessed in May 2018.

[73] DiPietro P., Balash P., Wallace, M. A Note on Sources of CO_2 Supply for Enhanced-Oil-Recovery Operations. SPE Economics and Management, 2012. April.

[74] Herzog H. Scaling up carbon dioxide capture and storage: From megatons to gigatons. *Energy Economics*, 33:597–604, 2011.

[75] Kwak, D. H. and Kim, J.K. Techno-economic evaluation of CO_2 enhanced oil recovery (EOR) with the optimization of CO_2 supply. *International Journal of Greenhouse Gas Control*, 58:169–184, 2017.

[76] AbuZahra, M. Perspective from Emirates Steel Project/UAE. In *CCS Pathways to Commercialisation*, London, November 2015. Masdar Institute.

[77] Thurber, M.C. and Morse, R. K. *The Global Coal Market: Supplying the Major Fuel for Emerging Economies*. Cambridge University Press, 2015.

[78] Zhang, L. and Ren, B. and Huang, H. and Li, Y. and Ren, S. and Guoli Chen, G. and Zhang, H. CO_2 EOR and storage in Jilin oilfield China: Monitoring program and preliminary results. *Journal of Petroleum Science and Engineering*, 125:1–12, 2015.

[79] Wei, N. and Li, X. and Dahowski, R. T. and Davidson, C. L. and Liu, S. and Zha, Y. Economic evaluation on CO_2-EOR of onshore oil fields in China. *International Journal of Greenhouse Gas Control*, 37:170–181, 2015.

[80] Mac Dowell, N. and Fennel, P. S. and Shah, N. and Maitland, G. The role of CO_2 capture and utilization in mitigating climate change. *Nature Climate Change*, 7:243–249, 2017. Perspective.

[81] International Energy Agency. Carbon Capture and Storage: The Solution for deep emissions reductions. OECD/IEA 2015, 2015.

[82] Xiuzhang W. Shenhua Group Carbon Capture and Storage Demonstration. *Corner Stone: The Official Journal of the World Coal Industry*, 2014. January.

[83] Aycaguer, A. and Lev-On, M. and Winer, A. Reducing Carbon Dioxide Emission with Enhanced Oil Recovery Projects: A Life Cycle Assessment Approach. *Energy Fuels*, 15:303–308, 2001.

[84] Jaramillo, P. and Griffin, M. and McCoy, S. Life Cycle Inventory of CO_2 Enhanced Oil Recovery System. *Environmental Science and Technology*, 43(21):8027–8032, 2009.

[85] Faltison, J. and Gunter, B. In *Net CO_2 Stored in North America EOR Projects*, Society of Petroleum Engineers, Canadian Unconventional Resources and International Petroleum Conference, 2011. Society of Petroleum Engineers, Calgary, Alberta, Canada.

[86] Hertwich, E.G. and Aaber, M. and Singh, B., Stromman, A. A Life-cycle Assessment of Carbon Dioxide Capture for Enhanced Oil Recovery. *Chin. J. Chem. Eng*, 16(3):343–353, 2008.

[87] Stewart, R.J. and Haszledine, R.S. Can Producing Oil Store Carbon? Greenhouse Gas Footprint of CO_2-EOR, Offshore North Sea. *Environmental Science and Technology*, 49:5788–5795, 2015.

[88] Cooney, G. and Littlefield, J. and Marriott, J. and Skone, T. J. Evaluating the Climate Benefits of CO_2 Enhanced Oil Recovery Using Life Cycle Analysis. *Environmental Science & Technology*, 49(12):74917500, 2015.

[89] Scott, V. and Haszeldine, S. and Tett, S. F. B. and Oschlies, A. Fossil Fuels in a Trillion Ton World. *Nature Climate Change*, 5:419–423, 2015. Perspectives.

[90] Sean T. McCoy. *The Economics of CO_2 Transport by Pipeline and Storage in Saline Aquifers and Oil Reservoirs*. PhD thesis, Carnegie Mellon University, 2009.

[91] Leena Koottungal. 2014 worldwide EOR survey. Data report, Oil & Gas Journal, 2014.

[92] Godec, Michael. Global Technology Roadmap for CCS in Industry: Sectoral Assessment CO_2 Enhanced Oil Recovery. Technical report, Advanced Resources International, 2011.

[93] Advanced Resources International. Basin Oriented Studies for Enhanced Oil Recovery: Permian Basin. U.S. Department of Energy/Office of Fossil Energy, 2006. February.

[94] Jason Gaines. In *Monell Unit CO_2 Flood: Patrick Draw Field, Sweetwater County, Wyoming*. Andarko Petroleum Corporation, 2008.

[95] James Page. In *Salt Creek Field: CO_2 Flood Conformance*. Andarko Petroleum Corporation, 2009. EORI - Wyoming CO_2 Conference, June 2009.

[96] Kovscek, A.R. Personal communication, January 23, 2017. Professor in Energy Resources Engineering at Stanford University.

[97] PennEnergy Research. 2016 worlwide eor survey. 2016 update, Oil & Gas Journal, 2016.

[98] Jessen, K. and Kovscek, A.R. and Orr, Jr., F. M. Increasing CO_2 Storage in Oil Recovery. *Energy Conv. & Manage*, 46(11-12):1941–1956, 2005.

[99] Perera, M. S. A. and Gamaje, R. P. and Rathnaweera, T. D. and Ranathunga, A. S. and Koay, A. and Choi, X. A Review of CO_2-Enhanced Oil Recovery with a Simulated Sensitivity Analysis. *Energies*, 9:481, 2016.

[100] Thomas, S. Enhanced oil recovery: An overview. *Oil Gas Science Technology Review*, 63(IFP):9–19, 2008.

[101] Jackson, D. D. and Andrews, G.L. and Claridge, E.L. In *Optimum WAG ration vs. Rock wettability in CO_2 flooding*, In Proceedings of SPE Annual Technical COnference and Exhibition, Las Vegas, NV, USA, 22-26 September, 1985.

[102] Tiffin, D. L. and Yellig, W. F. Effects of mobile water on multiple-contact miscible gas displacements. *Society of Petroleum Engineering Journal*, 23:447–455, 1985.

[103] V. A. Kuuskraa. In *Maximizing Oil Recovery Efficiency and Sequestration of CO_2 with "Next Generation CO_2-EOR Technology*, Advanced Resources International, 2008.

[104] Schlumberger. Pore-Pressure Gradient Definition. http://www.glossary.oilfield.slb.com/Terms/p/pore-pressure_gradient.aspx, 2017. Accessed on January 10, 2017.

[105] James P. Meyer. Summary of Carbon Dioxide Enhanced Oil Recovery CO_2EOR Injection Well Technology. Background report, American Petroleum Institute, 2007.

[106] Jarrell, P.M. and Fox, C. and Stein, M. and Webb, S. *Practical Aspects of CO_2 Flooding.* SPE Monograph Series Vol. 22. Society of Petroleum Engineers, 2002.

[107] R. Span and W. Wagner. A New Equation of State for Carbon Dioxide, Covering the Fluid Region from the Triple Point Temperature to 1100 K at Pressures up to 800 MPa. *J. Phys. Chem. Ref. Data.*, 25:1509–1596, 1996.

[108] S. T. McCoy and E. S. Rubin. The effect of high oil prices on EOR project economics. *Energy Procedia*, 1:4143–4150, 2009.

[109] Mike Stell. In *An Auditor's View of Booking Reserves in CO_2-EOR Projects and the ROZ, Ryder Scott Company*, 16th Annual CO_2 Flooding Conference, December 2010, 2010.

[110] House, K. Personal communication, Fall 2016. Visiting Professor at Stanford University.

[111] Azzolina, N.A. and Nakles, D.V. and Gorecki, C.D. and Peck, W.D. and Ayash, S.C. and Melzer, L.S. and Chatterjee, S. CO_2 storage associated with CO_2 enhanced oil recovery: A statistical analysis of historical operations. *International Journal of Greenhouse Gas Control*, 37:384–397, 2015.

[112] Burke, L. Carbon Dioxide Fluid-Flow Modeling and Injectivity Calculations. Technical report, U.S. Geological Survey, 2011.

[113] DOE-NETL. Improving Domestic Energy Security and Lowering CO_2 Emissions with Next Generation CO_2 Enhanced Oil Recovery (CO_2-EOR). Prepared by Advanced Resources International 2011/1504, U.S. Department of Energy, National Energy Technology Laboratory 2014, 2011.

[114] DOE-NETL. Acquisition and Development of Selected Cost Data for Saline Storage and Enhanced Oil Recovery (EOR) Operations. Prepared by Advanced Resources International 2014/1658, U.S. Department of Energy, National Energy Technology Laboratory 2014, 2014.

[115] DOE-NETL. FE/NETL CO_2 Transport Cost Model: Description and User's Manual (EOR). Technical Report 2014/1660, U.S. Department of Energy, National Energy Technology Laboratory 2014, 2014.

[116] IEA Greenhouse Gas R&D Program (IEA GHG). In *CCS Cost Network, 2016 Workshop*, August, 2016/09, 2016.

[117] P. Bains, P. Psarras, and J. Wilcox. CO_2 capture from the industry sector. *Progress in Energy and Combustion Science*, 63:146–172, 2017.

[118] Richard S. Middleton. A new optimization approach to energy network modeling: anthropogenic CO_2 capture coupled with enhanced oil recovery. *International Journal of Energy Research*, 37:17941810, 2013.

[119] Middleton, R. S. and Levine, J. S. and Bielicki, J. and Viswanathan, H. S. and Carey, J. W. and Stauffer, P. H. Jumpstarting commercial-scale CO_2 capture and storage with ethylene production and enhanced oil recovery in the U.S. Gulf. *Greenhouse Gases: Science and Technology*, 5(3):241253, 2015.

[120] U.S. Energy Information Administration . Wholesale Electricity and Natural Gas Market Data. `http://www.eia.gov/electricity/wholesale/`. Accessed on January 10, 2017.

[121] Carbon dioxide transport and storage costs in netl studies. Technical report, National Energy Technology Laboratory (NETL), 2013. March.

[122] Carbon Capture and Sequestration Technologies Program Massachusetts Institute of Technology. Carbon Management GIS: CO_2 Pipeline Transport Cost Estimation. Updated in june 2009, National Energy Technology Laboratory, U.S. Department of Energy, 2006.

[123] T. P. Wright. Factors affecting the costs of airplanes. *Journal of aeronautical sciences*, 3:122–128, 1936.

[124] M. J. Anzanello and F. S. Fogliatto. Learning curve models and applications, literature review and research directions. *International Journal of Industrial Ergonomics*, 41:573–583, 2011.

[125] Rochedo, P. and Szklo, A. Designing learning curves for carbon capture based on chemical absorption according to the minimum work of separation. *Applied Energy*, 108:383–391, 2013.

[126] Riahi, K. and Rubin, E. S. and Taylor, M. and Schrattenholzerm L. and Hounshell, D. Technological learning for carbon capture and sequestration technologies. *Energy Ergonomics*, 26:539–564, 2004.

[127] Azavedo, I. and Jaramillo, P. and Rubin, E. S. and Yeh, S. Technology Learning Curves and the Future Cost of Electric Power Generation. In *Presentation to the EPRI 18th Annual Energy & Climate Change Research Seminar, Washington, D.C.*, 2013. May.

[128] Kramer, G.J. and Haigh, M. No quick switch to low-carbon energy. *Nature*, 462:568–569, 2009.

[129] Napp, T. and Bernie, D. and Thomas, R. and Lowe, J. and Hawkes, A. and Ghambir, A. Exploring the Feasibility of Low-Carbon Scenarios Using Historical Energy Transition Analysis. *Energies*, 10(1), 2017. 116.

[130] NASDAQ. Crude Oil: WTI (NYMEX) Price. `http://www.nasdaq.com/markets/crude-oil.aspx?timeframe=1y`, 2017. Accessed on January 17, 2017.

[131] Z. Dai, H. Viswanathna, R. Middleton, F. Pan, W. Ampomah, C. Yang, W. Jia, T. Xiao, S.Y. Lee, B. McPherson, R. Balch, R. Grigg, and M. White. CO_2 Accounting and Risk Analysis for Co_2 Sequestration at Enhanced Oil Recovery Sites. *Environmental Science and Technology*, 50(14):7546–7554, 2016. June.

[132] Kossoy, A. and Peszko, G. and Oppermann, K. and Prytz, N. and Klein, N. Blok, K. and Lam, L. and Wong, L. and Borkent, B. State and Trends of Carbon Pricing 2015 (September). Technical report, World Bank, Washington, D.C., 2015.

[133] Noy, D. J. and Holloway, S. and Chadwick, R. A. and Williams, J. D. O. and Hannis, S. A. and Lahann, R. W. Modelling large-scale carbon dioxide injection into the Bunter Sandstone in the UK Southern North Sea. *International Journal of Greenhouse Gas Control*, 9:220–233, 2012.

[134] Williams, J. D. O. and Holloway, S. and Williams, G. A. Pressure constraints on the CO_2 storage capacity of the saline water-bearing parts of the Bunter Sandstone Formation in the UK Southern North Sea. *Petroleum Geoscience*, 20(2):155–167, 2014.

[135] Comptroller and Auditor General. Carbon capture and storage: the second competition for government support. Ordered by the House of Commons,

Department for Business, Energy & Industrial Strategy, January 2017. National Audit Office.

[136] Committee on Climate Change. The Fifth Carbon Budget: The next step towards a low-carbon economy. Technical report, November 2015. Presented to the Secretary of State pursuant to section 34 of the Climate Change Act 2008.

[137] Ghambir, A. and Drouet, L. and McCollum, D. and Napp, T. and Bernie, D. and Hawkes, A. and Fricko, O. and Havlik, P. and Riahi, K. and Bosetti, V. and Lowe, J. Assessing the Feasibility of Global Long-Term Mitigation Scenarios. *Energies*, 10:89, 2017.

[138] Thibeau, S. and Bachu, S. and Birkholzer, J. and Holloway, S. and Neele, F. and Zhou, Q. Using pressure and volumetric approaches to estimate CO_2 storage capacity in deep saline aquifers. *Energy Procedia*, 63:5294–5304, 2014.

[139] Heinemann, N. and Wilkinson, M. and Pickup, G. E. and Haszeldine, R. S. and Cutler, N. A. CO_2 storage in the offshore UK Bunter Sandstone Formation. *International Journal of Greenhouse Gas Control*, 6:210–219, 2012.

[140] Smith, D. J. and Noy, D. J. and Holloway, S. and Chadwick, R. A. The impact of boundary conditions on CO_2 Storage capacity estimation in aquifers. *Energy Procedia*, 4:4828–4834, 2011.

[141] Williams, J. D. O. and Jin, M. and Bentham, M. and Pickup, G. E. and Hannis, S. D. and Mackay, E. J. Modelling carbon dioxide storage within closed structures in the UK Bunter Sandstone Formation. *International Journal of Greenhouse Gas Control*, 18:38–50, 2013.

[142] ETI 2016. A Summary of Results from the Strategic UK CO_2 Storage Appraisal Project, funded by DECC, 2016. Strategic UK CCS Storage Appraisal Project, funded by DECC, commissioned by the ETI and delivered by Pale Blue Dot Energy, Axis Well Technology and Costain.

[143] Mechleri, E. and Brown, S. and Fennel, P. S. and Mac Dowell, N. CO_2 capture and storage (CCS) cost reduction via infrastructure right-sizing. *Chemical Engineering Research and Design*, 119: 130–139, 2017.

[144] Mechleri, E. and Fennel, P. S. and Mac Dowell, N. Optimisation and evaluation of flexible operation strategies for coal-and gas-CCS power stations

with a multi-period design approach. *International Journal of Greenhouse Gas Control*, 59:24–39, 2017.

[145] Mac Dowell, N. and Staffell, I. The role of flexible CCS in the UK's future energy system. *International Journal of Greenhouse Gas Control*, pages 1–18, 2016.

[146] Mac Dowell, N. and Shah, N. The multi-period optimisation of an amine based CO_2 capture process integrated with a super-critical coal-fired power station for flexible operation. *Computers & Chemical Engineering*, 74:169–183, 2015.

[147] Xie, J. and Zhang, K. and Li, C. and Wang, Y. Preliminary study on the CO_2 injectivity and storage capacity of low-permeability saline aquifers at Chenjiacun site in the Ordos Basin. *International Journal of Greenhouse Gas Control*, 52:215–230, 2016.

[148] Deng, H. and Stauffer, P. H. and Dai, Z. and Jiao, Z. and Surdam, R. C. Simulation of industrial-scale CO_2 storage: Multi-scale heterogeneity and its impacts on storage capacity, injectivity and leakage. *International Journal of Greenhouse Gas Control*, 10:397–418, 2012.

[149] Bannach, A. and Hauer, R. and Streibel, M. and Kuhn, M. and Stienstra, G. Stable large-scale CO_2 storage in defiance of an energy system based on renewable energy: Modelling the impact of varying CO_2 injection rates on reservoir behaviour. *Energy Procedia*, 76:573–581, 2015.

[150] Farhat, K. and Benson, S.M. A technical assessment of CO_2 Interim Sotrage in deep saline aquifers. *International Journal of Greenhouse Gas Control*, 15:200–212, 2013.

[151] International Energy Agency Grennhouse Gas R&D Programme. Injection Strategies for CO_2 Storage Sites. Technical Report 2010/04, 2010. June.

[152] Wiese, B. and Numtz, M. and Klatt, M. and Kuhn, M. Sensitivities of injection rates for single well CO_2 injection into saline aquifers. *Chemie der Erde*, 70:165–172, 2010.

[153] Birkholzer, J. T. and Zhou, Q. Basin-scale hydrogeologic impacts of CO_2 storage: Capacity and regulatory implications. *International Journal of Greenhouse Gas Control*, 3(6):745–756, 2009.

[154] Bachu, S. Review of CO_2 storage efficiency in deep saline aquifers. *International Journal of Greenhouse Gas Control*, 40:188–202, 2015.

[155] Global CCS Institute. White Rose CCS Project. https://www.globalccsinstitute.com/projects/white-rose-ccs-project, 2015. Accessed on August 30, 2016.

[156] Dixon, P. and Mitchell, T. Lessons learned: Lessons and evidence derived from UK CCS Programmes, 2008-2015. Technical report, Carbon Capture and Storage Association, 2016.

[157] Furnival, S. and Wright, S. and Dingwall, S. and Bailey, P. and Brown, A. and Morrison, D. and De Silva, R. Subsurface Characterisation of a Saline Aquifer Cited Commercial Scale CO_2 Disposal. *Energy Procedia*, 63:4926–4936, 2014.

[158] Mendelevitch, R. The role of CO_2-EOR for the development of a CCTS infrastructure in the North Sea Region. *International Journal of Greenhouse Gas Control*, 20:132–159, 2014.

[159] Mijic, A. and LaForce, T. C. and Muggeridge, A. H. CO_2 injectivity in saline aquifers: The impact of non-Darcy flow, phase miscibility, and gas compressibility. *Water Resources Research*, 50:4163–4185, 2014.

[160] Hortle, A. and Michael, K. and Azizi, E. Assessment of CO_2 storage capacity and injectivity in saline aquifers - comparison of results from numerical flow simulations, analytical and generic models. *Energy Procedia*, 63:3553–3562, 2014.

[161] Hassanzadeh, H. and Pooladi-Darvish, M. and Elsharkawy, A. M. Predicting PVT data for CO_2 brine mixtures for black oil simulation of CO_2 geological storage. *International Journal of Greenhouse Gas Control*, 2:65–77, 2008.

[162] Reynolds, C. A. *Two-phase flow behaviour and relative permeability between CO_2 and brine in sandstones at the pore and core scales*. PhD thesis, Imperial College London, 2016.

[163] Spiteri, E. J. and Juanes, R. and Blunt, M. J. and Orr Jr, F. M. Relative-Permeability Hysteresis: Trapping Models and Application to Geological CO_2 Sequestration. In *SPE Annual Technical Conference and Exhibition*. Society of Petroleum Engineers, 2005. Dallas, Texas.

[164] Raza, A. and Rezaee, R. and Gholami, R. and Rasouli, V. and Bing, C. H. and Nagarajan, R. and Hamid, M. A. Injectivity and quantification of capillary trapping for CO_2 storage: A review of influencing parameters. *Journal of Natural Gas Science and Engineering*, 26:510–517, 2015.

[165] Killough, J. E. Reservoir simulation with history dependent saturation functions. *Society of Petroleum Engineers Journal*, 16(1):37–48, 1976.

[166] Juanes, R. and Spiteri, E. J. and Orr, F. M. and Blunt, M. J. Impact of relative permeability hysteresis on geological CO_2 storage. *Water Resources Research*, 42(12):1–13, 2006.

[167] Carneiro, J. and Martinez, R. and Suarez, I. and Zarhloule Y. and Rimi, A. Injection rates and cost estimates for CO_2 storage in the west Mediterranean region. *Environmental Earth Science*, 73:2951–2962, 2015.

[168] Hosa, A. and Esentia, M. and Stewart, J. and Haszeldine, S. Injection of CO_2 into saline formations: Benchmarking worldwide projects. 89:1855–1864, 2011.

[169] Vernon, J. P. and Kendall, J. M. and Stork, A. L. and Chadwick, R. A. and White, D. J. and Bissell, R. C. . Comparison of geomechanical deformation induced by megatonne-scale CO_2 storage at Sleipner, Weyburn, and In Salah. *Proceedings of the National Academy of Science*, pages E2762–E2771, 2013.

[170] Leetaru, H. E. and Frailey, S. M. and Damico, J. and Mehnert, E. and Birkholzer, J. and Zhou, Q. and Jordan, P. D. Understanding CO_2 Plume Behavior and Basin-Scale Pressure Changes during Sequestration Projects through the use of Reservoir Fluid Modelling. *Energy Procedia*, 1:1799–1806, 2009.

[171] Furuvik, N. I. and Halvorsen, B. M. Simulation of CO_2 injection in fractured oil reservoir. In *Proceedings of the 56th SIMS*, October 2015. Linkoping, Sweden.

[172] Chadwick, R. A. *Offshore CO_2 storage: Sleipner natural gas field beneath the North Sea*, chapter 10, pages 227 –250. Woodhead Publishing Limited, 2013.

[173] Mathias, S. A. and Gluyas, J. G. and Mackay, E. J. and Goldthorpe, W. H. A statistical analysis of well production rates from UK oil and gas fields - Implications for carbon capture and storage. *International Journal of Greenhouse Gas Control*, 19:510–518, 2013.

[174] IHS Global Inc. Oil & Natural Gas Transportation & Storage Infrastructure: Status, Trends & Economic Benefits. Technical report, American Petroleum Institute, 2013.

[175] Mathias, S. A. and Gluyas, J. G. and Gerardo J. and Bryant, S. L. and Wilson, D. On relative permeability data uncertainty and CO_2 injectivity estimation for brine aquifers. *International Journal of Greenhouse Gas Control*, 12:200–212, 2013.

[176] Pickup, G.E. and Jin, M. and Mackay, E.J. Simulation of Near-Well Pressure Build-up in Models of CO_2 Injection . In *ECMOR XIII - 13th European Conference on the Mathematics of Oil Recovery*, number B34. ECMOR, September 2012.

[177] S. Posch and M. Haider. Optimization of CO_2 compression and purification units (CO_2CPU) for CCS power plants. *Fuel*, 101:254–263, November 2012.

[178] G. Pipitone and O. Bolland. Power generation with CO_2 capture: Technology for CO_2 purification. *International Journal of Greenhouse Gas Control*, 3(5):528–534, September 2009.

[179] The European Parliament and the Council of the European Union. DIRECTIVE 2009/31/EC OF THE EUROPEAN PARLIAMENT AND OF THE COUNCIL. Office Journal of the European Union, April 2009. `http://eur-lex.europa.eu/legal-content/EN/TXT/PDF/?uri=CELEX:32009L0031&from=EN`, Accessed on January 22, 2018.

[180] J. Yan, M. Anheden, and C. Bernstone. Impacts of Non-condensable Components on CCS. In *IEA CO_2 Specification working group meeting*, Stockholm, 2008. http://ieaghg.org (accessed on March 20, 2015).

[181] M. B. Toftegaard, J. Brix, P. A. Jensen, P. Glarborg, and A. D. Jensen. Oxy-fuel combustion of solid fuels. *Progress in Energy and Combustion Science*, 36(5):581–625, 2010.

[182] Eickhoff, C. and Brown, A and Neele, F. Techno-economic issues and trade-offs for CO_2 purity in CCS chains. *Energy Procedia*, 114:6698 6707, 2017.

[183] Lilliestrle, A. and Mlnvik, M. J. and Tangen, G. and Jakobsen, J. P. and Tolla, S. Munkejord, S. T. and Morin, A. and Strset, S. . The IMPACTS project: The impact of the quality of CO_2 on transport and storage behaviour. *Energy Procedia*, 51:402–410, 2014.

[184] V. A. Kuuskraa, M. L. Godec, and P. Dipietro. CO_2 Utilization from Next GenerationCO_2 Enhanced Oil Recovery Technology. *Energy Procedia*, 37:6854–6866, 2013.

[185] N. Mac Dowell, A. Alhajaj, M. Konda, and N. Shah. Multiscale whole-systems design and analysis of co$_2$ capture and transport networks. *21st European Symposium on computer aided process engineering*, 29:1205–1209, 2011.

[186] A. Alhaja, N. Mac Dowell, and N. Shah. Multiscale Design and Analysis of CO_2 Capture, Transport and Storage Networks. *Energy Procedia*, 37:2552–2561, 2013.

[187] Energy Technologies Institute. Carbon capture and storage: Building the UK carbon capture and storage sector by 2030 - scenarios and actions. Insights report, ETI, 2015.

[188] Kazuya Goto, K. and Kazama, S. and Furukawa, A. and Serizawa, M. and Aramaki, S. and Shoji, K. Effect of CO2 purity on energy requirement of CO_2 capture processes. *Energy Procedia*, 37:806 812, 2013.

[189] Walspurger, S. and van Dijk, H. A. J. EDGAR CO2 purity: type and quantities of impurities related to CO_2 point source and capture technology: a Literature study. Technical report, ECN, 2012.

[190] International Energy Agency. *Emissions from coal fired power Generation, Osamu Ito*, Workshop on IEA High Efficiency, Low Emissions Coal Technology Roadmap, 2011. November.

[191] E. de Visser, C. Hendriks, M. Barrio, M. J. Mø lnvik, G. de Koeijer, S. Liljemark, and Y. Le Gallo. Dynamis CO_2 quality recommendations. *International Journal of Greenhouse Gas Control*, 2(4):478–484, 2008.

[192] International Energy Agency Greenhouse Gas R&D Programme. CO_2 Pipeline Infrastructure. Technical report. 2013/18, December, 2013.

[193] A Shafen and T Carter. Geological Sequestration of Greenhouse Gases. In M Kutz and A Elkamel, editors, *Environmentally Conscious Fossil Energy Production*. Wiley & Sons, 2010.

[194] M. Chaczykowski and A. J. Osiadacz. Dynamic simulation of pipelines containing dense phase/supercritical CO_2-rich mixtures for carbon capture and storage. *International Journal of Greenhouse Gas Control*, 9:446–456, 2012.

[195] B. Wetenhall, J.M. Race, and M.J. Downie. The Effect of CO_2 Purity on the Development of Pipeline Networks for Carbon Capture and Storage Schemes. *International Journal of Greenhouse Gas Control*, 30:197–211, November 2014.

[196] H. Mahgerefteh, S. Brown, and G. Denton. Modelling the impact of stream impurities on ductile fractures in CO_2 pipelines. *Chemical Engineering Science*, 74:200–210, 2012.

[197] A. Cosham, D. G. Jones, K. Armstrong, D. Allason, and J. Barnett. The Decompression Behaviour of Carbon Dioxide in the Dense Phase. In *Proceedings of the 2012 9th International Pipeline Conference*, number 90461, page 447, 2012.

[198] G. Heddle, H. Herzog, and M. Klett. The Economics of CO_2 Storage. Technical report, Laboratory for Energy and the Environment, Massachussetts Institute of Technology, 2003. http://lfee.mit.edu (accessed on April 10, 2015).

[199] E. de Visser, C. Hendriks, G. de Koeijer, S. Liljemark, M. Barrio, A. Austegard, and A. Brown. Towards Hydrogen and Electricity Production with Carbon Dioxide Capture and Storage: D 3.1.3 DYNAMIS CO_2 quality recommendations. Technical report, Ecofys, 2007. https://www.sintef.no (Accessed on May 1, 2015).

[200] J. P Meyer. Summary of Carbon Dioxide Enhanced Oil Recovery (CO_2-EOR) Injection Well Technology prepared for the American Petroleum Institute). Technical report, American Petroleum Institute, 2005. http://www.api.org (accessed on April 20, 2015).

[201] GCP 2001 - 2017. The Global Carbon Project. `http://www.globalcarbonproject.org/`. Accessed on 20 January 2018.

[202] Neele, F. and Koornneef, J. and Jakobsen, J. P. and Brunsvold, A. and Eickhoff, C. Toolbox of effects of CO2 impurities on CO2 transport and storage systems. *Energy Procedia*, 114:6536 6542, 2013.

[203] ZEP. Business models for commercial CO_2 transport and storage. Technical Report June, 2014.

[204] Q Zhang, C. F. Heuberger, I. E. Grossmann, A. Sundaramoorthy, and J. M. Pinto. Air Separation with Cryogenic Energy Storage: Optimal Scheduling Considering Electric Energy and Reserve Market Participation. *AIChe Journal*, page 12, 2015.

[205] F. Vega, B. Navarrete, M. Cano, and E. Portillo. Development of Partial Oxy-combustion Technology: New Solvents Applied to CO_2 Capture in Fossil-fuels Power Plants. *Energy Procedia*, 63:484–489, 2014.

[206] H. Stadler, F. Beggel, M. Habermehl, B. Persigehl, R. Kneer, M. Modigell, and P. Jeschke. Oxyfuel coal combustion by efficient integration of oxygen transport membranes. *International Journal of Greenhouse Gas Control*, 5(1):7–15, 2011.

[207] S. Engels, F. Beggel, M. Modigell, and H. Stadler. Simulation of a membrane unit for oxyfuel power plants under consideration of realistic BSCF membrane properties. *Journal of Membrane Science*, 359(1-2):93–101, 2010. Elsevier B.V.

[208] V. White, R. Allam, and E. Miller. Purification of Oxyfuel-Derived CO_2 for Sequestration or EOR. *Energy Procedia*, 1(1):399–406, 2009.

[209] D.U. Peng and D.B. Robinson. A New Two-Constant Equation of State. *Ind. Eng. Chem., Fundam.*, 15:59–64, 1976.

[210] D. Kopke and R. Eggers. Phase Equilibria measurements and their application for the CO_2 seperation from CO_2 rich gases. In *Proceedings of the IEAGHG International oxy-combustion network*, Yokohama, 2008.

[211] A. Nehrozoglu. Advanced CO_2 Cycle Power Generation. Technical report, Foster Wheeler Power Group, Inc. for US Department of Energy, July 2003. http://www.osti.gov (accessed on April 1, 2016).

[212] International Energy Agency Greenhouse Gas R&D Programme. Oxy combustion processes for co_2 capture from power plant. Technical report, July 2009. Report number 2005/9.

[213] V.S. Angus, B. Armstrong, and K.M. de Rerrck. Carbon Dioxide: International Thermodynamic Tables of the Fluid State, Bd. 3. Von S. Angus, B. Armstrong und K. M. de Rerrck. *Chemie Ingenieur Technik*, 49(7):594, July 1977. Pergamon Press Ltd., Oxford and New York 1976.

[214] G.H. Zenner and L.I. Dana. Liquid-Vapour Equilibrium Compositions of Carbon DIoxide - Oxygen - Nitrogen Mixtures. *Chem. Eng. Prog. Symp. Ser*, 59(44):36–41, 1963.

[215] G. De Guido, S. Lange, Moioli S., and L.A. Pellegrini. Calculation of CO_2 freezing points in mixtures using SRK and PR EoSs. *Journal of Energy Challenges and Mechanics*, 1(4), 2014.

[216] Aspen Tech. *Aspen Economic Evaluation Family*. Aspen Technology Inc., 2014.

[217] Aspen Tech. *Aspen Capital Cost Estimator: User's Guide*. Aspen Technology Inc., 2012.

[218] United States Department of Labor: Bureau of Labor Statistics. Databases, Tables & Calculators by Subject: CPI Inflation Calculator. `https://www.bls.gov/data/inflation_calculator.htm`. Accessed on January 10, 2017.

[219] R.J. Campbell. *Increasing the Efficiency of Existing Coal- Fired Power Plants*. Congressional Research Service, 2013.

[220] Offshore CO_2-EOR as Part of a National CCS Programme: Opportunities and Challenges. Senergy, Hughes, D.S., February 2014.

[221] Energy Research Partnership. Prosepects for CO_2EOR in the UKCS. Technical report, ERP, October 2015. http://erpuk.org/project/co2-eor/ (accessed October 21, 2015).

[222] M. Netsuil and Ditl P. Comparison of methods for dehydration of natural gas stored in underground gas storages. *Inzyniera i aparatura chemiczna*, 87, 2010.

[223] H. Hansen, A. Chiriac, N. Incoom, and A. Olsen. Design of a TEG dehydration train model using the glycol property package in HYSYS. Master's thesis, Aalborg University, 2013.

[224] A.J. Kidnay, W. R. Parrish, and McCartney D.G. *Fundamentals of natural gas processing*. CRC Press, 2011.

[225] R. Li, C. Miao, and Y. Wang. Purity Analysis of Industrial Triethylene Glycol by Capillary Gas Chromatography. *Journal of Chromatographic Science*, 36, 1998.

[226] F. Binci, F.E. Ciarapica, and G. Giacchetta. In review.

[227] The Dow Chemical Company. Letter addressed to Dow Customer, 2011.

[228] P.S. Prada and MNVSN Konda. Development of an Integrated CO_2 Capture, transportation and Storage Infrastructure for the UK and North Sea using an Optimisation Framework, 2010.

[229] EsriUKContent. OS Open Carto Tile Layer: UK Map, 2015.

[230] David M. Gay. IBM ILOG CPLEX Optimization Studio Getting Started with CPLEX, Version 12, Release 4. Technical report, 2011. http://cedric.cnam.fr/ (accessed on June 1, 2015).

[231] D. Benton. Decarbonising British Industry: Why industrial CCS clusters are the answer. Technical report, Green Alliance policy insight, March 2015. http://www.green-alliance.org.uk/ (accessed on May 1, 2015).

[232] ZEP. The costs of co_2 capture, transport and storage: Post-demonstration ccs in the eu. Technical report, European Technology Platform for Zero Emission Fossil Fuel Power Plants, 2011. http://www.zeroemissionsplatform.eu (accessed on May 6, 2015).

[233] Godec, Michael. In *CO_2-EOR and CCUS: Worldwide Potential and Commercial Drivers*, SPE Annual Technical Conference and Exhibition Special Session: CO_2-EOR as a Pathway for CCUS, 2014. Amsterdam, Netherlands, October 2014.

[234] Global CCS Institute. Large Scale CCS Facilities: Project Database. `https://www.globalccsinstitute.com/projects/large-scale-ccs-projects`, 2017. Accessed on November 1, 2017.

[235] C. Kolster, E. Mechleri, S. Krevor, and N. Mac Dowell. CO_2 price calculation as a function of purity for CO_2 compression and purification units' cost data. `http://doi.org/10.5281/zenodo.1230482`, 2018.

Appe

A1 A]

A1 MI]

MIICE M
with the foll

A2 Mo

Model env

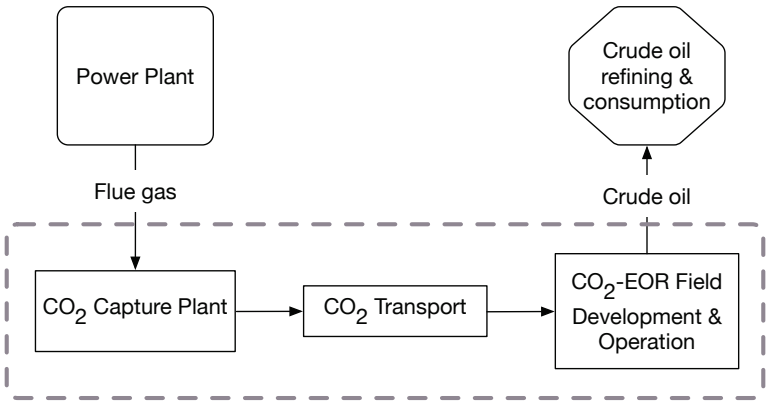

Figure A1: Conceptual representation of the CCS + CO_2-EOR model envelope (dotted line box) without considering physical flow streams

A3 CCS and CO_2 enhanced oil recovery field development and cost modeling

CO_2 capture cost in literature and model-based assumptions

Table A1: Operating costs for CO_2 capture as reported by Worley Parsons and adjusted to a $MtCO_2$ basis - all cost values adjusted to 2016 US$.

Parameter	Worley Parsons Report	Adjusted Calculations for this Study
Type of power plant considered	Pulverized coal firing	idem
Type of capture technology	Post-combustion amine scrubbing	idem
Net Power Output	546 MW	approx. 110 MW
Capture rate	90%	90%
CO_2 Captured	4.98 Mt/year	1 Mt/year
Power associated with capture plant	87 MW	17.5 MW
Cost of electricity consumed	$30.25 million/year	$6.07 million/year
Variable O&M	$4.53 million/MWh	$0.69 million/year
Fixed O&M	$11.41 million	$2.29 million

CO_2 transport costs

Table A2: Capital and operating costs for transport pipelines from source to sink required for projects of 1- 4MtCO_2/year capture rates (M$ = $ million)

Cost type	Function of	1 MtCO_2/year	2 - 3MtCO_2/year	$\geq$ 3 MtCO_2/year
Pipeline Capital Costs				
Materials	Diameter (D) & Length (L)	7.223 M$	11.115 M$	15.377 M$
Labor	D & L	28.209 M$	32.976 M$	36.672 M$
Miscellaneous	D& L	7.825 M$	11.287 M$	13.815 M$
Right of Way	D& L	2.976 M$	3.172 M$	3.1547 M$
CO_2 surge tank	Fixed	1.332 M$	idem	idem
Pipeline control system	Fixed	0.120 M$	idem	idem
Total Capital Costs		47.686 M$	60.003 M$	75.567 M$
Pipeline Operating Costs				
Operating & Maintenance	L	0.561 M$	idem	idem
Total Operating Costs		0.561 M$/year	idem	idem

EOR field characteristic ranges

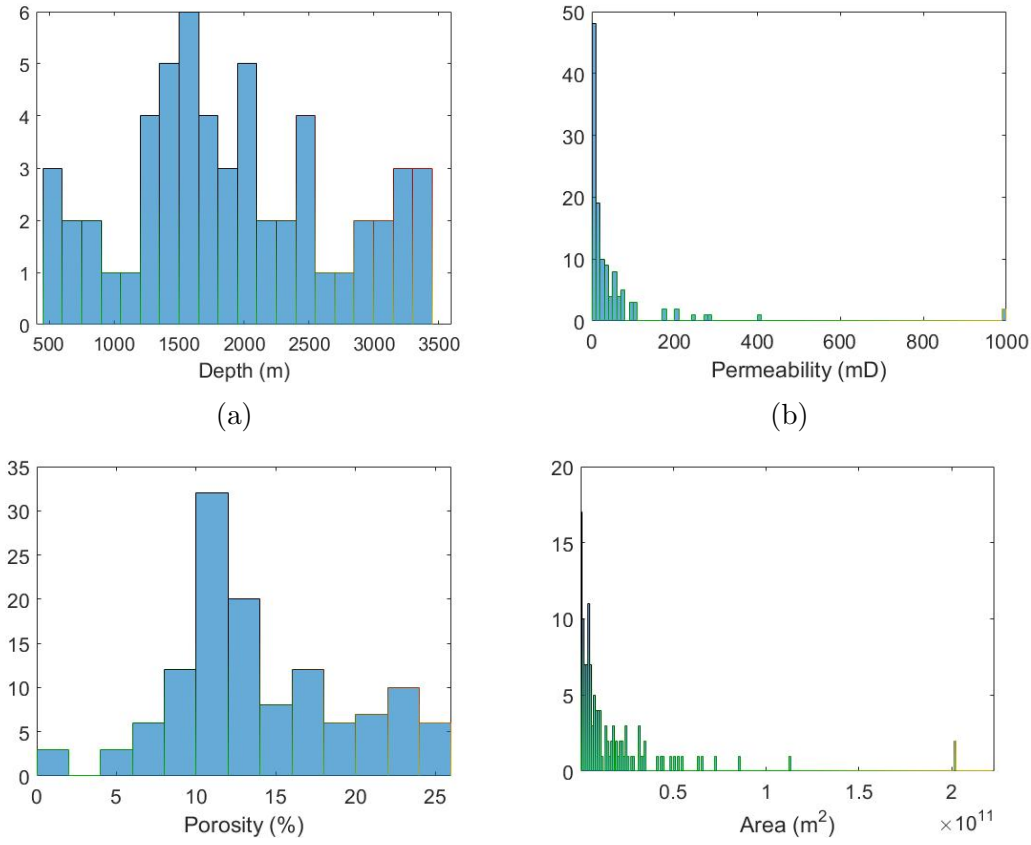

(a) (b) (c) (d)

Figure A2: Distributions of reservoir characteristics including depth (m), porosity (%), permeability (mD) and field area (m^2) for oil fields with CO_2-EOR activity in the U.S. as well as Prudhoe Bay hydrocarbon miscible injection field based on Oil & Gas Journal 2014 Survey data.

CO

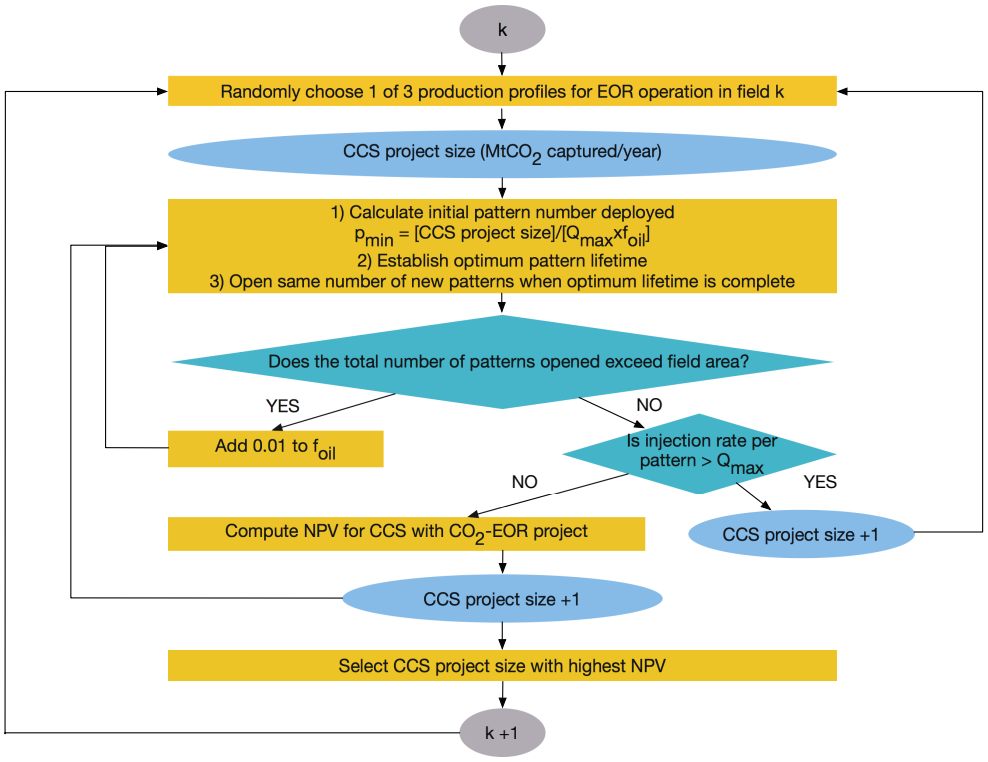

Figure A3: Flow diagram describing the decision strategy process for CO_2-EOR pattern deployment within a field k.

EOR production profile fit parameters

Table A3: Parameters of logistic and exponential equations of curve fits for production profiles of oil and CO_2 as a percentage of OOIP and HCPV respectively

Oil production fit	d	a	b	c	RMSE/R-Square
Low	0.0	0.105	9.813	0.4213	0.001414/0.9977
Medium	0.01	0.1774	4.86	0.447	0.002853/0.9954
High	0.09	0.3818	3.449	0.3415	
CO_2 production fit	d'	a'	b'	c'	RMSE/R-Square
Low	0.33	0.3155	0.8515	0.1492	0.01481/0.9751
Medium	0.4	0.6357	0.9292	0.5785	0.009409/0.997
High	0.4792	1.276	0.9086	1.078	

Cost inflation factors

Table A4: Inflation factors used to convert US$ costs from literature to constant 2016 US$ based on the Bureau of Labor Statistics Consumer Price Index inflation calculator[218].

Year of cost reported	Inflation factor to 2016 US$
2004	1.270
2010	1.100
2013	1.030
2014	1.017

Compound annual growth rates

A compound annual growth rate (CAGR) is used to compare results of cumulative CCS capacity deployed by 2050 and cumulative oil production rates to both industries' growth rate predictions. The CAGR describes a rate at which an industry would need to grow by every year, if this were at a steady rate, to achieve a final industry objective size. These rates are calculated against values of oil production from CO_2-EOR in the US, which was at 156.95 MMbbl/year in 2015[233] and the global value for CO_2 captured in 2016 of 27 $MtCO_2$/year[234].

Slow and fast industry growth scenarios

In a slow deployment scenario, we assume that the 5-year demonstration period is followed by a growth to materiality of 20% per year (lower than the exponential growth assumed), followed by a stagnated growth of 3% per year based on a low carbon technology study by Napp et al.[129]. Meanwhile, a much faster industry growth scenario considers that the first 5 years of project initiation has an upper bound of 2^{year} project investments. In the 10 years that follow, the number of projects that can be built is limited by a 40% growth rate year on year. The 10 years that follow see a slower allowable growth rate as momentum is reduced to a 20% growth rate and the 10 years that follow are limited by a 10% yearly growth rate.

A4 Five world scenario results

Cumulative CO_2 stored and oil produced

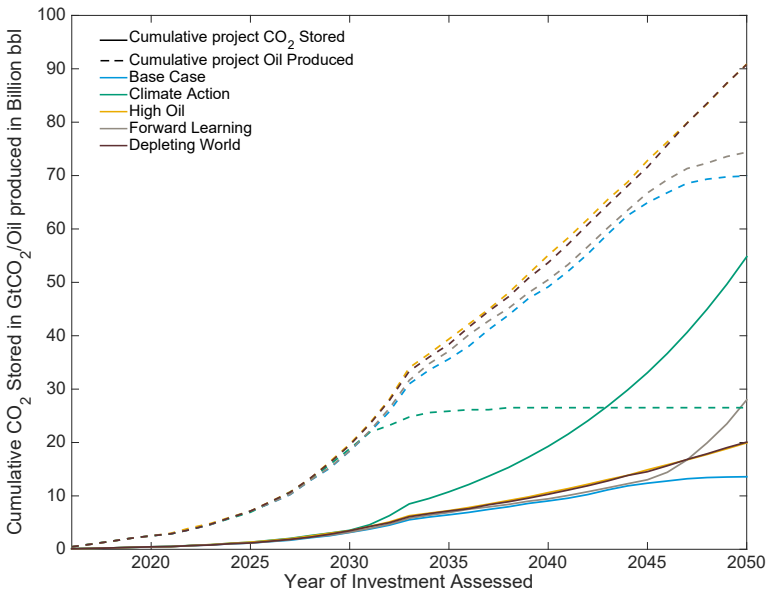

Figure A4: Graph showing cumulative CO_2 stored and oil produced as a result of successful projects obtained in each of the Five World Scenarios

Average field characteristics of successful projects

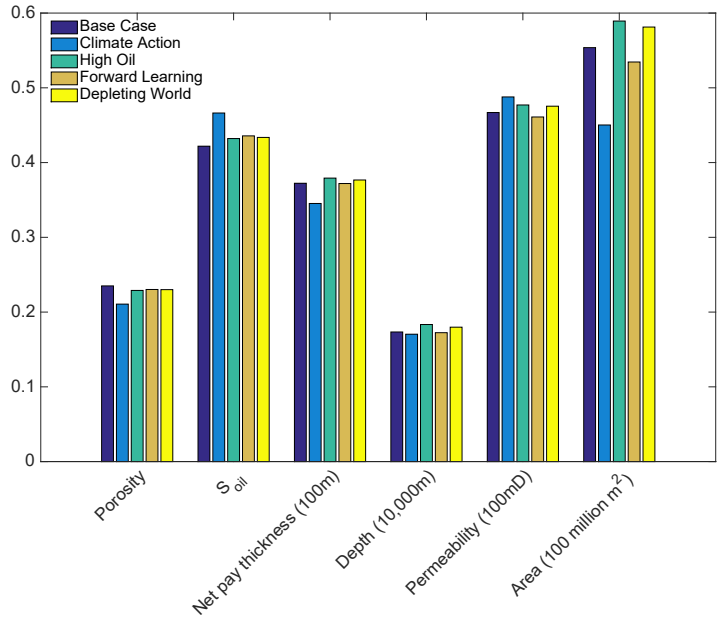

Figure A5: Bar chart showing the total average field characteristics for all successful projects resulting from each of the five world scenarios from the pool of 1000 fields

A5 Results showing sensitivities of CO_2 storage and oil production

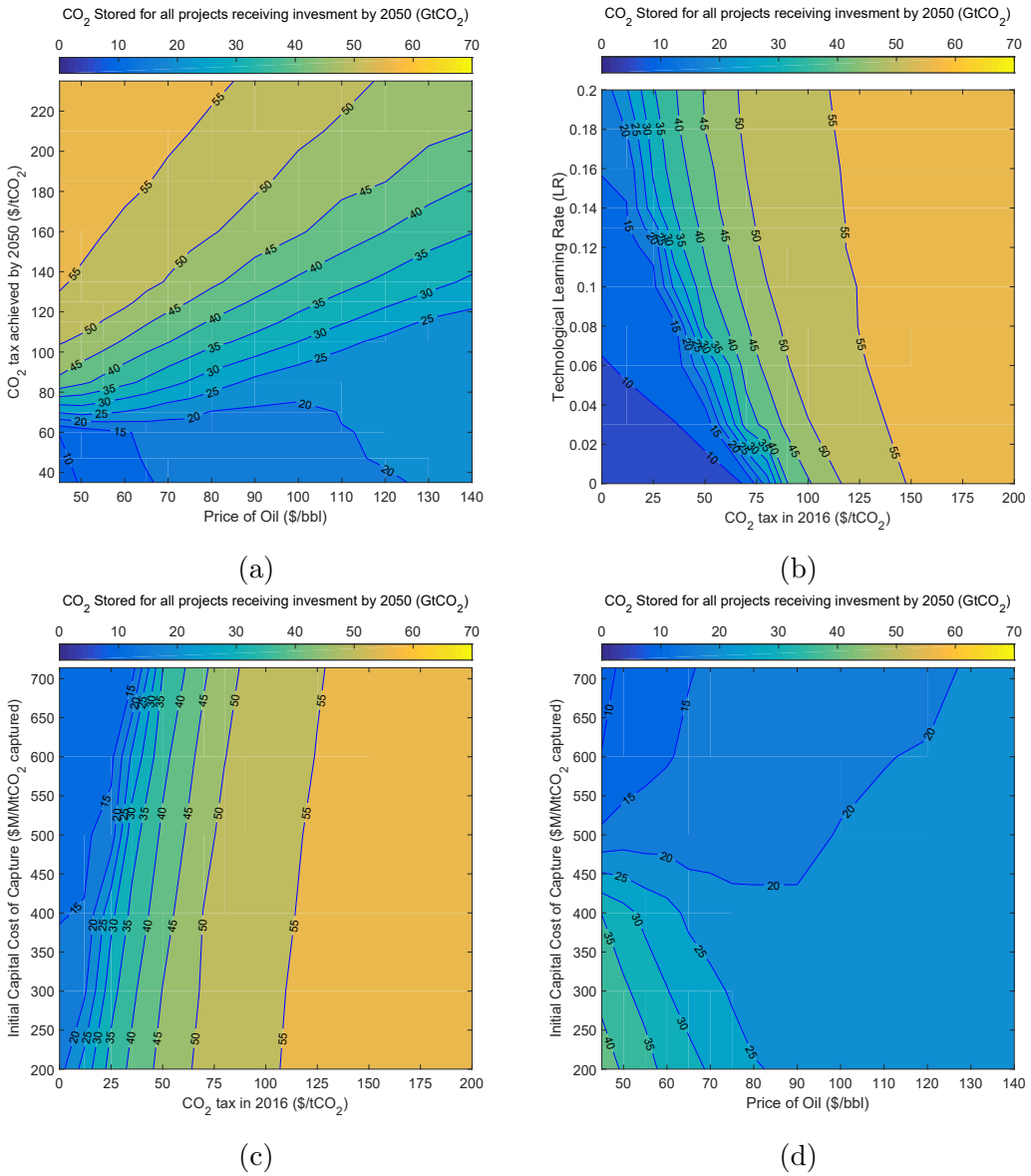

Figure A6: Heat maps showing contours of CO_2 storage achieved for all invested CCS with CO_2-EOR projects by 2050 as a function of (a) the CO_2 tax achieved by 2050 and the price of oil, (b) the CO_2 tax in 2016 and the amount of technological learning assumed, (c) the price of oil and the initial capital cost of capture assumed per $MtCO_2$ capture capacity in 2016, and (d) the price of oil and the initial capital cost of capture assumed per $MtCO_2$ capture capacity in 2016.

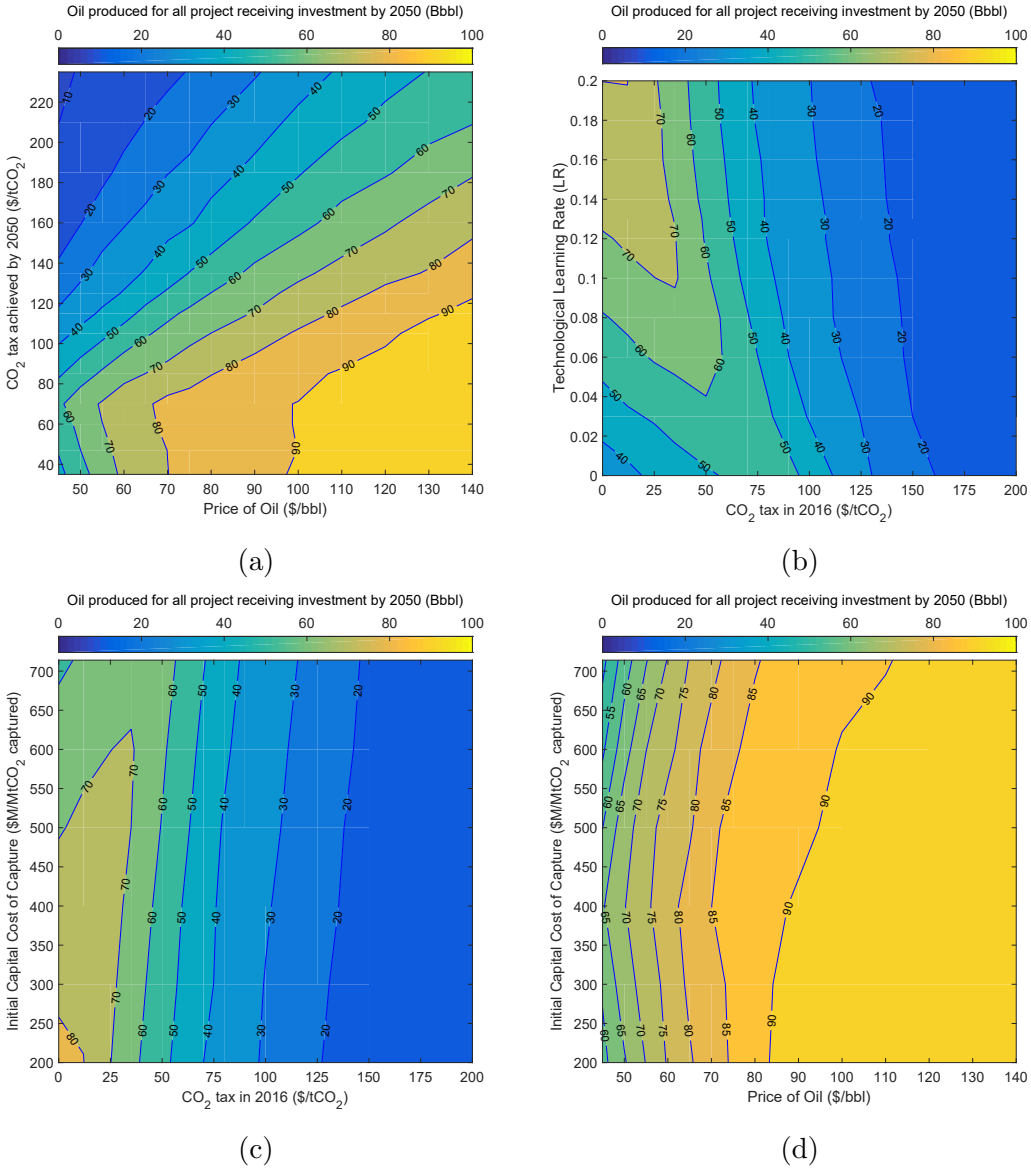

Figure A7: Heat maps showing contours of oil production for all invested CCS with CO_2-EOR projects by 2050 as a function of (a) the CO_2 tax achieved by 2050 and the price of oil, (b) the CO_2 tax in 2016 and the amount of technological learning assumed, (c) the price of oil and the initial capital cost of capture assumed per $MtCO_2$ capture capacity in 2016, and (d) the price of oil and the initial capital cost of capture assumed per $MtCO_2$ capture capacity in 2016.

A2 Appendix to Chapter 4

A1 Bunter Sandstone geological reservoir model

Table A5: Summary of geological reservoir model parameters

Parameter	Value	Unit
Average permeability	100	mD
Average porosity	0.2	
CO_2 density at STP	1.8393	kg/m^3
Brine density at STP	1095.7	kg/m^3
Brine salinity	130,000	ppm
Pore compressibility	4.5 x $10^{-}10$	Pa^{-1}
Initial average reservoir pressure	19.5	MPa
Average reservoir temperature	65	°C

A2 Gas saturation and reservoir pressure maps for set 1 injection scenarios

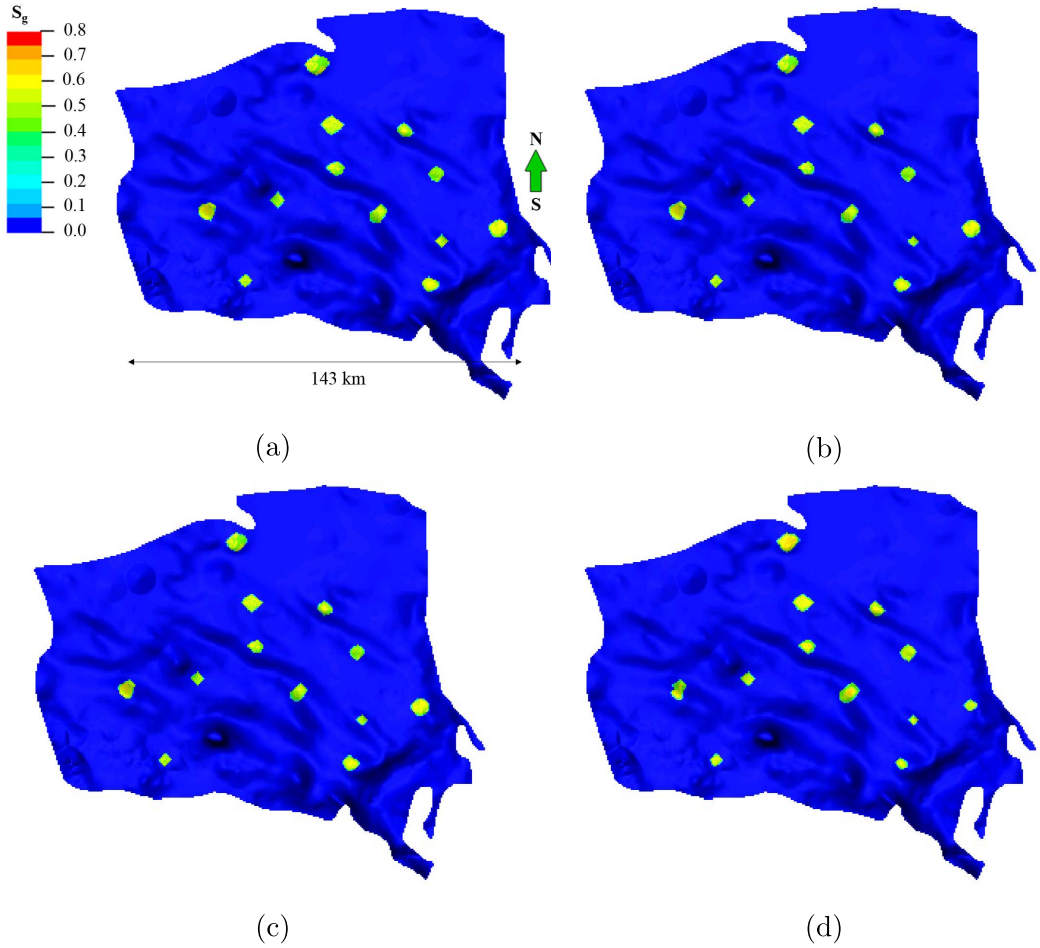

Figure A8: Gas saturation S_g after 50 years of constant injection at 2 $MtCO_2$/year/site (a), after 50 years of varying injection rate by 1.8 and 0.2 times 2 $MtCO_2$/year every 2.5 years (b), by 0.2 then 1.8 every 2.5 years (c), by 1.8 then 0.2 every 5 years (d) and by 0.2 then 1.8 every 5 years (e)

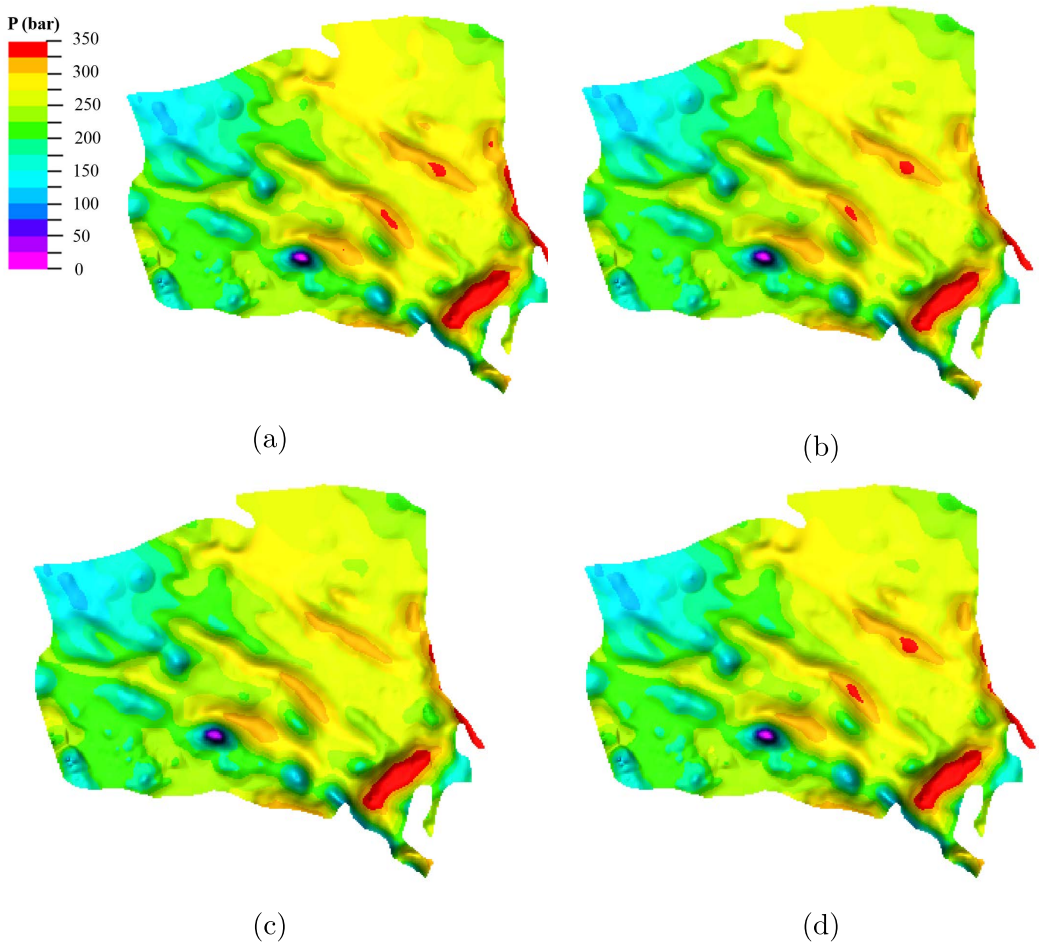

Figure A9: Reservoir pressure P after 50 years of constant injection at 2 $MtCO_2$/year/site (a), after 50 years of varying injection rate by 0.2 then 1.8 every 2.5 years (b), by 1.8 then 0.2 every 5 years (c) and by 0.2 then 1.8 every 5 years (d)

A3 Assumptions for set 2 injection scenarios of CO_2 capture deployment and storage demand for the Bunter Sandstone saline aquifer storage sink

Description of Drax scenarios 1 - 5

- Drax 1: A first demonstration plant capturing CO_2 at a rate of 2 $MtCO_2$/year seeks injection in the field and is split evenly between the 12 injection sites. Three larger scale CO_2 capture plants (equivalent to the emissions from one Drax power plant unit of 660 MWe) then gradually come on-line adding 4 $MtCO_2$/year to the target injection rate every 5 years, peaking at 2045. We then assume that after peak injection for 10 years, the demonstration plant comes off-line, reducing injection by 2 $MtCO_2$/year. Thereafter, assuming that increased renewable energy capacity factors to the UK electricity grid equate to a reduction in fossil fuel based energy, reduction in CO_2 storage

demand is of 2 $MtCO_2$/year. This is then followed by gradually shutting down the capture and power plants associated with them [1], as we transition to a zero carbon energy market towards the end of the century.

- Drax 2: Here, instead of assuming a gradual deployment of CO_2 supply, we assume that once the demonstration and first larger scale capture plant come on-line, 2 more capture plants are built simultaneously adding 8 $MtCO_2$/year to the field's target injection rate. CO_2 injection in the field peaks at 2040 and follows the same slow decline in CO_2 supply as described in Scenario 1.

- Drax 3: The same deployment assumptions as Scenario 1 are taken here, followed by a very fast decline in CO_2 injection demand, due to quicker decommissioning of coal fired power plants and faster insertion of renewable energy supply into the energy market. CO_2 storage supply in the field is no longer needed beyond the end of the century.

- Drax 4: Slow deployment of CO_2 capture and storage is assumed here, with additional CO_2 supply coming on-line in 10 years steps. Peaking target injection in 2060, this scenario assumes a fast decommissioning and storage demand reduction, reaching 0 injection by the end of the century.

- Drax 5: In this scenario we assume a larger scale deployment of CCS in the UK with storage demand from the Bunter field of interest. Starting off with the injection of 2 $MtCO_2$ for an initial 10 year period, one larger scale plant then adds 4 $MtCO_2$/year to the CO_2 supply, before adding 2 more CCS plants by 2045 followed by another 2 in 2050 and achieving peak taget injection of 22 $MtCO_2$. By 2055, the 25 year old demonstration plant stops capturing CO_2 reducing supply by 2 $MtCO_2$/year. The reduction of target injection rate that follows stems from a gradual reduction in fossil fuel energy demand and shutting down of capture plants after a 30 year lifetime.

Target (objective) injection rates versus actual injection rates for Drax scenarios 1 and 4 and 2, 3 and 5

[1] We expect that the capture plants have a lifetime of 30 and at best 60 years

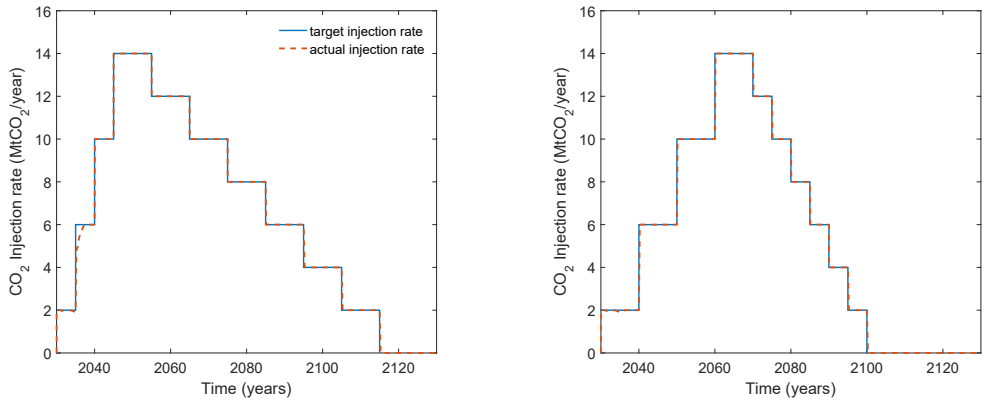

(a) (b)

Figure A10: Graphs contrasting objective injection rate and actual injection rate into the field as a result of deployment scenarios Drax 1 (a) and Drax 4 (b) with peak CO_2 target injection rates of 14MtCO_2/year.

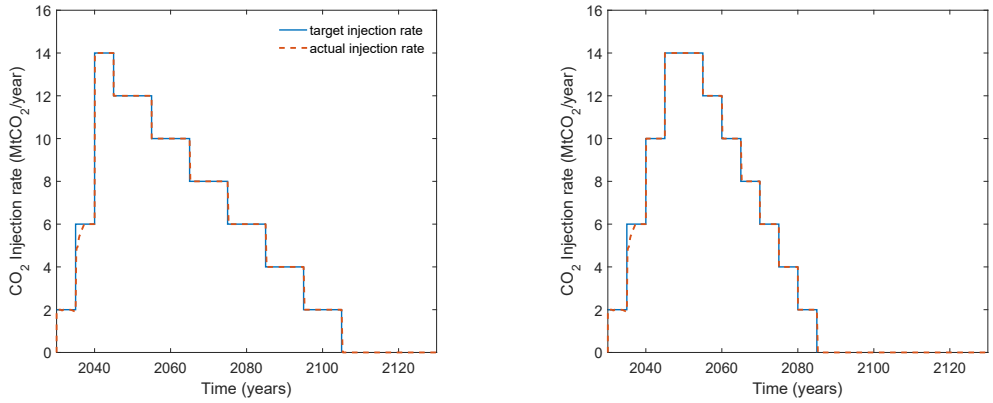

(a) Drax 2: Fast & accelerating deployment of CCS plants with a very slow decline

(b) Drax 3: Fast deployment of CCS plants 1-by-1 every 5 years with a fast decline

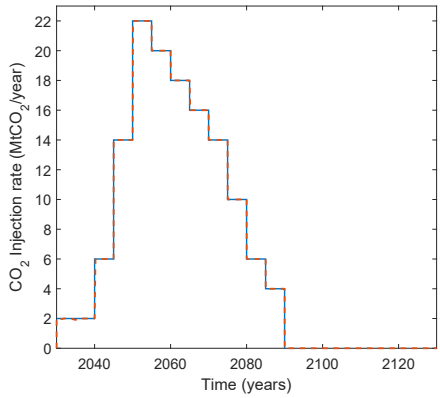

(c) Drax 5: Accelerated deployment of CCS peaking at 22 MtCO_2/year

Figure A11: Graphs showing the objective injection rate compared to the target injection rate for field injection in scenarios Drax 2, 3 and 5.

A3 Appendix to Chapter 5

A1 Process utility assumptions

Table A6: Aspen HYSYS process utility assumptions

Name	Fluid Type	Conditions Pressure,Temperature	Cost	Units
Electricity			0.0576	£/kW
Cooling Water	Water	105kPa$_g$; 20°C	0.00443	£/tonne
Propane	Refrigerant	105kPa$_g$;-40°C	0.0580	£/tonne
LP Steam	Steam	0kPa$_g$; 125 °C	0.002	£/MJ
Refrigerant 1	Propane	0 kPa$_g$; -24°C	0.003	£/MJ
Ethane	Refrigerant	105 kPa$_g$; -90°C	0.036000	£/tonne
Freon 12	Refrigerant	105 kPa$_g$; -29.8°C	0.170000	£/tonne

A2 CPU financial model MATLAB code

The financial model developed to derive the price of CO_2 at which the CO_2CPU investments would meet minimum required rates of return, assuming there is a market for CO_2 sequestration is published for open-access and can be downloaded on MATLAB with the following link: `http://doi.org/10.5281/zenodo.1230482`[235].

A3 Transport network optimisation problem

This part of the appendix to Chapter5 presents the equations and constraints that give the objective functions x (product purity), y (CAPEX in £/t$_{CO_2}$) and z (OPEX in £/t$_{CO_2}$). The following set of equations give the purity of the sum of CO_2 streams from each type of plant, the capital cost incurred per tonne of CO_2 captured for the sum of each type of plant and the operational cost incurred per tonne of CO_2 captured for the sum of each type of plant in the following order: gas CCGT plants, coal plants, industrial plants (one steel plant). The variables for each equation are defined in Table A7.

$$\begin{aligned} \sum_{v} \left[Flow\_gas\,(j) * A2\,(v)\right] &= CO2\_1\,(j) \quad \forall j, \\ \sum_{u} \left[Flow\_coal\,(k) * A1\,(k) * binary1\,(u,k)\right] &= CO2\_2\,(k) \quad \forall k, \\ \sum_{u} \left[Flow\_ind\,(l) * A1\,(u) * binary1\,(u,l)\right] &= CO2\_2\,(l) \quad \forall l, \end{aligned} \tag{A1}$$

$$\begin{aligned}
\sum_{v}\left[Flow_gas\left(j\right)*CAP_post\left(v\right)\right] &= CO2CAPEX1\left(j\right) \quad \forall j,\\
\sum_{u}\left[Flow_coal\left(k\right)*CAP_oxy\left(u\right)*binary1\left(u,k\right)\right] &= CO2CAPEX2\left(k\right) \quad \forall k,\\
\sum_{u}\left[Flow_ind\left(l\right)*CAP_oxy\left(u\right)*binary1\left(u,l\right)\right] &= CO2CAPEX3\left(l\right) \quad \forall l,
\end{aligned} \tag{A2}$$

$$\begin{aligned}
\sum_{v}\left[Flow_gas\left(j\right)*OP_post\left(v\right)\right] &= CO2OPEX1\left(j\right) \quad \forall j,\\
\sum_{u}\left[Flow_coal\left(k\right)*OP_oxy\left(u\right)*binary1\left(u,k\right)\right] &= CO2OPEX2\left(k\right) \quad \forall k,\\
\sum_{u}\left[Flow_ind\left(l\right)*OP_oxy\left(u\right)*binary1\left(u,l\right)\right] &= CO2OPEX3\left(l\right) \quad \forall l,
\end{aligned} \tag{A3}$$

$$\begin{aligned}
x = \left[\sum_{j} CO2_1\left(j\right)+\sum_{k} CO2_2\left(k\right)+\sum_{l} CO2_3\left(l\right)\right] /\\
\left[\sum_{j} Flow_gas\left(j\right)+\sum_{k} Flow_coal\left(k\right)+\sum_{l} Flow_ind\left(l\right)\right]
\end{aligned} \tag{A4}$$

$$\begin{aligned}
y = \left[\sum_{j} CO2CAPEX1\left(j\right)+\sum_{k} CO2CAPEX2\left(k\right)+\sum_{l} CO2CAPEX3\left(l\right)\right] /\\
\left[\sum_{j} Flow_gas\left(j\right)+\sum_{k} Flow_coal\left(k\right)+\sum_{l} Flow_ind\left(l\right)\right]
\end{aligned} \tag{A5}$$

$$\begin{aligned}
z = \left[\sum_{j} CO2OPEX1\left(j\right)+\sum_{k} CO2OPEX2\left(k\right)+\sum_{l} CO2OPEX3\left(l\right)\right] /\\
\left[\sum_{j} Flow_gas\left(j\right)+\sum_{k} Flow_coal\left(k\right)+\sum_{l} Flow_ind\left(l\right)\right]
\end{aligned} \tag{A6}$$

Table A7: Optimization variables for transport network problem

Optimization Variable	Description
CO2_1(J)	Purity of CO_2 stream from sum of gas plants (J) with post combustion capture (V) in mass fraction
CO2_1(K)	Purity of CO_2 stream from sum of coal plants (K) with oxy-combustion capture (U) in mass fraction
CO2_1(L)	Purity of CO_2 stream from industrial plants (L) with oxy-combustion capture (U) in mass fraction
CO2Capex1 (J)	Total CAPEX from gas plants (J) using technology V in £M per Mt_{CO_2} captured per year
CO2Capex2 (K)	Total CAPEX from coal plants (K) using technology U in £M per Mt_{CO_2} captured per year
CO2Capex3 (L)	Total CAPEX from industrial plants (L) using technology U in £M per Mt_{CO_2} captured per year
CO2Opex1 (J)	Total OPEX from gas plants (J) using technology V in £M per Mt_{CO_2} captured per year
CO2Opex2 (K)	Total OPEX from coal plants (K) using technology U in £M per Mt_{CO_2} captured per year
CO2Opex3 (L)	Total OPEX from industrial plants (L) using technology U in £M per Mt_{CO_2} captured per year